Vessel's Performance modelling

Developing a digital twin for the propulsion system, a Spliethoff group case

Stamatis Mavroudis

TU Delft

Vessel's Performance Modelling

Developing a Digital Twin for the propulsion system, a Spliethoff Group case

by

S. Mavroudis

to obtain the degree of Master of Science
at the Delft University of Technology,
to be defended publicly on Wednesday December 11, 2019 at 2:00 PM.

Student number:	4739817	
Thesis number:	SDPO.19.042.m	
Project duration:	February 25, 2019 – December 11, 2019	
Thesis committee:	Prof. Ir. J.J. Hopman	Chairman
	Ir. J.W. Frouws	TU Delft mentor
	Dr. Ir. E.B.H.J.van Hassel	TU Delft mentor
	Dr. Ir. H.J de Koning Gans,	TU Delft
	Ir. M. Berg,	Spliethoff Group supervisor

This thesis is confidential and cannot be made public until December 31, 2024.

An electronic version of this thesis is available at `http://repository.tudelft.nl/`.

TU Delft

Preface

This thesis is submitted as the final requirement to obtain my degree as Master of Science in the field of Marine Technology at the faculty of Mechanical, Marine and Materials Engineering a the Delft University of Technology.

First, I would like to sincerely thank Max van den Berg and Karel van Zijl from Spliethoff, for believing in me and giving me the opportunity to work on such a interesting topic. Max as my daily supervisor, was always willing to offer me help and his door was always open for questions. Karel thank you for believing in this project and making it a reality. I could not forget to thank Robert van de Ketterij for his valuable feedback on my work.

I would also like to thank my supervisors from the TU Delft, Koos Frouws and Edwin van Hassel who have read many versions of this report. Your feedback on my work throughout the project and our discussions were very useful and they kept me focused in the right direction.

Many thanks go to my friends and my family for supporting me and being so understanding for the limited time that I spent with them the last year. In particular, I would like to thank my girlfriend Nicole for always being there for me. Your positive vibes proved to be always effective to inspirit me, even at times when the pressure was high.

Finally, I would like to thank and express my gratitude to John S. Latsis Public Benefit Foundation because without the scholarship you offered to me, this journey would be more difficult. I hope that one day I will have the opportunity to play my part in the Foundation.

S. Mavroudis
Delft, December 2019

Abstract

Spliethoff is a shipping company operating around 120 vessels. The vessels of Spliethoff are generating a lot of operational data as they sail around the globe. In the presented thesis it will be examined how this operational data can be used in the development of a vessel's performance model.

Two methods were examined for the development of a vessel's performance model. The first method, follows the traditional approach, in which every component of the propulsion system is examined separately. The resistance of the vessel was modeled by combining the results from the model tests with information retrieved from the Holtrop and Mennen method [20]. Empirical methods were used to take into account the added resistance caused from the environmental conditions. In order to create models for the machinery of the propulsion plant, information from the manufacturers were used and/or reference values available in the literature. A special case is the propeller's model, which was developed by combining the available open water tests with information from the well documented Wageningen B-series. The available historical data were used during the development of the model to verify that the results provided from the developed sub-models agree with the actual measurements and to identify where modifications are needed.

The second method is a Machine Learning (ML) approach. In this model the input values are the operational conditions of the vessel (speed, draft, trim, weather conditions, etc.) and the target output is the vessel's fuel consumption. This model relies entirely in the available historical data, since a large dataset is necessary in the training phase. The method of the Support Vector Machines was used for the development of the ML model, since this method is capable of handling non-linear problems, and additionally requires less historical data and less time to be trained compared to other methods. In addition, it was examined whether a vessel's performance model can be developed by combining the two methods described in the previous paragraph. Thus, two additional models were created based on the principles introduced by Leifsson et.al. [30].

In order to test the developed performance models, historical data regarding Schippersgracht's last year of operation were used. The database consists of datapoints which were recorded with a 5-minute interval (around 45000 datapoints), during the operation of the vessel. Both the operating conditions (speed, draft, trim, weather conditions) and the corresponding shaft power and fuel consumption are available. Thus, the inputs that the models require in order to perform a calculation were provided from the database. Based on these inputs, the vessel's fuel consumption was calculated from the performance models, for every datapoint. Finally, for every datapoint comparisons were performed, between the calculated fuel consumption by the models and the measured fuel consumption stored in the database. It was found that by all the 4 models, around 80% of the examined dataset (Schippersgacht's last year of operation) was calculated with an error less than 10%. It should be noted that from the examined dataset the non-steady conditions (vessel accelerating or decelerating, not stable heading, etc) were not filtered out.

In order to further examine the models' accuracy, the errors distribution was created for every component with strong influence on the vessel's fuel consumption (speed, draft, waves, swell, wind). Based on these graphs it is concluded that the all the developed models are well tuned and all perform equally good in all conditions. The daily fuel consumption for the dataset regarding Schippersgracht's last year of operation was calculated and compared with the measured one. It was found that for about 90% of the days examined, the daily fuel consumption was calculated with an error less than 10%. In addition, five voyages were selected, with duration ranging from 4-11 days, and in all of them the voyage's total fuel consumption was calculated with an error less than 3.5%.

The main conclusions about the developed performance models is that all the models resulted in more less the same accuracy. The model based on the traditional approach has the advantage that it offers more information and more outputs can be taken, compared to the ML approach which only provides an output about the fuel consumption. On the other hand, the model based on the ML approach is significantly faster and allows many iterations to be performed in a short period of time. Regarding the models which were developed

based on the principles introduced by Leifsson [30], they did not further improve the accuracy, and they do not have additional advantages, compared to the two aforementioned models (ML approach and traditional approach).

Finally, two case studies were performed. In the first case study it is presented how the model, developed following the traditional approach, can be used to examine how modifications in the propulsion system will influence the vessel's fuel consumption. The case of switching from fixed rpm (that is currently used) to a variable rpm system was examined, which is a real scenario that the company is considering. It was calculated that installing the variable rpm system and a frequency converter will result in annual savings of around 250,000 €, while the investment's payback time is estimated to be around two years. In the second case study a future voyage simulation algorithm was developed. This algorithm receives as inputs the voyage plan (route and speed) and performs a calculation for the voyages fuel consumption by taking into account the weather predictions. The voyage simulation algorithm, is making use of the ML model. A few cases were examined in order to examine for how many days in advance the calculation is reliable (due to the uncertainty of the weather predictions) and about the time interval that should be used in the algorithm. However, clear conclusions were not derived and further examination is suggested (by examining more voyages).

Contents

List of Figures

List of Tables

Glossary

ANN Artificial Neural Networks. 9

BBM Black Box Model. 10, 15, 18

CPP Controlable Pitch Propeller. 14

DCS Data Collection System. 1

EEDI Energy Efficiency Design Index. 1

GBM Grey Box Model. 10, 15, 18

GHGs Green House Gases. 1

GMM Gaussian Mixture Models. 9

GP Gaussian Processes. 9

GT Gross Tonnage. 1

HSFO High Sulphur Fuel Oil. 1

IMO International Maritime Organization. 1

KPIs Key Performance Indicators. 7

LSFO Low Suphur Fuel Oil. 1

ML Machine Learning. 9, 15

NR Noon Reports. 9

PMS Performance Monitoring System. 3, 16

PTO Power Take Off. 14

SEEMP Ship Energy Efficiency Management Plan. 1

SPA-JIP Service Performance Analysis Joint Industry Project. 56

STA-JIP Sea trial Analysis Joint Industry Project. 56

WBM White Box Model. 10, 15, 18

1 Introduction

1.1. Context

The international shipping is responsible for the carriage of about 90% of world trade and it is vital to the functioning of the global economy [3]. The contribution of shipping to the global emissions of Green House Gases (GHGs), is significant and it is comparable to the contribution of a major national economy [3]. More specifically, in 2012 international shipping was estimated to account for 2.2% of the global CO_2 emissions, and this percentage is estimated to increase between 50% and 250% by 2050 [4], depending on future economic and energy developments. The International Maritime Organization (IMO) 2nd GHG study [2] showed that there is the potential to reduce the ship's energy consumption and CO_2 emissions by up to 75% by applying operational measures and implementing existing technologies. Thus, despite the fact that shipping offers a substantially lower carbon intensity compared to the other freight modes [3], additional measures have been taken in order to further increase the vessels' energy efficiency. By 2012, all the new ships should comply with the Energy Efficiency Design Index (EEDI) and in addition all the ships both already existing and new should have a Ship Energy Efficiency Management Plan (SEEMP) [4]. In addition, the EU decided that by 2018 ships larger than 5000 Gross Tonnage (GT), using EU ports, have to monitor (and report by 2019) their fuel consumption and CO_2 emissions [1]. Reporting data regarding fuel consumption and emissions from ships larger than 5000 GT will be required as well for global shipping by 2019 under the IMO Data Collection System (DCS) regulation. The global 0.50% sulphur cap (IMO 2020) will enter into force in 2020, and more that 70,000 ships will be affected by the regulation [14]. In order to avoid running on fuel of better quality and higher price, many shipowners have chosen to install scrubbers. However according to a study by Clarksons, in the beginning of 2019 around 10% the existing fleet, by tonnage capacity, was equipped with scrubbers, while the corresponding percentage of the world's orderbook is 31% [12]. It cannot be foreseen how the demand of the High Sulphur Fuel Oil (HSFO) and Low Suphur Fuel Oil (LSFO) will be in 2020, but an influence on the prices is likely to happen.

In addition, a factor that raises the interest towards more energy-efficient shipping is the high variations in the prices of marine fuels over the last years (as presented in Figure 1.1). When the fuel price is in high levels, shipowners are putting more effort into increasing the energy efficiency, which is translated to cost reduction. It is estimated that in 2013, the bunker costs could account for 50-60% of the total vessel's operating costs [52]. Today the fuel price is lower compared to 2013, but still, the fuel cost has a significant contribution to the total operational costs. With the fuel costs accounting for such a high percentage of the total operational costs, it can be seen that even a small reduction in fuel consumption can be a significant cost reduction for a shipping company.

This situation results in an increased effort to achieve a more energy-efficient shipping. The methods to achieve it, have been categorized into structural, operational, technical and alternative fuels according to DNV GL [10]. The present research is only tied to the operational measures. Operational measures are related to the way that the vessel is operated and maintained and include measures such as trim optimization, hull and propeller cleaning, weather routing, and better scheduling (just in time arrival) [10]. These measures are attractive since they can be applied to all vessels, including the already existing ones, while the cost of the

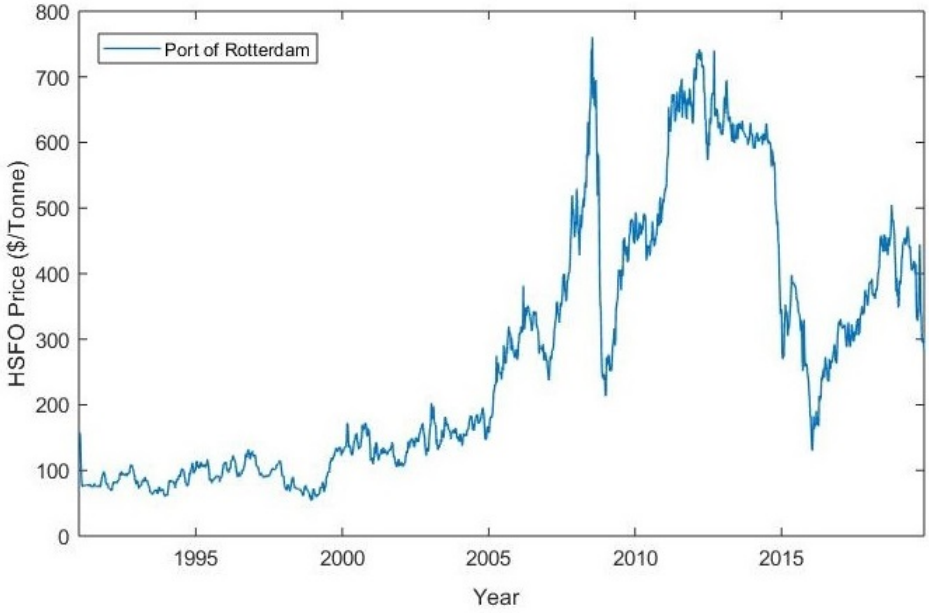

Figure 1.1: Price of HSFO in the Port of Rotterdam over the last 20 years [42]

investment is maintained low.

However, in order to implement the measures mentioned above, and more general in order to optimize the vessel's performance (in terms of energy efficiency), there should be a way to evaluate the performance of the vessel. Thus, the process of optimizing the energy efficiency of the vessel is tied to the monitoring and the evaluation of the latter. The monitoring will provide the required data which will be used for the evaluation. Many shipping companies are not relying any more to the noon reports, and they choose to collect high frequency data (i.e. every 5 minutes, or in other cases every 15 seconds). On the other hand the evaluation is the process of assessing the performance compared to a reference. The evaluation process is complex due to the fact that the vessel is operating in a complex environment, influenced by many factors (such as the weather conditions).

A vessel is a complex system consisting of many sub-systems. The configuration of these sub-systems, their efficiencies, and their mutual interactions determine the overall energy efficiency and operational performance. However, these interactions are complex, and thus the operational performance is hard to be determined. The resistance of a vessel is influenced from parameters such as draft and trim (which are directly connected with the wetted surface of the vessel) and from factors such as the weather conditions. Waves, wind, and currents can increase the resistance significantly, especially when their direction is against the vessel's course. In addition, heavy weather also results in drift forces, which makes the ship deviate from its course, resulting in additional resistance. The resistance is also influenced from the fouling effect on the propeller and the hull. In addition, minor effects can be caused when the vessel is sailing in shallow waters and from the variations of the water temperature and salinity. However, the operational performance is not determined only from the vessel's resistance. The configuration of the propulsion plant, the current state of the machinery, and their efficiencies play as well a significant role in the overall operational performance. Despite that many systems on-board are automated, the human has still control of many settings regarding the operation of the vessel. The way that the crew and the captain are operating the vessel has an impact on the operational performance. However, despite the complexity of the vessel's operating environment, usually, little is known for the vessel's operational performance out of the design conditions. The vessel's energy demand is examined during the design phase, only for the design conditions in calm seas. The vessel is rarely sailing under the idealistic design conditions, and many shipping companies do not have a way to evaluate the vessel's performance in that case.

There is a need for evaluation methods which will enable the assessment of the vessel's performance un-

der any operating conditions. This can be achieved with a performance model. A performance model can be defined as model which receives as an input the operating conditions of the vessel (speed, draft, trim, weather conditions, etc) and gives as an output the reference fuel consumption for the given inputs. A very detailed performance model capable of providing an accurate estimation of the vessel's power/fuel demand under all possible conditions that the vessel may encounter can also be seen as a digital twin of the propulsion system. The development of such a model will result in a more effective performance evaluation and will open the way to act towards operational performance optimization.

1.2. Thesis plan of approach

1.2.1. Motivation

Nowadays, the shipping industry is being reshaped by digitalization, which is a key enabler for making the maritime industries more innovative, efficient, and fit for future operations. The main enabling factors are the increased vessels' connectivity, advanced sensor technology, offering more reliable and economical solutions in a broader range of applications, and the developments in cloud computing and advanced data analytics, making the storage and analysis of data more affordable. This new era in shipping offers new ways and methods to maximize profit and verify compliance with regulatory demands. Examples which worth to be mentioned are the newly established companies offering solutions in the area of vessels' performance optimization based on real-time collection and analysis of the operational data. The digital era in shipping enables the opportunity to use the digital twin concept, which can be used in various ways to create value for the industry.

Spliethoff is a shipping company, established in 1921, with the headquarters based in Amsterdam. The company endeavors to find ways to maximize the vessels' operational efficiency and reduce the environmental footprint. Working towards achieving this goal, the following projects have been carried out by Spliethoff.

The development of a vessel's Performance Monitoring System (PMS) was researched by R. Grutterink [17], who also performed an initial data analysis. Afterwards, M. Berg [49] continued building on this research, working towards the development of a Ship Energy Efficiency Management Plan (SEEMP) and the role of the PMS within it. In the revised SEEMP, there is a transition towards a more data-drive decision making and communicative culture. M.Berg [49] focused on how and how much value can be created from the use of the PMS and researched what information should be provided from the PMS to achieve this. This research resulted in the development of reference performance curves for the vessel (fuel consumption or required power versus the vessel's speed) under various operational conditions (waves, wind, draft), which were examined separately. These curves proved to be very useful for evaluating the vessel's performance and making conclusions about past trips. Spliethoff is now looking forward to a more detailed evaluation method where a more extensive range of effects will be taken into account. This model will offer new opportunities to the company concerning operational performance optimization.

This research will be implemented in the S-type vessels of Spliethoff group. The main reason is that these vessels are the main fuel consumers within the company's fleet. Thus, the company started the process of installing sensors to these vessels to collect data in order to gain knowledge and set the basis for optimizing the vessels energy efficiency.

1.2.2. Objective

The objective of the presented thesis can be formulated by the following sentence.

Develop a performance model for the S-type vessels of Spliethoff group

The secondary research questions are the following:

- Which are the state of the art methods to create a performance model?
- Which effects should be taken into account? Are the required information available to do so?
- How the model can be used to simulate future or past voyages (and calculate the fuel consumption)?

The performance model to be developed can also be expressed as a digital twin of the vessel's propulsion system.

1.2.3. Scope

The proposed diploma thesis will continue building further on the research done by R.Grutterink [17] and M.Berg [49]. As was aforementioned, the goal of the project is to create a performance model that will be able to reproduce past events based on the stored operational data and predict future situations by considering weather predictions. Particular effort should be put to develop a model which will be close to the realistic conditions without introducing significant simplifications. Thus, the model to be developed will have to take into account the main parameters affecting the operational performance of the vessel and will have to provide results in a high level of accuracy. For the scope of this project, the vessel's operational performance is constrained to the power demand and fuel consumption.

In the following paragraph, the areas that will be researched are discussed. Since the parameters with influence on the resistance of a vessel were discussed in Section 1.1, in this section will be treated briefly. The vessel's fuel consumption is determined mainly from the resistance of the hull and the performance of the propulsion plant components. The vessel's resistance is an area of high importance, as it is influenced both from parameters such as vessel's speed, draft, trim, and from the environmental conditions (waves, currents, wind). In addition, there is influence from shallow water sailing, course keeping efforts, and hull fouling. Thus, particular effort will be put to create a model for the vessel's resistance, which will be able to take the aforementioned parameters into account. The propeller's characteristics and the engine's performance will be studied, also taking into account their mutual interaction. In addition, the shaft generator, which provides the required electric power and is an additional load to the main engine, should also be included in the model. The model to be developed will be receiving as inputs a set of parameters (i.e wind speed, wave height, draft etc) and will give as output the fuel consumption under the given input parameters.

In order to calculate the fuel consumption for an entire trip, the voyage simulation algorithm will be developed. The performance model will be incorporated into this algorithm. The voyage simulation algorithm will make the projection of the performance prediction model over time. The inputs to the algorithm will be the route under study, the weather predictions, the speed profile, and operational parameters such as draft and trim. The route to be followed will be divided into waypoints. The performance model will be used on each of these waypoints to predict the fuel consumption under the conditions that the vessel will have to encounter. By considering the outputs from all the waypoints, the fuel consumption for the entire voyage can be calculated. Further explanation is given in Figure 1.2 where the distinction between the performance model and the voyage simulation algorithm is highlighted. As the main objective of this project is to develop an accurate performance model and not to develop a voyage optimization algorithm, the algorithm will be constrained to the fuel prediction under the given inputs.

Research will be done in order to identify the approach and the modelling methods which will result in a reliable and accurate performance model. In addition, the approach that will be followed by the voyage simulation algorithm will be examined.

The study will be based on the S-type vessels from the Spliethoff fleet. For the development of the model, information regarding the design characteristics, propulsion plant configuration, propeller's open water diagram, and engine's consumption map is expected that will have to be acquired. Since there are minor deviations on the design characteristics of the S-class vessels and additionally not significant differences are observed in the the PMS regarding their operational performance, one of them will be selected in order to collect this information. In addition, data collected from the PMS regarding the operation of the S-type vessels will be used. Despite that the design characteristics from one vessel will be used, the operational data from the entire class will be used in order to increase the sample's size. The developed model is expected to be applicable to the entire S-class fleet.

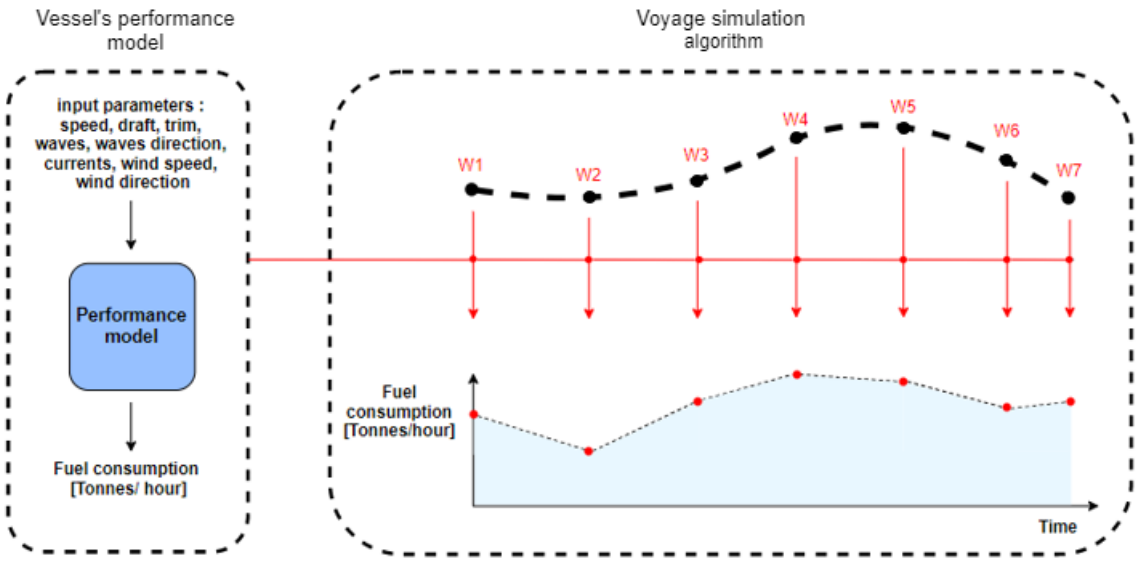

Figure 1.2: Vessel's performance model and voyage simulation algorithm interaction

1.2.4. Activities

The following activities will be the main core of this project.

Literature
The first activity of the project will be literature research. The focus will be to explore the available methodologies which can be applied in the performance model development. The literature research will be continued throughout the most part of the project, as in each activity relevant literature will have to be reviewed.

Method selection
This part will deal with the selection of the method that will be followed in the performance model development. An overview of the available data that can be provided by the company will be presented, as that have a major role in the methodology selection. Which parameters will be the input to the performance model, which systems will be included and what methods will be used for the modelling of the systems are questions that will be answered in this part. In addition, the approach that will be followed by the calculation algorithm will be determined.

Performance model development and validation
In this section information from the process of the model development will be presented. The accuracy of the derived model is very important for the scope of the project and so it will be examined as well in this section.

Voyage simulation algorithm development
In this part the algorithm for the calculation of the vessel's fuel consumption for an entire trip will be developed.

Case studies
In this section incidents from past voyages where it was identified that there was room for improvement of the operational performance will be used to indicate how the developed tools (performance model and algorithm) can result to fuel consumption reduction within Spliethoff.

2

Literature review

In this chapter the literature relevant to the vessels' performance models will be reviewed. Their applications will be briefly presented and the methods that are used for their development will be discussed. Finally, the literature gap will be identified.

2.1. Literature review

A first detailed description of a performance monitoring and evaluation system was given by Carlton [8], where both the structure of the system was discussed but also its role within a shipping company. Carlton [8] discussed the importance of developing a database with operational data under various operational and environmental conditions in order to create a reference for the vessel's performance. In addition, it was highlighted how the development of the vessel's reference performance, and the data collection can be used both for operational and chartering decision making. Regarding the evaluation of the vessel's performance it was briefly discussed how Key Performance Indicators (KPIs) can be used for that purpose. The methods that are currently used in the vessel's performance evaluation are the following [37].

- Comparing the measured energy consumption with older measurements corresponding to the same conditions.
- Using a model to calculate the vessel's *'reference'* energy consumption for the given conditions and comparing it with the measured energy consumption.

The first method is also known as the filtering method since from the entire database only the data corresponding to the same conditions are used to evaluate the performance. However, due to the fact that there are many factors influencing the vessel's energy consumption, there will not be many data referring to exact the same conditions, which makes the evaluation of the vessel's performance with this method difficult to be applied.

In the second method a model is used to calculate the vessel's reference energy consumption, this model is called vessel's performance model. An exact definition for the performance model is not available, however a simple description is given by Aldous [5]. Aldous states that "*A vessel's performance model is developed in order to estimate the response in the dependent variable (fuel or power demand) to each operational (speed, draft, trim, time out of dock) and environmental condition given the ship's fixed design parameters (hull geometry, propeller characteristics, engine configuration)*". The evaluation of the vessel's performance with this method is usually performed by comparing the measured fuel consumption/power with the reference one for exactly the same conditions, which is calculated with the performance model. The challenge in this method is identified in the development of an accurate performance model, which arises due to the high complexity and the large number of factors influencing the vessel's energy consumption.

So far Spliethoff was using the first method to evaluate the vessel's performance. Reference fuel consumption curves (versus speed through water) were created for different environmental conditions [49] and the performance evaluation was performed by comparing the measured fuel consumption with the reference curve

which corresponded to similar environmental conditions. However, in contrast with the filtering method, the applications of a vessel's performance model are not limited only to the evaluation of the vessel's energy efficiency. According to Aldous [5] and Leifsson et.al. [30] the main applications of a vessel's performance model are the following:

- Operational real time optimization

  By taking into account the voyage's operational parameters (i.e. draft and required time of arrival) and environmental conditions (currents, wind, waves, etc) the vessel's performance model can be used to derive the values of the controllable parameters (i.e. trim and speed). Weather routing is taking into account weather predictions and the destination of the vessel and tries to minimize the voyage's cost by controlling the speed and the route to be followed. However, usually the way that the influence of the weather conditions on the vessel's energy efficiency is taken into account is oversimplified. Thus, it can be seen that an accurate and detailed performance model can increase the potential for savings through the weather routing service.

- Maintenance

  By combining an accurate performance model with a performance monitoring system, a tool can be created which will help in the process of detecting faults and the scheduling of maintenance. By comparing the actual vessel's performance with the reference one for the same conditions, valuable conclusions can be derived about the hull and propeller fouling. In addition, possible faults in the equipment of the propulsion system can be identified.

- Evaluation of technological interventions

  New technologies which are examined from the company as solutions to improve the vessel's energy efficiency can be evaluated in order to quantify cost versus benefit and the economic risk of the investment. Performance models can also be used to prove or disprove manufacturers' claims (post analysis in this case). Thus a performance model can also be used as a simulation or design tool.

- Charter party analysis.

  A vessel's performance model can provide to a shipping company valuable information about the fuel consumption under different conditions (speed, draft and weather conditions) that can be used when the terms of a contract are negotiated.

The wide range of applications in which a performance model can be used for, is the reason why Spliethoff is interested in the development of a performance model. Therefore, the development of the latter will be examined in the present thesis. In the following paragraphs different types of performance models will be analysed.

Based on the available literature, there are mainly two different methods for the development of a vessel's performance model. The first method is the traditional approach which is used for many years. In this approach, the components that compose the ship propulsion system are examined separately. Usually, the resistance of the vessel is modeled by combining empirical or semi-empirical methods with results from model tests. In a similar way, the phenomena influencing the vessel's resistance (i.e. weather conditions, shallow water sailing, etc) are taken into account with empirical or semi-empirical models. In order to calculate the fuel consumption, the machinery has also to be examined. The gearbox's and the shaft's efficiency, in most studies considered as constant. On the other hand for the diesel engine, a simple relation is used for the fuel-power dependency, based on information which are provided from the manufacturer. The engine's performance can also be modeled based on thermodynamic relationships, however this approach requires more effort. The advantage of the this method is that the model can relatively easily be modified in order to be used for different vessels, or to account for modifications in the propulsion system. On the other hand, it is challenging to derive an accurate model as a lot of assumptions and simplifications have to be made during the development process. In addition, Logan [31] highlights that the method to model every resistance component independently cannot take into account possible interactions between them which makes the modelling inconsistent.

Journee [23][24] published in 2003 his studies where he used results from full scale experiments (full-scale sea keeping experiment in [23] and calm water performance tests in [24]) to create the vessel's performance model. In both studies he used a combination of empirical methods and experimental results to develop a model for every component of the propulsion chain. The model was used to assess the impact on the fuel consumption on different operations (i.e. operating the twin screw vessel only on one propeller). The results from the model show good agreement with the measured values, however due to the fact that there was a small number of measurements available, the model's accuracy was not examined extensively.

Eljardt [11] developed as well a vessel's performance model falling under this method, in his study towards the development of a fuel oil consumption monitoring and trim optimization system. In this research the effects from the sea state, the wind, the course keeping and the shallow water were taken into account, however the accuracy of the developed model is not discussed.

Two recent studies where a large number of operational data (from an automated recording system) were used for the evaluation of the models are the following. Hansen [19], developed a performance model and researched the ways that it can be used in the performance monitoring. Additionally, he examined how the influence of biofouling on the vessels energy consumption can be measured. Although the accuracy of the model is not discussed directly from Hansen, it appears from the presented results, that there is good agreement between the results from the model and the measured data. Tsujimoto and Orihara [48] developed a performance model to be used in combination with the performance monitoring system for the performance assessment. The effects of waves, wind, hull drifting and steering forces were taken into account. The models applicability in the performance monitoring system was evaluated extensively [35]. The agreement between the measured data and the calculated from the model appears to be very good. However, it should be noted here that this is partially due to the fact that from the evaluation dataset situations which corresponded to non-steady state conditions were filtered out.

Finally, in the research conducted from Geertsma et. al. [13], a performance model for a frigate's propulsion plan was developed. The performance model was used to perform simulations to examine the impact of different control strategies on the diesel engine's performance. In this research a very detailed physical model was developed for the diesel engine based on thermodynamic relationships. According to the author the model was able to predict the system's behaviour with an error less than 5%.

The second method which is identified in the literature is the data-driven models also referred to as "*Machine Learning*" (ML) models. Noting that there are conflicting opinions about the definition of Machine Learning (ML), many researchers consider as ML all the methods where learning from data is involved (from simple regression to highly complex algorithms), however others disagree and consider as ML only the advanced methods. In ML a model is trained based on a large number of data to predict the target output for the given set of input variables. For the training phase a large dataset is required where both the input and the output values are known. The characteristic of the performance models developed with this method is that they can be used to make predictions for the output of the exact system that the data for the training were collected from. Thus, with this type of models modifications in the propulsion system cannot be examined

Pedersen [37] used different regression methods (linear regression, non-linear regression, Artificial Neural Networks (ANN) and Gaussian Processes (GP)) to develop a vessel's performance model. It was found that the accuracy of the models based on ANN and GP outperform the accuracy of the models based on the simple regression methods, however the difference between the ANN and GP model was reported to be insignificant. In addition, two different ANN models were examined. In one case data from Noon Reports (NR) were used, whereas in the second high frequency data, which were collected from an automated system. In the model in which high frequency data were used, an error of 0.8-1.7% was reported, whereas in the model in which NR data were used, an error of about 7% was reported.

Petersen [38] compared the performance of models developed based on ANN, GP and Gaussian Mixture Models (GMM) which were trained with high frequency data from an automated recording system. The accuracy of the developed model ranges in the same levels with that reported by Pedersen [37].

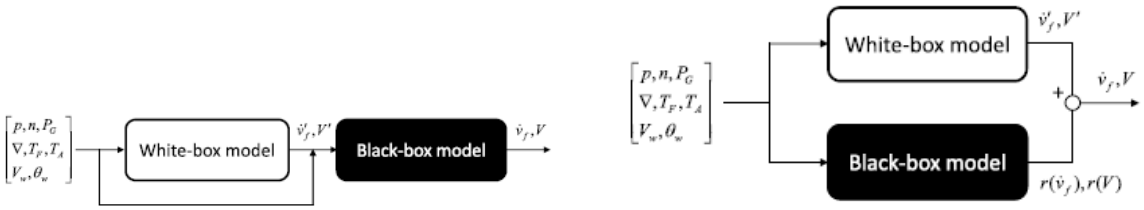

(a) Serial grey box performance model (b) parallel grey box performance model

Figure 2.1: Grey box model methods proposed by Leifsson et.al [30]

Senteris used as well ANN to develop a performance model for a VLCC tanker. The model was used to assess the hull's condition in terms of biofouling. The presented results show an agreement between the measured and the predicted data corresponding to an R^2 higher that 0.98, however, it should be noted that this result was based on a small dataset.

Leifsson [30] characterized the models falling under the first described method (modelling every component of the propulsion chain with physical, empirical methods and/or results from model or full scale tests) as White Box Model (WBM). For the models falling under the second method (developing a model entirely based on operational data) he used the term Black Box Model (BBM). It should be noted that this distinction is not absolute since in the models which are developed with the traditional step by step approach, a submodel can also be developed based on black box modeling methods, which means that the final model will be a hybrid model. On the other hand, according to many researchers, in ML there are both white box model and black box models. In addition, Leifsson introduced the idea of combining a WBM with a BBM which results in the development of a Grey Box Model (GBM). The methods he proposed, which were also applied for the development of a containership's performance model can be seen in Figure 2.1.

As it is also presented in Figure 2.1a, in the serial GBM, the WBM performs a prediction for a given set of input parameters, and then the same set of inputs including the WBM's prediction, is passed by to the BBM to perform the final prediction of the target output. In the parallel method (Figure 2.1b, the WBM performs an initial prediction for the target output and a BBM is used as a correction factor. The conjecture is that the WBM will retain what is known about the physical behavior of a ship regarding the balance between propulsion power and vessel resistance, and the BBM will scale the output from the WBM to fit operational data of a given ship, and include the effects of phenomena that are not modeled in the WBM. Leifsson developed both a WBM, a BBM and two GBM (serial and parallel). Leifsson [30] reported that the BBM and GBM presented 65% lower Root Mean Square Error (RMSE), whereas a difference cannot be identified between the performance of the BBM and GBM. However, it should be noted that in the WBM, significant simplifications have been made. An example is that the influence of waves on the vessel's energy consumption has not been taken into account. For the BBM component a Feed-Forward Neural Network was used in all cases.

A similar approach was followed from Coraddu et.al. [9] and the results from this research are in agreement with the findings reported from Leifsson [30]. However, an oversimplified WBM was used as well in this case. Coraddu reported that despite the fact that the BBM and GBM resulted in the same level of accuracy, the GBM required less historical data for the training phase.

After analysing the literature relevant to the vessels' performance modelling, the following conclusions were derived. Firstly, it is observed that there is increased research interest in the development of vessels' performance models especially the recent years. There are many studies on the development of performance models, however, in most of them the accuracy of the developed models is not examined sufficiently. In addition, in recent years the interest in developing vessels' performance models based on ML methods arose. The latter is mainly a result of the enormous increase of the available historical operational data due to the automation of the recording system. Since, the ML approach is preferred from the researchers there are not many studies examining how the large datasets of historical operational data can be used in the development of a vessel's performance model based the traditional approach (modelling every component of the propulsion plant). In addition, in a few studies where a performance model was developed by both the two methods (ML and traditional approach), significant simplifications were made in the model developed by the traditional ap-

proach and thus, the comparison was not performed on equal basis. Finally, it was observed that in most studies, the performance models were developed to be used as the evaluation method in the performance monitoring system (i.e. fouling detection, fault detection), and as a consequence, other application have not been examined.

3

Method selection

In this chapter, the methods to be followed both for the development of the vessel's performance model and for the voyage simulation algorithm will be selected. This selection is highly dependent on the data that the company has in possession and can provide. Thus, an overview of the available data will be given before the selection is made.

3.1. Information for the S-type class

As it was mentioned in chapter 1.2, the project will be based on the S-type vessel from the Spliethoff fleet. The S-type class consists of 11 general cargo vessels which are divided in two series, the short S-type with length of 168 m and the long S-type with length of 173 m. In Chapter 1 was mentioned that the performance model will be based on the S-type vessels, to be more specific, the vessels of 168 m will be used. The S-type vessels are mainly sailing in transatlantic voyages, between the Baltic and the East coast of USA. The routes followed from the S-type vessels in 2018 can be seen in Figure 3.1.

Figure 3.1: Voyages operated in 2018

In addition the speed profile of the S class, based on the available historical data of the past 2 years, is presented in Fig 3.2. It can be seen that the vessels spend almost 35% of the time in port. On the other hand, around 50% of the time the vessel was sailing with speed in the range of 13-18 knots. It is important to mention that the design speed of the vessels is 20 knots but as we can see, the vessels rarely sail at this speed.

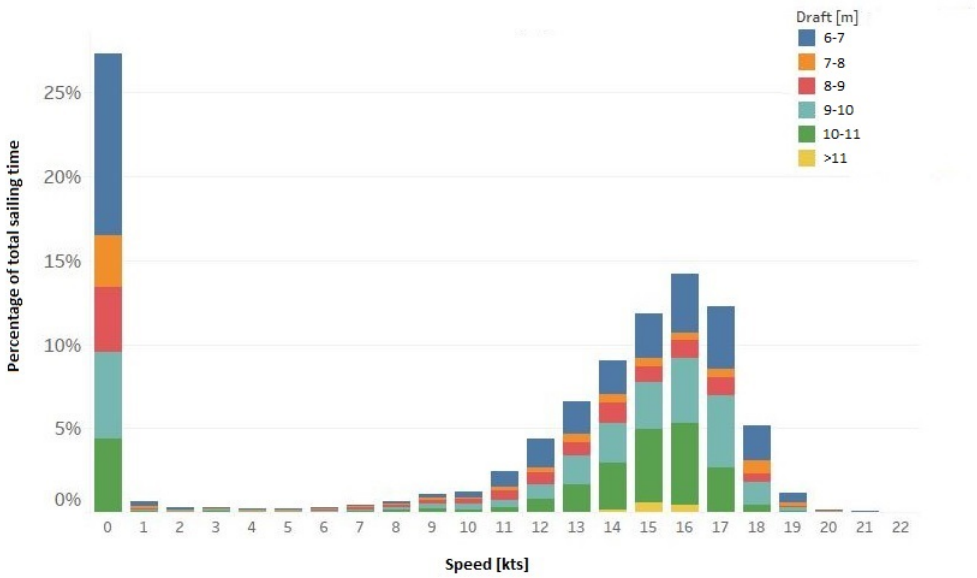

Figure 3.2: Speed profile of S class vessels (2018)

A representation of the propulsion plant is given in Figure 3.3. The mechanical power is provided from one diesel engine rated at 12 MW and the electrical power from the Power Take Off (PTO). The vessel is also equipped with an auxiliary and an emergency electrical power generation system consisting of 3 and 1 diesel generators, respectively. The vessel is propelled by a Controlable Pitch Propeller (CPP), with a diameter of 6.2 m. A frequency converter is not installed in the vessels, and as a result, the propeller is fixed to rotate at 105 rpm when the PTO is in operation. The use of the auxiliary electrical power generation system is limited to extreme weather conditions when the output of the main engine is not enough to both propel the ship and run the PTO, and when the ship is in port, as the thrusters can be set in operation only when powered from the diesel generators.

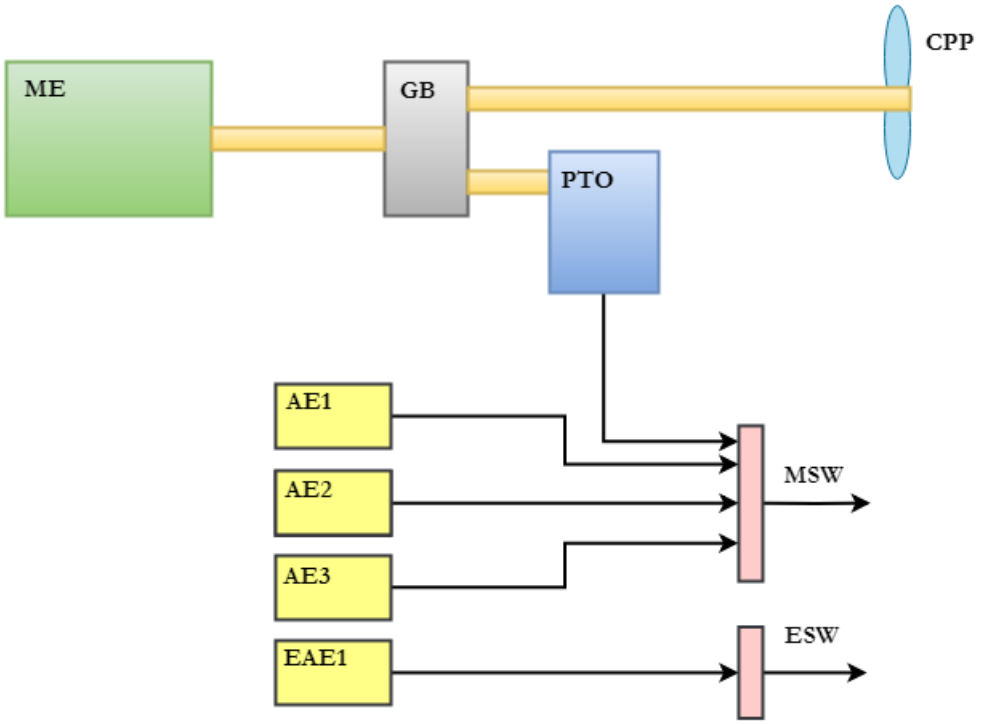

Figure 3.3: Propulsion plant representation of S-type vessels

3.2. Data availability

In this section, an overview of the data that the company has in possession will be presented. In addition, it will be discussed whether the modeling methods (presented in Chapter 2) can be applied in the present research. It should be noted the categorization which was performed from Leifsson [30] will be used in this research as well. Thus the models falling under the traditional approach (using empirical, semi-empirical methods and/or results from model tests to create a model for every component of the propulsion chain) the term WBM will be used. For the ML approach the term BBM will be used. The models in which the two approaches are combined will be called GBM.

Applicability of a WBM approach

For this project, access is granted to the documentation that was provided to the company from the shipyard and the system's manufacturers. A first overview was performed to the available documentation to gain an insight into whether the required information for a WBM approach is available.

As it was explained in Chapter 2, a WBM consists of sub-models accounting for every component of the propulsion chain. Regarding the modelling of the vessel's resistance (including the influence of environmental conditions), the already available models, proposed from other studies, require information about the main dimensions and the form coefficients of the vessel. This information can be collected from the documentation that was provided to the company from the shipyard. In addition, regarding the calm water resistance, self propulsion tests and sea trials are available (not for the full range of speed) and can be used for extra information. Thus, a sub-model for the total vessel's resistance (calm water resistance, wave added resistance, wind resistance etc.) can be developed.

On the other hand, in order to determine the overall performance of the propulsion plant, the machinery (propeller, gearbox, shaft, shaft generator, engine) should also be examined. However, the manufacturers do not offer detailed documentation neither for the design characteristics nor for the performance of these systems. For instance, the propeller's performance is provided for a narrow range of operating values and more specifically, only for 3 P/D values. Limited information are provided regarding the engine's performance while for the shaft, the PTO, and the gearbox there is no information.

It is concluded that the construction of a WBM for the vessel's operational performance, based on the principles described in Chapter 2, is possible, even though not all the required information is available. For the components where the required information is not available, findings from the literature can be used.

Applicability of a BBM approach

As was mentioned in section 1.2 within Spliethoff, a Performance Monitoring System (PMS) is implemented. This system is continuously collecting data from the operating systems onboard and convert them to useful information regarding the performance of the vessel. The system also performs some basic calculations to compute additional parameters from the measured data. The whole process is automated and for the data which are measured on board a data point is created every 5 minutes. The data is temporarily stored on board until it is sent in small groups to the shore every 1 hour. The data collected from the PMS is combined with weather information based on the time and the position of the vessel and they construct a new database. It is important to note that the weather data is not measured on-board but is provided by a weather provider. Thus, since the data which is stored in the PMS regarding the weather are based on weather models (and not actual measurements), it is expected that occasionally there will be deviation between the predicted and the actual weather conditions. However, a study was performed within the company and it was concluded that the accuracy of the weather data is sufficient for the type of the applications that the company is interested in [53].

Parameters such as draft and static trim are also stored in the aforementioned database. However, these parameters are not measured from the automated system every 5 minutes; instead, their values are collected from the Noon Reports (NR). An overview of the parameters for which there is available data (either measured, calculated, or externally provided) and are related to this project is given in Table 3.1. It should be noted, that there is not consistency in the measurement of the water depth. Some vessels use occasionally the water depth logger, whereas others do not. More information about the structure of the Performance monitoring system and about how the data are collected, transmitted and stored can be found in the research work of R.Grutterink [17].

The database contains data for the variables presented in Table 3.2, for about the last two years. Thus a vessel's performance model following the ML approach (BBM) can also be developed. It is important to note that the black box approach is relying entirely on the available data from the PMS, and thus the quality of the data is crucial. It is expected that in the PMS data errors will be present mainly due to the following reasons. The sensors that are used for the onboard measurements sometimes get damaged, and thus the recorded data are wrong. However, this issue can usually be identified relatively easily since the recorded values will be out of the range of the expected value (i.e. a value of 50 MW for the shaft power). In addition, the sensors tend to drift and calibration is required. However, if calibration is performed according to the intervals proposed from the manufacturer, not important issues are expected. Electrical noise and errors in data transmission, are also influencing the quality of the database. On the other hand, sensors provide a measurement with a certain inaccuracy. The accuracy of the sensors for which there is available information is presented in Table 3.2. It should be noted that these are the values which are provided from the sensors' manufacturers, and thus, it is expected that the actual accuracy will not perfectly match with the reported one. On the other hand, it should be mentioned that the sensors installed onboard are state of the art sensors from a reliable manufacturer, which automatically correct for effects caused from the temperature fluctuations. An example is the temperature's influence on the volume of the fuel, which is accounted automatically from the sensor. As it was aforementioned, the weather data are as well connected with uncertainty. For the case of the weather data, it is difficult to identify cases where the actual weather conditions do not match with those stored in the PMS.

Power	***Weather***	***Position***	***Noon Reports***
Shaft rpm	Currents speed	Latitude	Mean draft
Shaft torque	Currents direction	Longitude	Static trim
Shaft power	Wave height	Speed over ground	Draft fore
PTO power	Wave period	Heading	Draft aft
Main engine fuel flow rate	Swell height	Water depth	
Auxiliary DG fuel flow rate	Swell period	Speed through water(logger)	
	Total wave direction		
	Total wave height		
	Wind direction		
	Wind speed		
	Sea water temperature		

Table 3.1: Available data on the PMS database

Sensor	**Accuracy**	**Unit**
Fuel flow	0,2 %	Liters/min
Torque	0,25 %	Nm
Thrust	1 %	N

Table 3.2: Sensors' accuracy

However despite the aforementioned issues the most significant factor affecting the quality of the data stored in the PMS is the speed through water. Due to the fact that the speed loggers of the vessels present erratic behavior, it was decided within Spliethoff to use the calculated speed through water based on the speed over ground (from GPS) and the currents' data. However this does not solve entirely the issue with the quality of speed through water signal, since in this case errors occur due to the fact that the currents' data are not perfect. It should be noted that speed loggers with erratic behavior is not an issue only within Spliethoff. The case of erratic speed loggers is extensively described from Antola et.al [32], where a method to overcome this issue is presented as well, however this is out of the scope of the presented thesis.

The data about the currents is also provided from the weather provider. It is known within the company that the current's predictions are not accurate enough in areas close to the shore, areas enclosed by the shore (i.e. English channel, Baltic) and the East coast of North America due to the Gulf stream. The data points marked as E2 in Figure 3.4 correspond to a situation where the vessel was sailing through the English channel and the predictions about the currents were wrong. In this graph, it can be seen how bad predictions about currents result in wrong values about the speed through water. In addition, the datapoints marked as E1 is an example of outliers caused from incorrect measurements from the sensors, from electrical noise or from errors during the transmission.

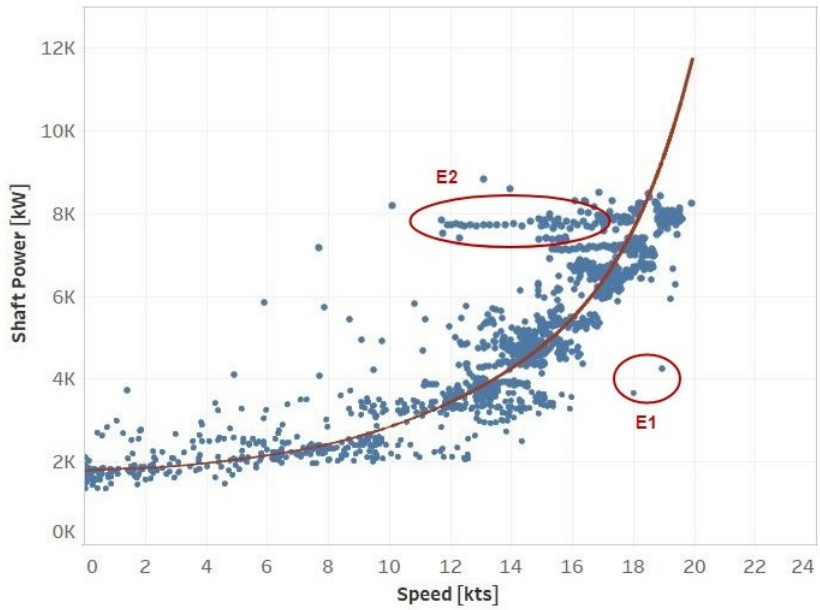

Figure 3.4: Shaft power measurements compared to the baseline

3.3. Vessel's performance model method selection

In the previous paragraphs, an overview of the available data was given. The outcome is that both a WBM and a BBM approach can be followed, and as a consequence, the same applies for a GBM. Since the data availability do not arise a restriction on the model selection, it is decided to develop both a WBM and a BBM. In addition, based on the WBM and the BBM, the GBM proposed by Leifsson et.al [30] and Coraddu et. al. [9], will be developed as well (the main principle of the GBM methods was discussed in Chapter 2 and schematic representation was given in Figure 2.1). By examining different methods (WBM, BBM, GBM), answers will be given to questions such as, which method leads to more accurate results, which model is faster, which model is more suitable for the company's needs, and is the performance of the models in agreement with the literature findings.

A decision has to be made regarding the variables and the effects that will be included in the model. In figure 3.5, we can see a simplified diagram with the main variables affecting the required power that is needed to drive the ship through the water at a certain speed. The shaft and the gearbox are not depicted in the diagram as their losses usually are taken into account as constant. We can see that there are effects for which the required parameters are not measured and so they cannot be taken into account, or a different method should be followed in order to do so. For instance, the added resistance due to course keeping effort/ steering can be estimated if the rudder angle is known. However, this value is not measured from the automated logging system and makes the estimation of this resistance component more difficult. The same situation is observed regarding the hull and propeller fouling. Regarding the state of the hull and propeller fouling is not an available information, as the evaluation software that is used does not give a clear indication about it. Spliethoff representatives estimate that fouling on this ship type has limited influence in the S-type vessels, as they are sailing in high speeds and often in ice conditions fact, which helps to the removal of marine plants and bacteria from the propeller and the wetted surface of the hull. Finally, the effects of poor maintenance and aging of the machinery can not be taken into account as there is no available information.

In addition, it should be noted that as it was mentioned in Chapter 1, the vessel's performance model will be incorporated to the voyage simulation algorithm in order to make calculations of the fuel consumption for future voyages, taking into account the weather predictions. Thus, the inputs that will be used in the performance model should be possible to be predicted for a future voyage.

The effects that will be taken into account in the model will be explained in more detail in the next chap-

ter. In addition, reasoning will be provided for the components which will not be taken into account.

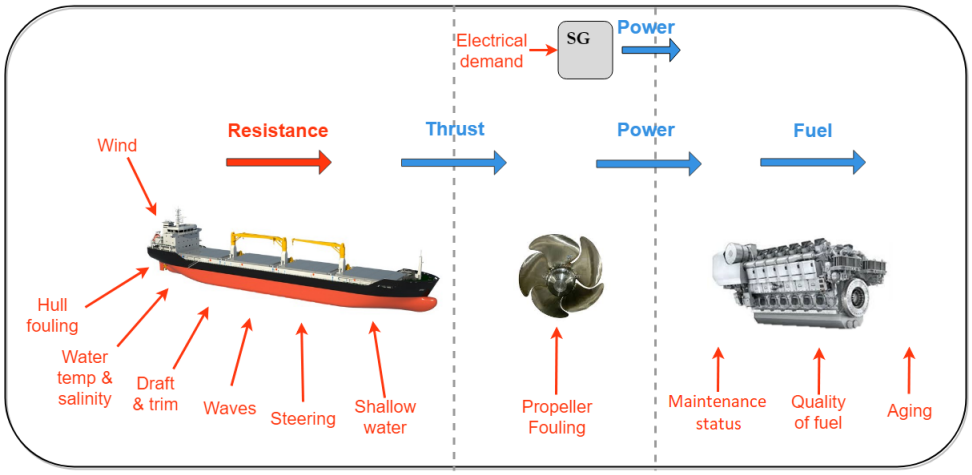

Figure 3.5: Power decomposition

3.4. Voyage simulation algorithm method selection

A significant amount of research is performed in the area of voyage optimization. An extensive review can be found in the work of Psaraftis et.al. [40]. Many studies have proposed methods to optimize speed or route for a trip to minimize the costs, while some researchers treat both route and speed, as controlled variables for a more generic solution. However, these studies are out of the scope of this project. The focus of this research is to develop an accurate vessel's performance model. As a second step, a simple algorithm will be developed to calculate the overall fuel consumption under a given route. This algorithm will incorporate the performance model and will enable the examination of future voyages or reproduction of old ones, under different inputs (i.e. speed, route). Thus, the voyage simulation algorithm can be seen as a secondary tool that will be developed to contribute in the process of proving the value of the performance model within the shipping company.

The algorithm will be receiving as input the route (waypoints) that has to be followed, the desired speed profile, and the loading conditions (draft and trim). Based on the weather predictions offered by the weather provider, and by making use of the vessel's performance model (which will have been already developed), a calculation of the fuel consumption for the entire trip will be performed. It is essential to mention that the desired speed in some cases (i.e harsh weather conditions) might not be possible to be attained and so a strategy should be decided on how this situation will be treated. It is expected that the route will have to be constrained to the part that the vessel is under normal operation and not when the ship is maneuvering, as the performance model will not be able to make accurate predictions for the fuel consumption under these circumstances. A flowchart for the calculation algorithm is presented below (Wactive corresponds to active waypoint).

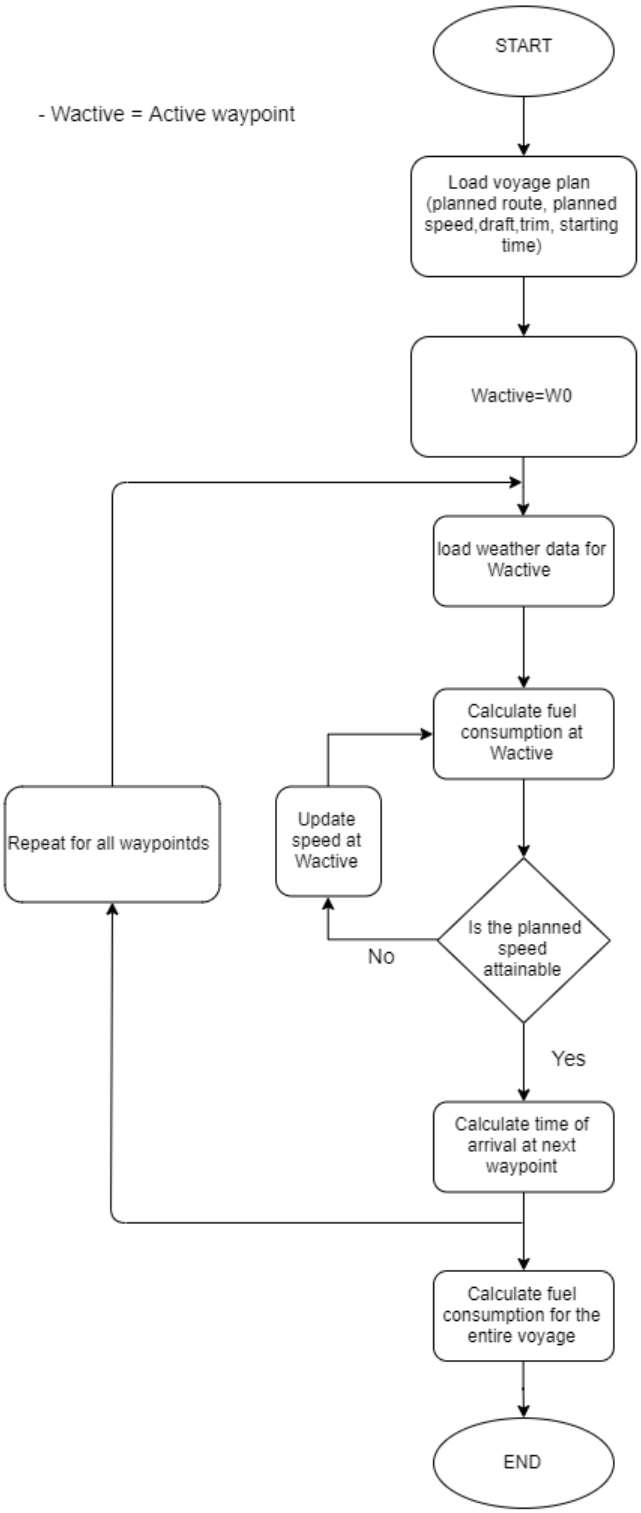

Figure 3.6: voyage simulation algorithm flow chart

4

WBM development

In this chapter the development of the WBM will be described. Initially, the structure and the components of the WBM will be presented. Following, the available information related to the model development will be discussed. All the components will be presented and the methods used in the development will be explained. Finally, the accuracy of the model will be examined.

4.1. WBM structure

An introduction to the WBM was given in Chapter 2. In this paragraph, more information will be presented about the structure of the model that will be developed in this research. A step-by-step approach will be followed, and every component, which is part of the system, will be examined separately. In Figure 4.1 the structure of the model is presented.

In order to calculate the fuel consumption, which is the final output of the model, the following steps should be performed. Initially, the calm water resistance should be determined based on the sailing conditions of the vessel (speed, draft, trim). Then, the added resistance due to waves, wind, and shallow water should be calculated. When the total resistance of the vessel is known, the thrust that the propeller should deliver can be calculated. Following, from the open water diagram, the operating point of the propeller can be determined, and the required shaft power can be calculated. If the shaft's efficiency, the gearbox's efficiency, and the electric power demand from the PTO are taken into account, the required power from the engine can be determined, and finally, the fuel consumption can be derived.

The parameters influencing a vessel's fuel consumption were presented in Figure 3.5. However, as it is presented in Figure 4.1, some effects were not taken into account in the model to be developed. The main reasons for that are the following. As was mentioned before, in some cases, the required input values are not known. An example is the added resistance due to course keeping effort for which the rudder angle should be known in order to be estimated; however, this parameter is not stored in the PMS. In addition, as was aforementioned, the model will be incorporated into the voyage simulation algorithm, which will calculate the fuel consumption for a future voyage. Thus, the inputs which are given in the model should be possible to be predicted for a future voyage. The simplifications that were made are the following. Influence from fouling was not taken into account since Spliethoff's representatives estimate that fouling is not a significant influence for the S-type vessels. The influence of the steering effort in the resistance, the aging of the engine, the quality of fuel that is used, and the maintenance status were not taken into account since there is no available information. The influence of the water temperature is also ignored since it has a minor influence. More specifically, the influence of the temperature difference on the resistance is estimated to be less than 2.5 % compared to the reference condition of 15 °C [6].

Figure 4.1: WBM structure

4.2. Available documentation

In this paragraph, an overview of the vessel's available documentation, which is relevant to the model development will be given. Regarding the resistance of the vessel, the company has in possession self-propulsion tests which were performed from HSVA [1]. The model was tested in three different drafts, for a limited range of speeds. In addition, a CFD study was performed in 2018 from WESTCON [2] in order to investigate the influence of the trim in the resistance/power demand. Results were provided for three drafts, and in each case three speed values were tested and four trim values. The aforementioned reports will provide useful information regarding the resistance of the vessel and the propeller-hull interaction coefficients. The propeller's open water tests were performed from the Nagasaki Experimental Tank [3]. Three pitch ratio values were tested, and the available results do not cover the full range of advance coefficient values. More information about the conditions that were tested in all the aforementioned tests can be seen in Tables 4.1-4.3.

CFD test		
Draft [m]	**Speed [kts]**	**Trim [m]**
6.7	12.5/15.5/17.5	0/0.4/0.8/1.5
9	12.5/15.5/17.5	-0.5/0/0.7/1.4
10.25	12.5/15.5/17.5	-0.5/0/0.7/1.4

Table 4.1: Conditions tested in CFD

[1] Hamburg Ship Model Basin
[2] WESTCON is a maritime engineering company in Poland, subsidiary of WESTCON shipyards
[3] Mitsubishi Heavy Industries

Self propulsion test		
Draft [m]	**Speed [kts]**	**Trim [m]**
6.75	16.5-21.5 with 0.5 step	1.5
10	18-20.5 with 0.5 step	0
10.65	16-20.5 with 0.5 step	0

Table 4.2: Conditions tested in self propulsion test

Propeller open water test	
Pitch (0.7R)	**J**
0.3878	0.19-0.31
0.6934	0.33-0.55
1.0521	0.52-0.85

Table 4.3: Conditions tested in open water diagram

4.3. WBM development

4.3.1. Propeller

The S-type vessels are equipped with a 6.2 m diameter Controllable Pitch Propeller (CPP). As can be seen in Figure 4.2, the results from the open water tests provide limited information for the efficiency of the propeller. The propeller's performance was only examined for three values of pitch ratio (P/D) and not for the full range of the advance coefficient (J).

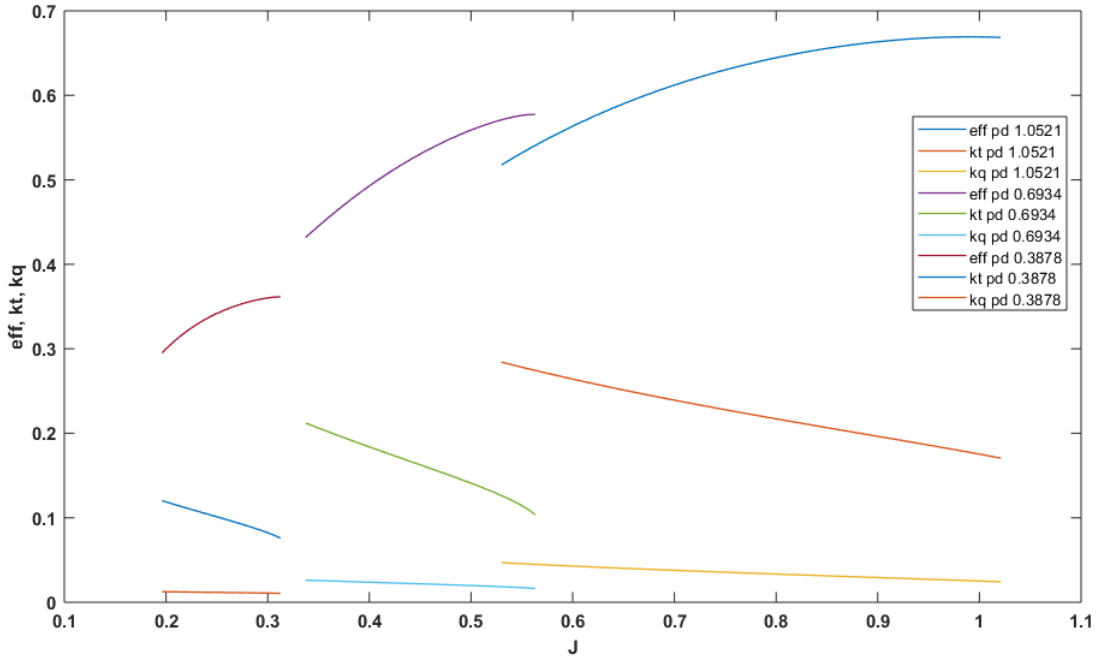

Figure 4.2: Open water test results

It is clear that, based on this information only, the development of a detailed model for the propeller is not possible. The procedure that was followed for the propeller's model development is presented in Figure 4.3.

The S-type propeller's performance will be compared to that of the Wageningen B-series for equivalent pitch ratios (and geometric characteristics) to examine whether the B-series performance characteristics can be used as a basis for the propeller model. For the reproduction of the performance characteristics of the Wageningen B-series, the equations reported by Oossanen [50] were used. The results are presented in the Figures 4.4-4.6.

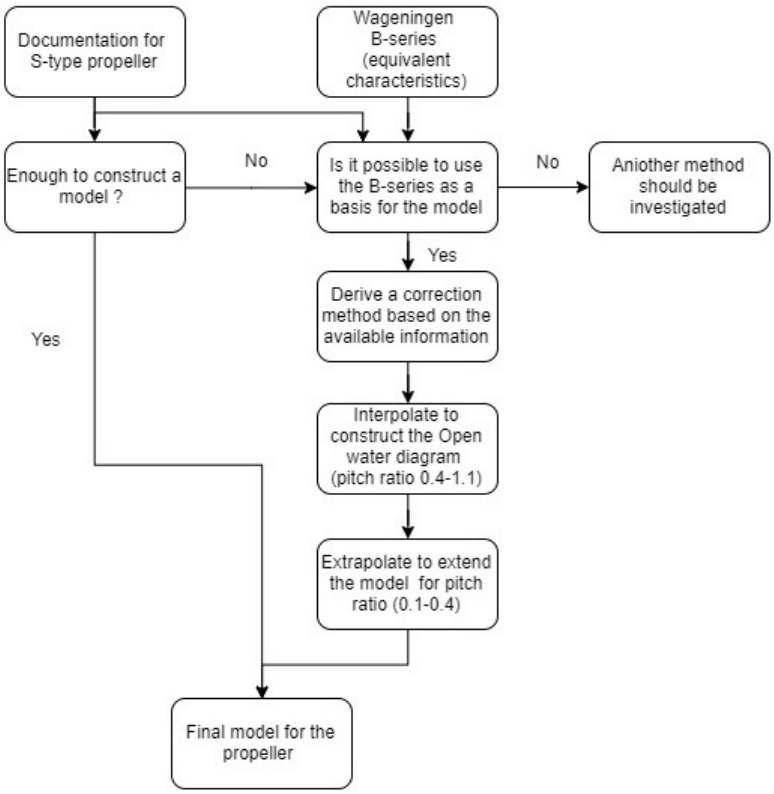

Figure 4.3: Procedure for the development of the propeller's model

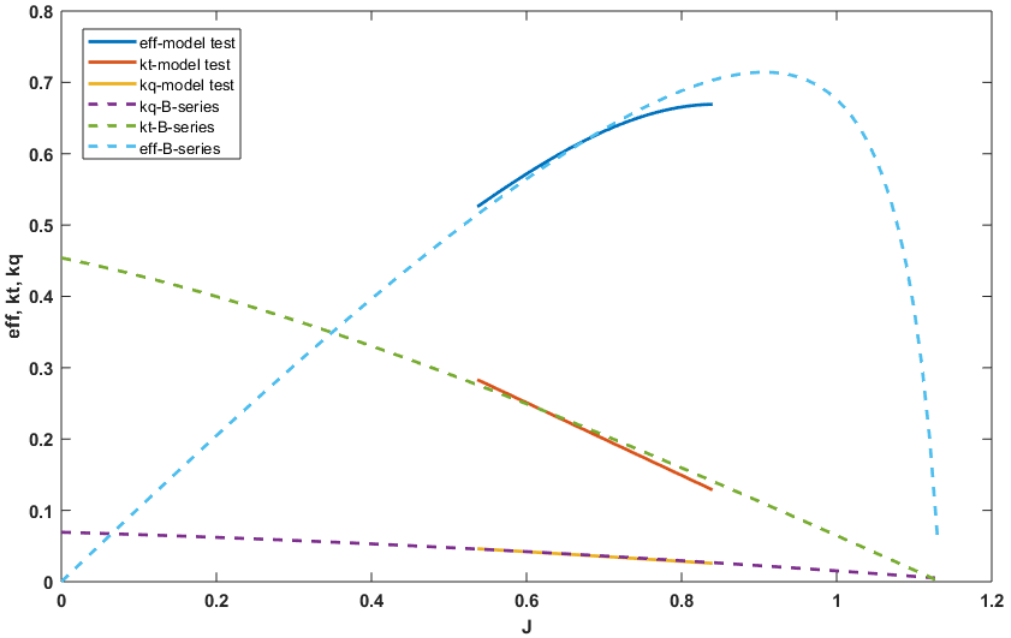

Figure 4.4: B-series and S-type propeller performance characteristics comparison (pitch ratio 1.0521)

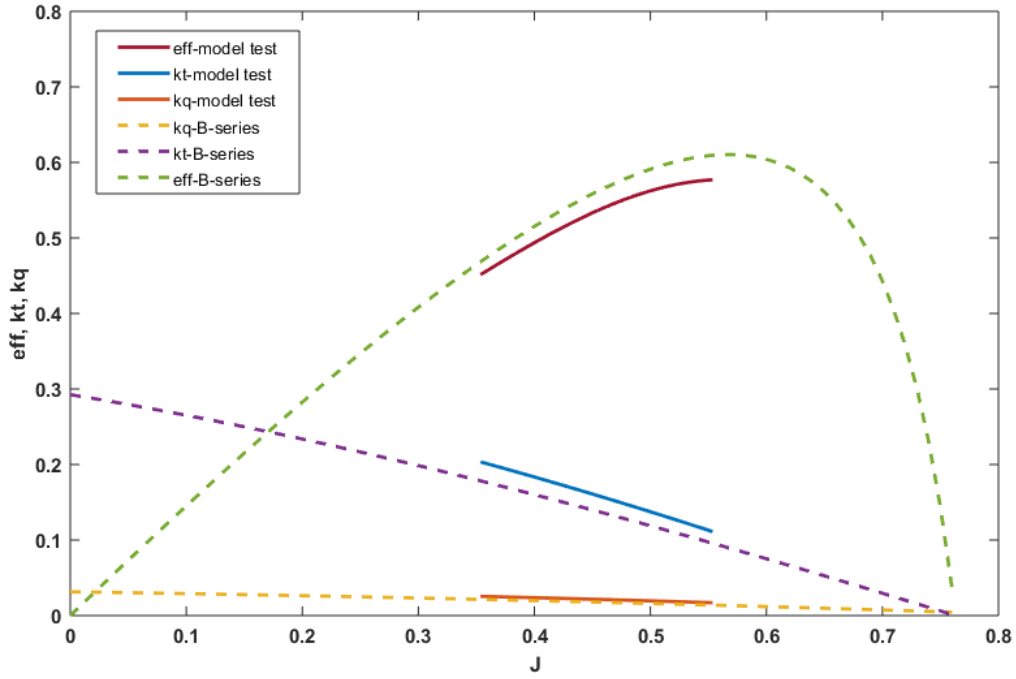

Figure 4.5: B-series and S-type propeller performance characteristics comparison (pitch ratio 0.6934)

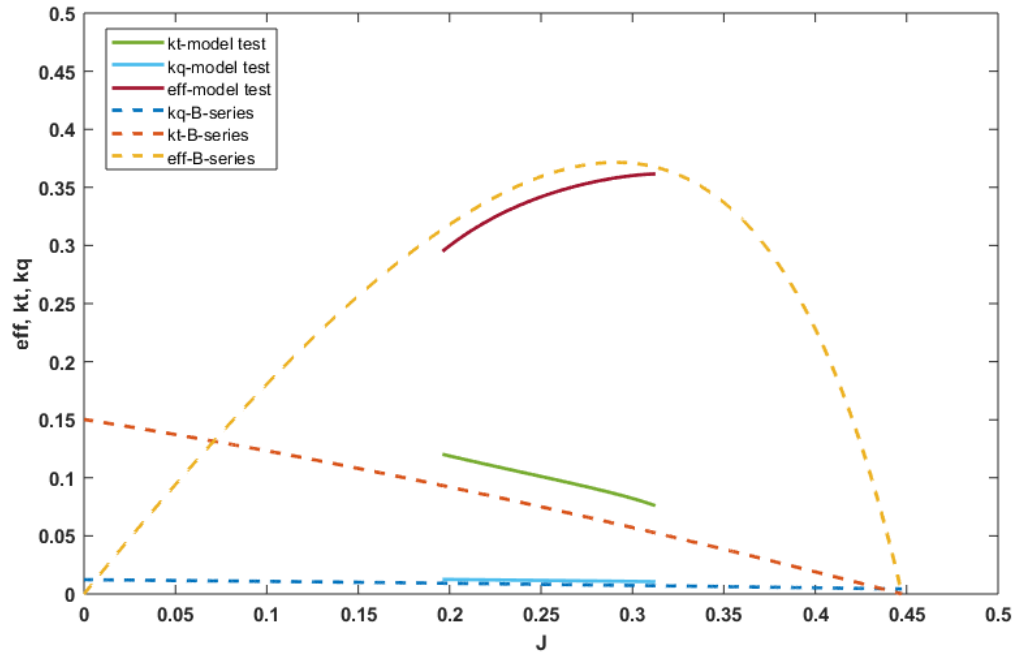

Figure 4.6: B-series and S-type propeller performance characteristics comparison (pitch ratio 0.3878)

From the information presented in Figures 4.4-4.6, it was decided that the Wageningen B-series could be used as a basis for the propeller's model. A correction factor was applied in order to adjust for the performance differences between the B-series and the S-type propeller. To derive the correction factor that should be applied in every case (depending on the advance coefficient and pitch ratio), the results of the open water tests of the S-type propeller were used (Figures 4.4-4.6). Based on the difference between the kt, kq of the S-type propeller and those of B-series a correction factor was derived for both parameters (kt, kq) for all the three pitch ratios. In order to cover the full range of J, an extrapolation was performed and then an

interpolation to cover the full range of pitch ratios. In Figures 4.7-4.8, the correction factor which were used for the kt and kq versus the advance coefficient and the pitch ratio are presented. In the z axis the correction factor is plotted expressed in percentage. The calculation of the correction factor is performed based on the following equation (for the case of kt). The correction factor for the kq is calculated in the same way.

$$kt_{difference} = \frac{kt_{Stype}(J, P/D) - kt_{Bseries}(J, P/D)}{kt_{Bseries}(J, P/D)} \tag{4.1}$$

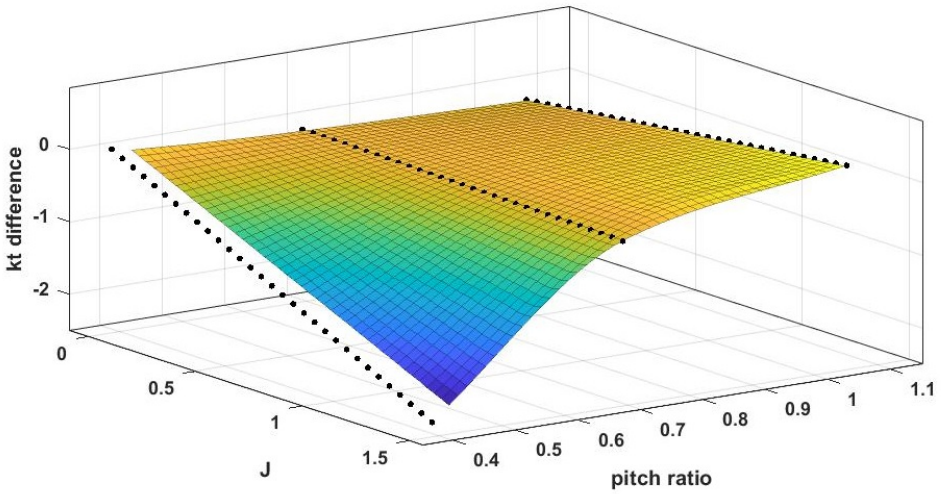

Figure 4.7: Surface for kt adjustment

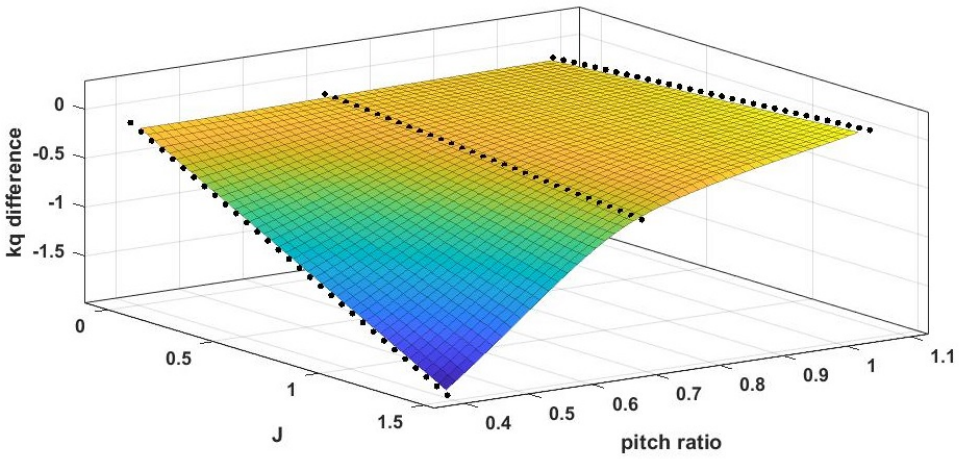

Figure 4.8: Surface for kq adjustment

By making use of the correction factors presented above, the open water diagram was created for the S-type propeller, for pitch ratio values within the range of 0.4-1.05. An example is presented in Figure 4.9, where the the performance characteristics are plotted for 14 pitch ratios.

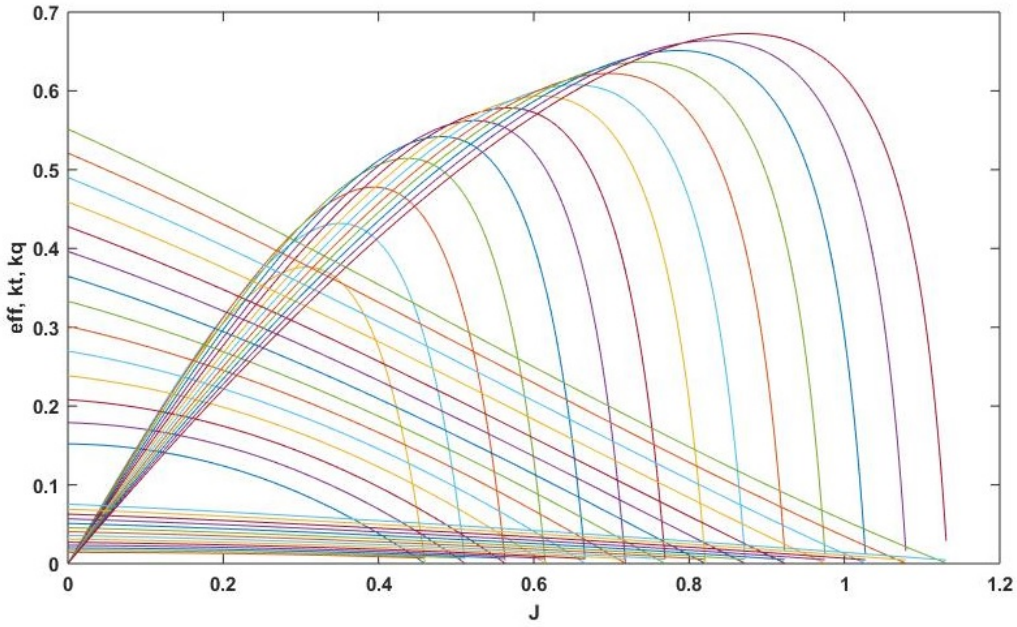

Figure 4.9: Open water diagram for 14 P/D values

Afterwards, the water diagram had also to be extended in pitch ratios lower than 0.4. For the S-type vessels the 0.4 pitch ratio value corresponds to the speed of around 12 knots. Thus if the model was not extended, situations, where the ship's speed was lower than 12 knots, would not be possible to be assessed. For this reason the kt, kq values should be extrapolated for lower pitch values. In order to identify which extrapolation method is the most suitable one, the diagram of kt,kq, versus the pitch ratio were created for several J values. An example is presented in Figures 4.10,4.11, which corresponds to J equal to 0.1 . The conclusion was that a linear extrapolation can be used for the kt values while a second-order polynomial extrapolation for the kq values (Figures 4.12,4.13). Thus with an iterative process an extrapolation was performed for all J values.

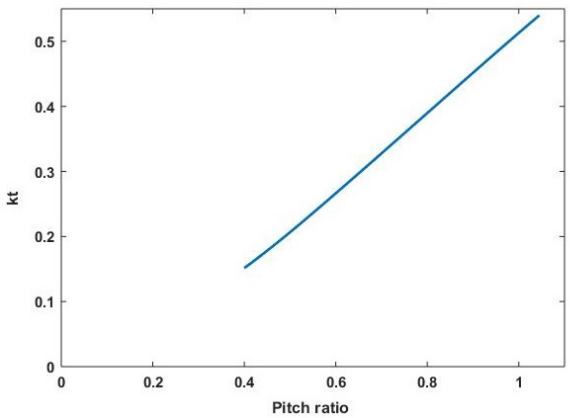

Figure 4.10: kt versus pitch ratio at J=0.1

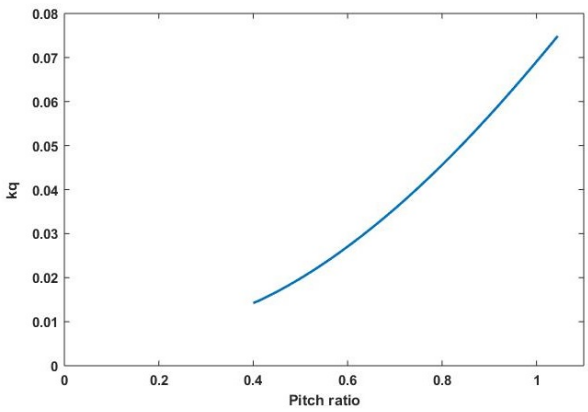

Figure 4.11: kq versus pitch ratio at J=0.1

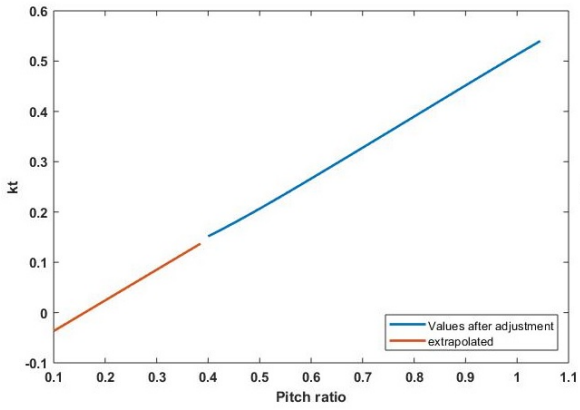

Figure 4.12: extrapolation of kt at J=0.1

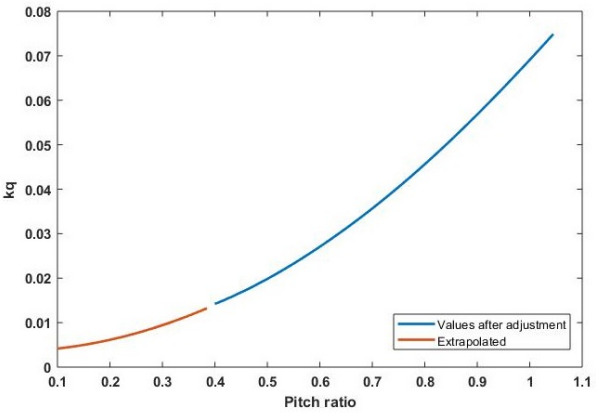

Figure 4.13: extrapolation of kq at J=0.1

Finally, based on the procedure presented above, the open water diagram of the S-type propeller was created using as a basis, the performance characteristics of the Wageningen B-series propellers, after applying correction factors on kq and k_t. The performance characteristics can be created for any selected number of pitch ratio values. In the Figure below, the open water characteristics are presented for 45 pitch ratio values. It is important to examine the accuracy of the propeller model since, due to the interpolations and extrapolations, it is possible that the model does not meet reality. This will be done in a later stage when the estimated, by the WBM, results for the shaft power will be compared to the shaft power measurements available from the PMS.

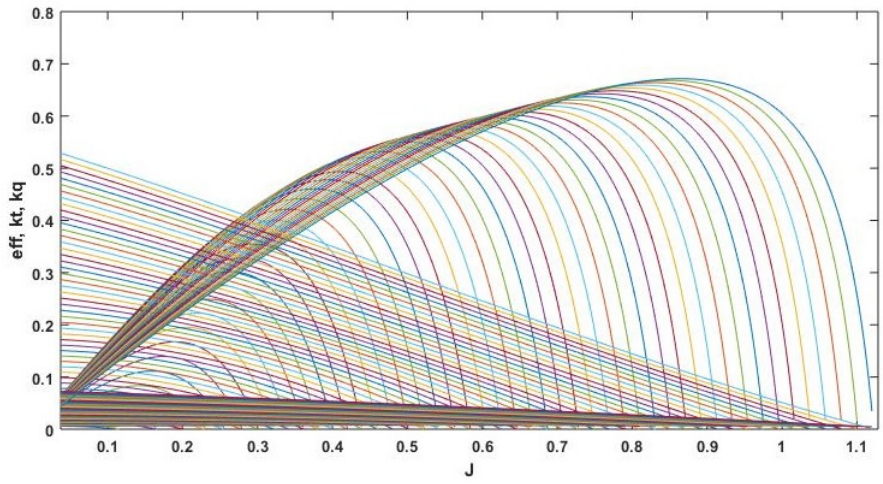

Figure 4.14: Open water diagram for 45 pitch ratio values

4.3.2. Propeller-Hull interaction coefficients

Wake fraction

The available information from the model tests and the CFD test regarding the wake fraction is presented in Figure 4.15.

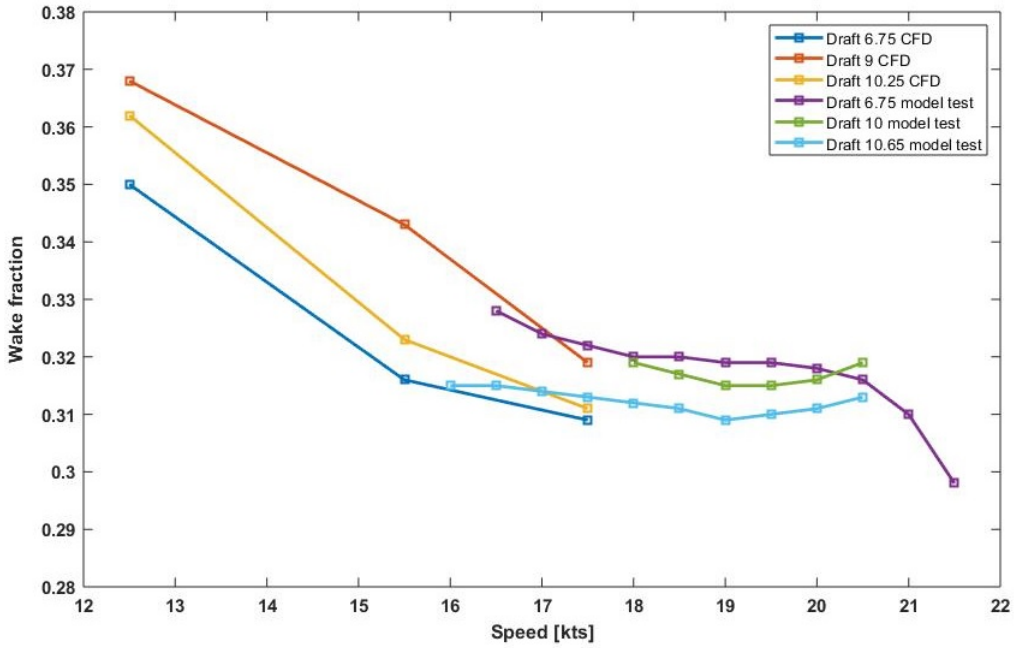

Figure 4.15: Wake fraction versus speed (available information)

According to Molland et al. [33], lower values are expected for the wake fraction as the speed is getting higher. Additionally, the same applies to the dependency on the draft, meaning that for a higher draft, a lower value is expected for the wake fraction. The latter is also reported from Journee [23] based on results from the model tests of a containership (performned by HSVA). It can be seen in Figure 4.15, that the results do not match with the literature findings [33]. The results from the CFD test present high variation versus speed. Similarly, the relation with the draft is not either as it is described in relevant literature [33]. However, an equation for the wake fraction as a function of the draft and speed cannot be developed completely based on the results of the model tests. The results based on the equation proposed from Holtrop and Mennen [20] are also compared to the results from the model tests and the CFD. An example can be seen in Figure 4.16.

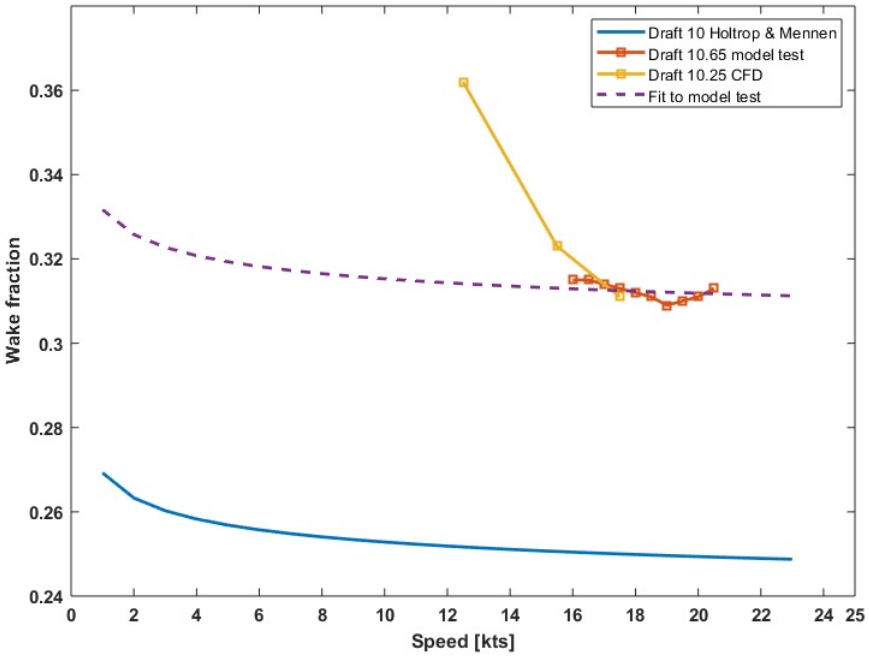

Figure 4.16: Wake fraction versus speed (fitted equation to be used)

In Figure 4.16, it is more clear that the CFD results present strong dependency with the speed. On the other hand, it is observed that the trend followed from the results of the model test is similar to the one from the results based on Holtrop and Mennen [20], despite the fact that there is a difference of about 25% between the values. It was decided to fit a curve to the results of the model tests to reproduce the trend observed in the results based on Holtrop and Mennen. In Figure 4.16 the fitted curve can be seen. This curve will be used for the wake fraction estimation at the draft of 10.65 m. The correction for different drafts will be done according to the equation proposed from Moor et al. [34], which is presented in the Appendix A. It should be noted that the influence of an overloaded propeller to the wake fraction was neglected (the same applies in the case of thrust deduction factor which is examined in the following section).

Thrust deduction factor

The available information from the model tests and the CFD test regarding the thrust deduction factor are presented in Figure 4.17.

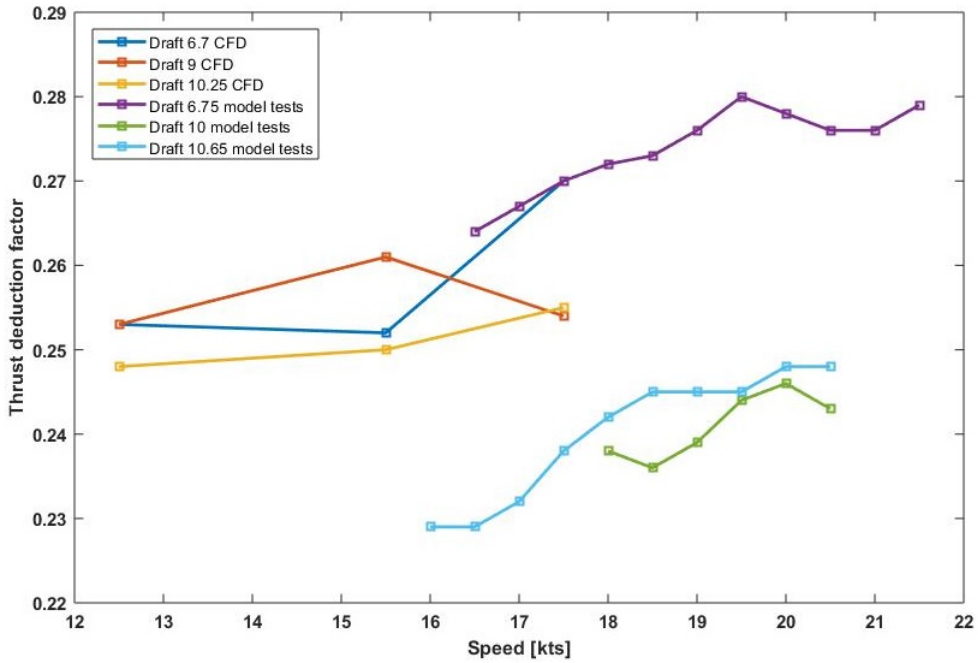

Figure 4.17: Thrust deduction factor versus speed

In the book of Molland et al. [33] the dependency of the thrust deduction factor to the speed is not discussed, and only the dependency to the draft is presented according to the equation proposed from Moor et.al [34]. In addition Holtrop and Mennen [20] proposed an equation which is independent of the speed. However in the literature there are studies in which a dependency of the thrust deduction factor to the speed is presented [27]. On the other hand, Journee [23] used again results from model tests to take into account the thrust deduction factor on the draft without considering a dependency on the speed.

For the wake fraction it is decided that a linear fit to the results of the model test at the draft of 10 m will be used (as presented in Figure 4.18) and the dependency to the draft will be taken into account by the equation proposed by Moor et al. [34].

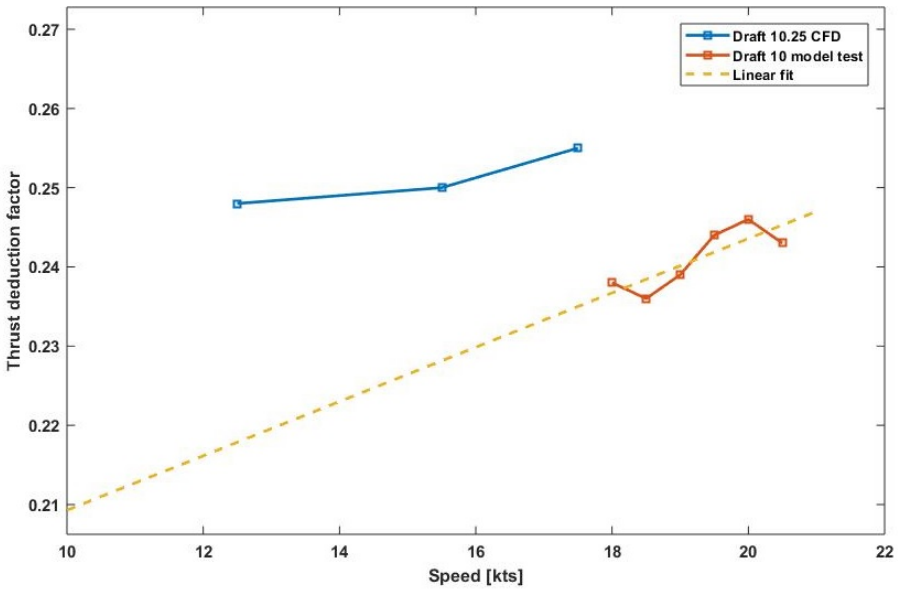

Figure 4.18: Thrust deduction factor versus speed

4.3.3. Relative rotative efficiency

The available results for the relative rotative efficiency are presented in Figure 4.19. The variance observed between the different draft is not considered important. The dependency to the speed will be taken into account with a linear fit to the results of 10 m draft.

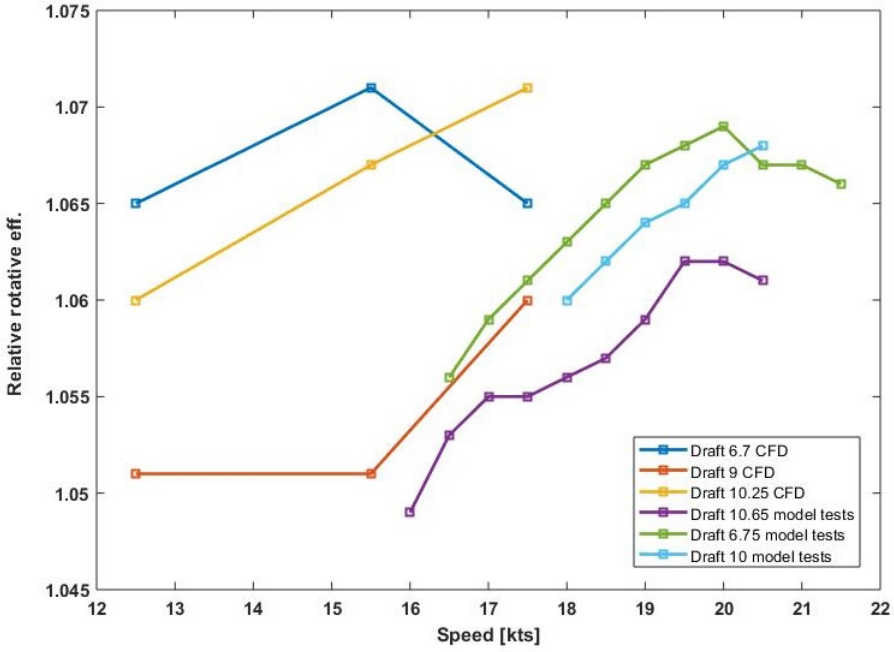

Figure 4.19: Relative rotative efficiency versus speed

4.3.4. Matching code

The matching code is an algorithm which was developed in order to find the operating point of the propeller. The propeller of the S-type vessels due to the configuration of the propulsion plant is rotating fixed at 105 rpm. Thus the matching code finds the pitch ratio for which the propeller will provide the required thrust. In addition, the efficiency of the propeller at the certain operating point is determined and thus the required shaft power can be calculated. The method that is implemented in the algorithm is the one proposed from Klein Woud and Stapersma [26].

4.3.5. Calm water resistance

The calm water resistance model should be able to provide an accurate estimation of the vessel's resistance for the input parameters which are the speed , the draft and the trim. A convenient way to create the resistance model would be based on the Holtrop Mennen method [21]. The Holtrop Mennen method is a statistical method for the resistance prediction of displacement hulls, developed from the analysis of a large number of model tests. This method is a handy solution as it can be used to create resistance curves for the full range of speed and draft. However, due to the fact that the Holtrop Mennen method is a statistical method, consisting of many regressions based on the main shape coefficients of the vessel, it's accuracy for an implementation on the S-type vessels had to be examined. Thus the Holtrop Mennen method was applied for the same drafts that the model tests were performed and the results were compared (as presented in Figures 4.20-4.22).

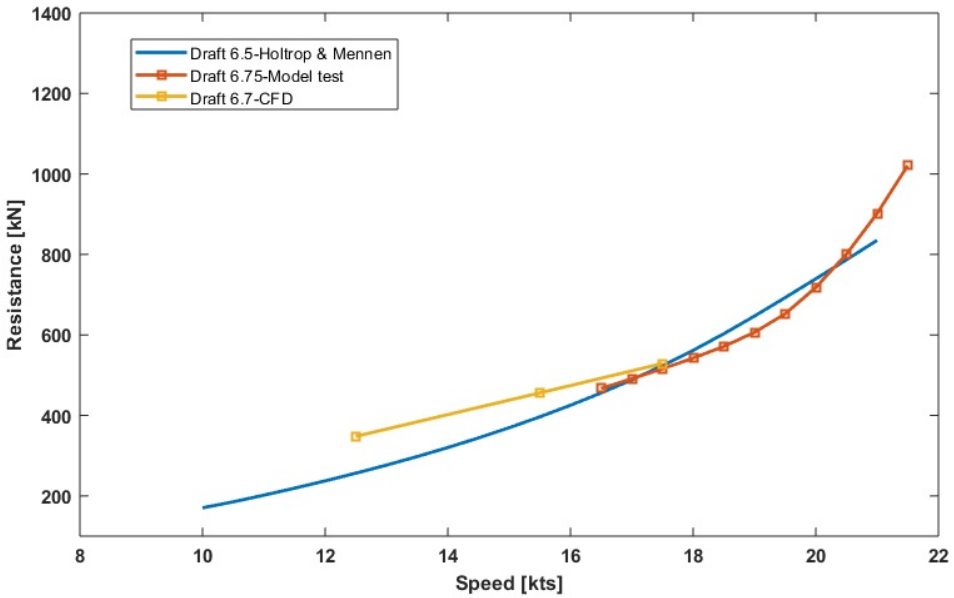

Figure 4.20: Resistance at 6.75 m draft (available documentation)

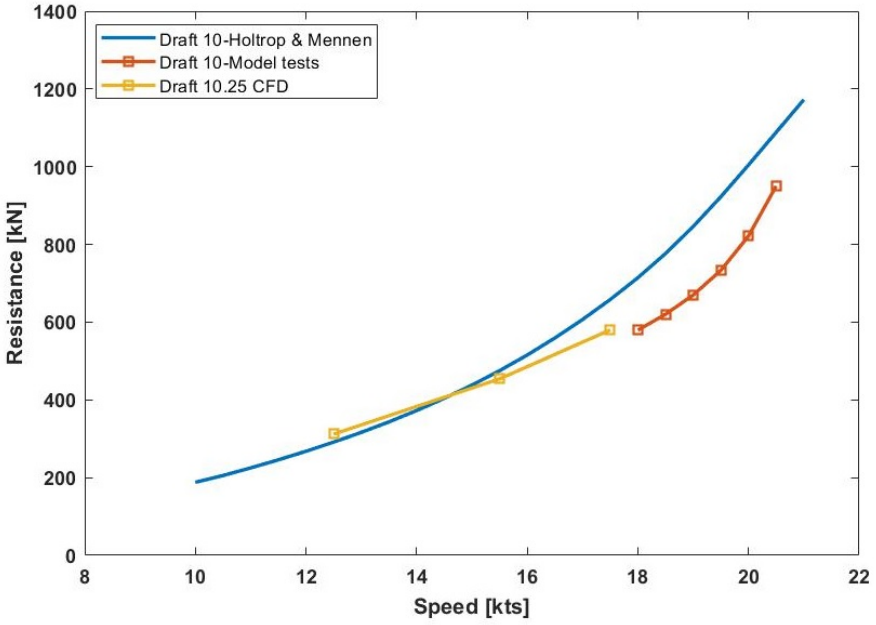

Figure 4.21: Resistance at 10 m draft (available documentation)

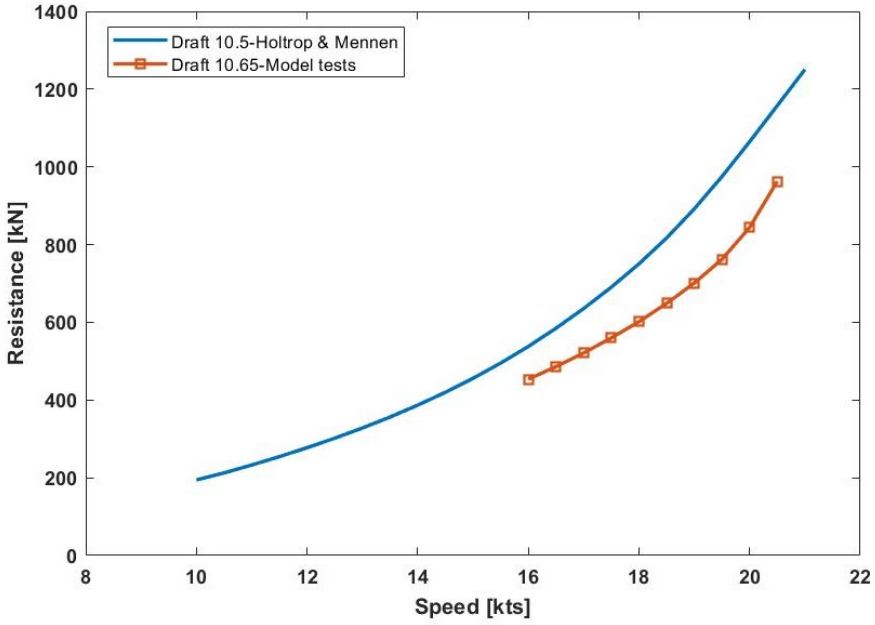

Figure 4.22: Resistance at 10.65 m draft (available documentation)

The conclusion was that that the Holtrop Mennen [20] method overestimates the resistance of the S-type vessels (about 25% in the speed range 18-20 kts) and thus cannot be used for the resistance estimation. A possible solution would be to use a correction factor to adjust the results from the Holtrop-Mennen method in order to match with the results from the model tests. However, it is clear from the graphs that the two curves (model test and Holtrop Mennen) have a different shape, and thus a correction method will not be easily derived. The complex adjustment, reverses the advantage of the Holtrop Mennen method, which is that it can be applied easily for the full range of speed and draft. Thus, it was decided that the model tests will be used, with the drawback that model tests are available only for 3 drafts and for a limited speed range. Thus a method to create a model for the resistance, which will cover the full range of draft and speed should be found.

Extension of calm water resistance curves for lower speeds

In order to extend the resistance curves from the model tests, at lower speeds, the steps of the procedure depicted in Figure 4.23 were followed. The presented procedure was performed for all the three available resistance curves from the model tests.

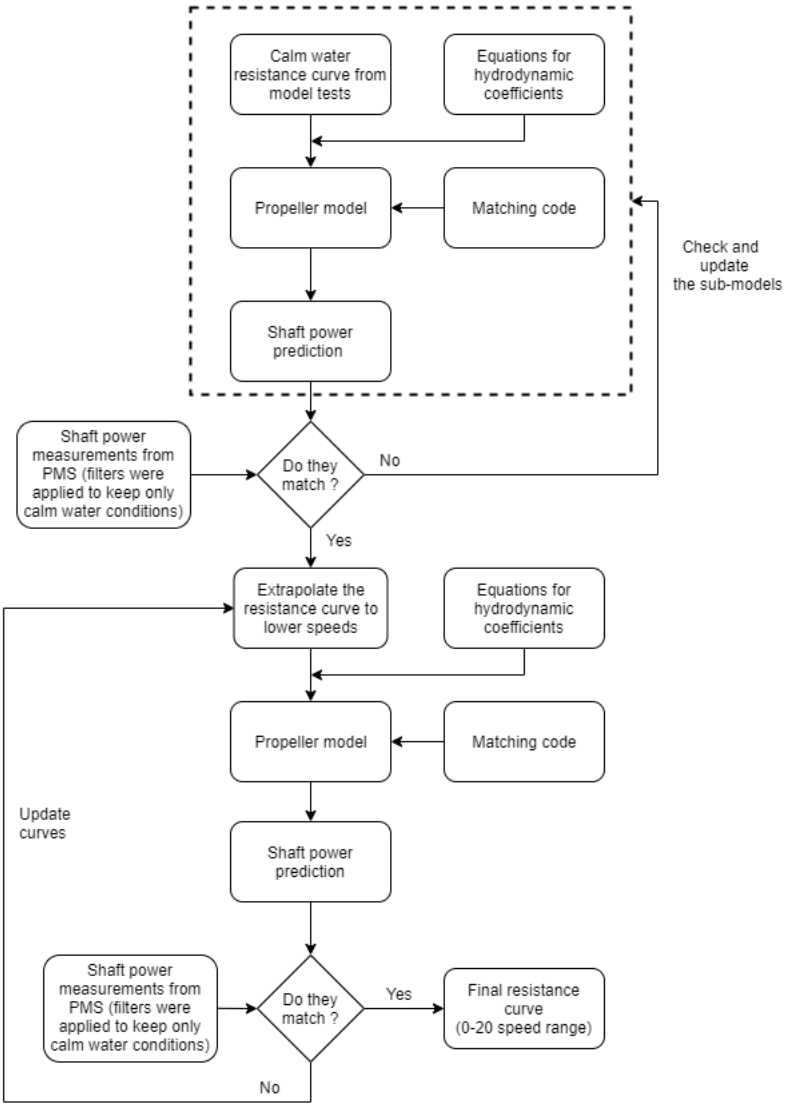

Figure 4.23: Procedure followed for the extension of the resistance curves

Firstly, the already developed components of the WBM (propeller model, matching code, equations for hydrodynamic coefficients) were used in combination with the resistance curves from the model tests (as presented in Figures 4.20-4.22), to calculate the corresponding shaft power curves. Then, each calculated shaft power curve was compared with the shaft power measurements available from the Performance Monitoring System. It is important to note that filters were applied to the data from the PMS in order to filter out data points which correspond to different draft than the one examined in each case (in each case data points which correspond in drafts ±0.25m of the draft under examination were filtered out). The data points were also filtered in order to include only the calm water conditions (data points which correspond in wave height higher than 1 m were filtered out).

The comparison is presented in the following Figures 4.24 - 4.26. It can be seen that the calculated shaft curves lie within the cloud of the measured shaft power (data from PMS). In addition, the calculated shaft power values are close with the measurements from the sea trials, as it can be seen in Figure F.1 presented in Appendix

F. Thus it was decided to extrapolate the resistance curves to lower speeds and use the propeller model, the hydrodynamic equations and the matching code to calculate the corresponding shaft power curves. Then, by comparing the shaft power curves (resulted based on the extrapolated resistance curves) with the measured shaft power data from the PMS, the final resistance curves (for the speed range 0-20 kts) were derived after some iterations. The final resistance curves are presented in Figure 4.27. In addition, the calculated shaft power, for the extended resistance curves, are presented in Figures 4.28-4.30, where shaft power measurements (for equivalent conditions) from the PMS are presented as well. Further examination about the agreement between the calculated (by the WBM components) shaft power curves with the shaft power measurements from the PMS will be performed after the extension of the model in the full range of draft.

In Figure 4.24, which corresponds to the case of 6.75 m draft, it is observed that the calculated shaft power curve lies closer to the center of the cloud compared to the cases of 10 m and 10.65 m draft (Figures 4.25-4.26. Perhaps, this can be explained due to the fact that the resistance curve of the 6.75 m draft, corresponds to a trimmed (1.5 m by stern) condition. This will be further examined after developing the trim model, based on which the trimmed resistance curve will be converted to zero-trim conditions.

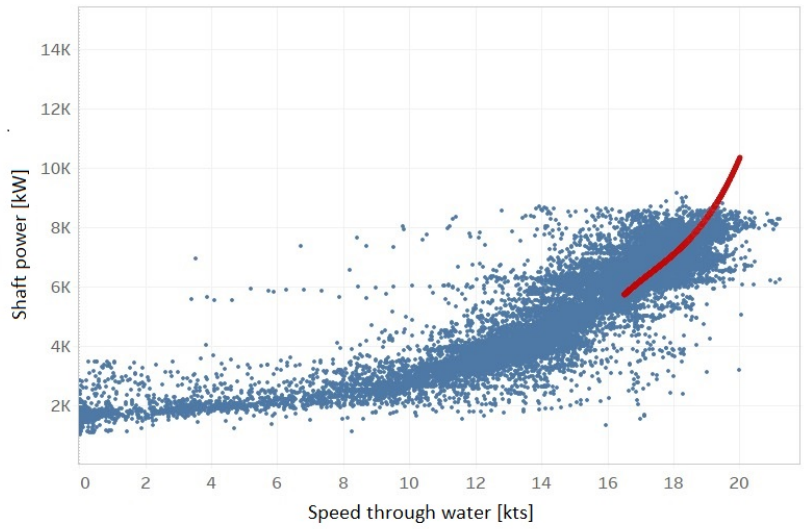

Figure 4.24: Shaft power estimated (based on resistance model tests results) and measured values (draft 6.75 m)

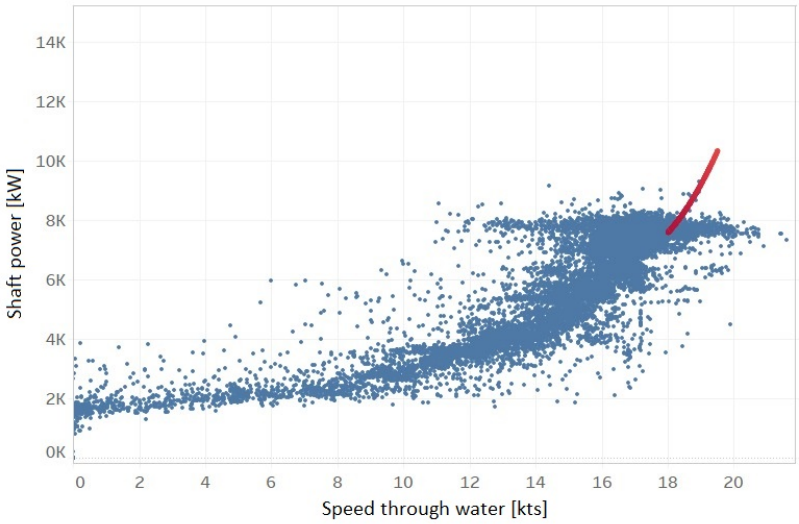

Figure 4.25: Shaft power estimated (based on resistance model tests results) and measured values (draft 10 m)

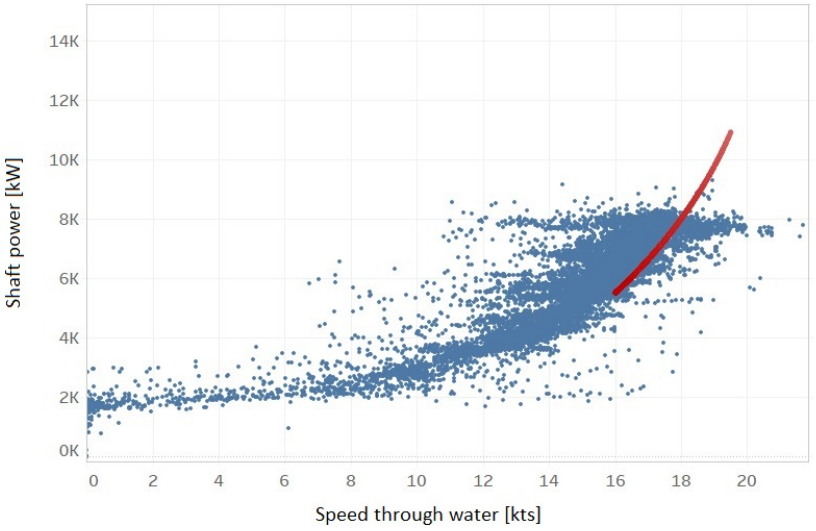

Figure 4.26: Shaft power estimated (based on resistance model tests results) and measured values (draft 10.65 m)

Various curves were examined for the extension of the existing resistance curves in lower speeds. The propeller model, the matching code and the equations for the propeller-hull interaction coefficients were used to assess whether the proposed curves for the extension in lower speeds resulted in shaft power estimations which are in agreement with the real measurements. In other words, various equations were fitted to the model tests and for each attempt the corresponding shaft power curve was estimated. Then, every shaft power curve was compared with the real measurements and finally the curve which fitted the best with the real measurements was selected. This procedure was performed for all the three available resistance curves.

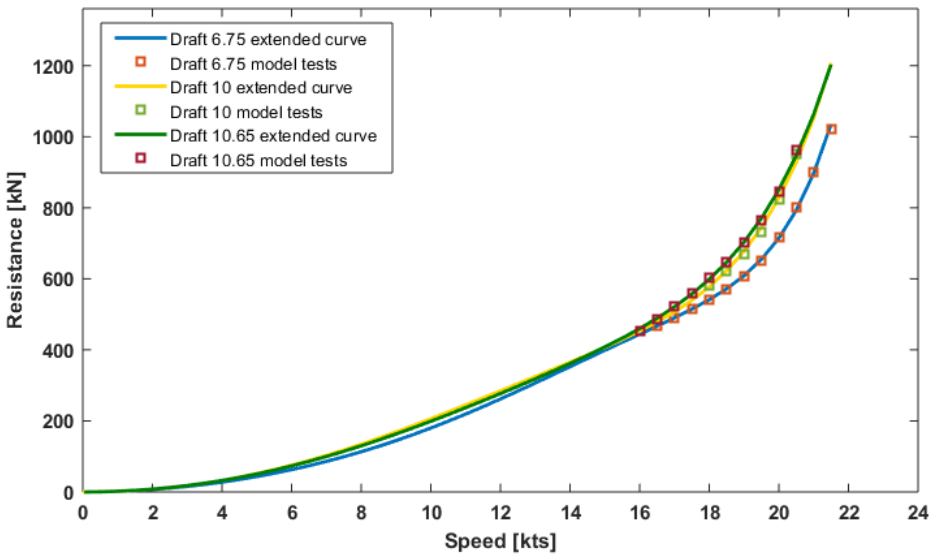

Figure 4.27: Extended resistance curves

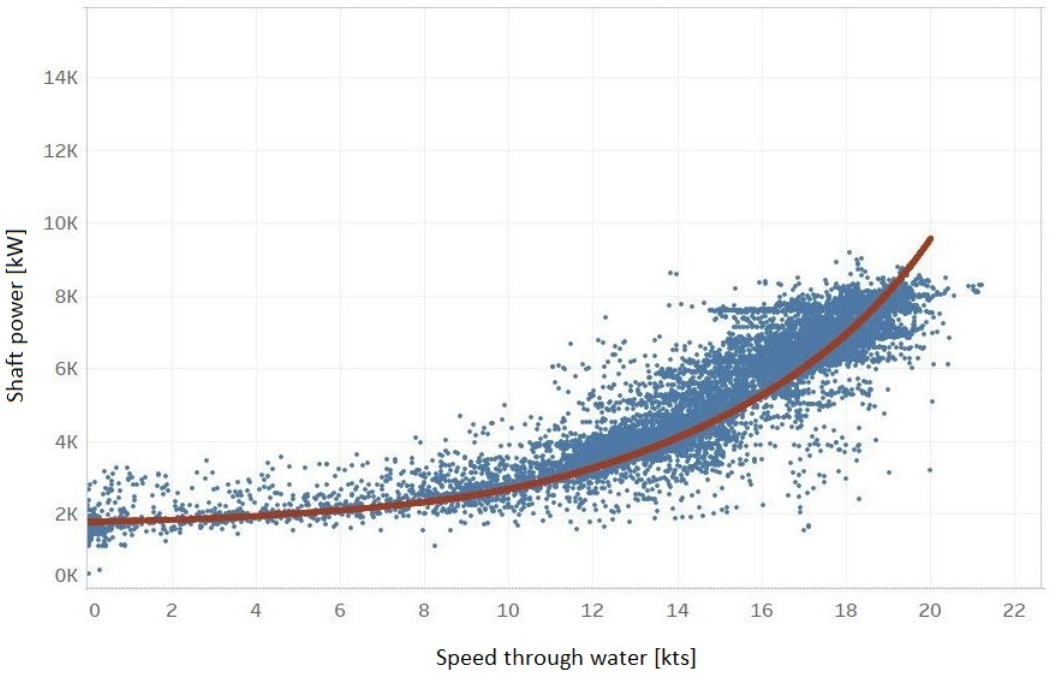

Figure 4.28: Shaft power estimated (based on extended curve) and measured values (draft 6.75 m)

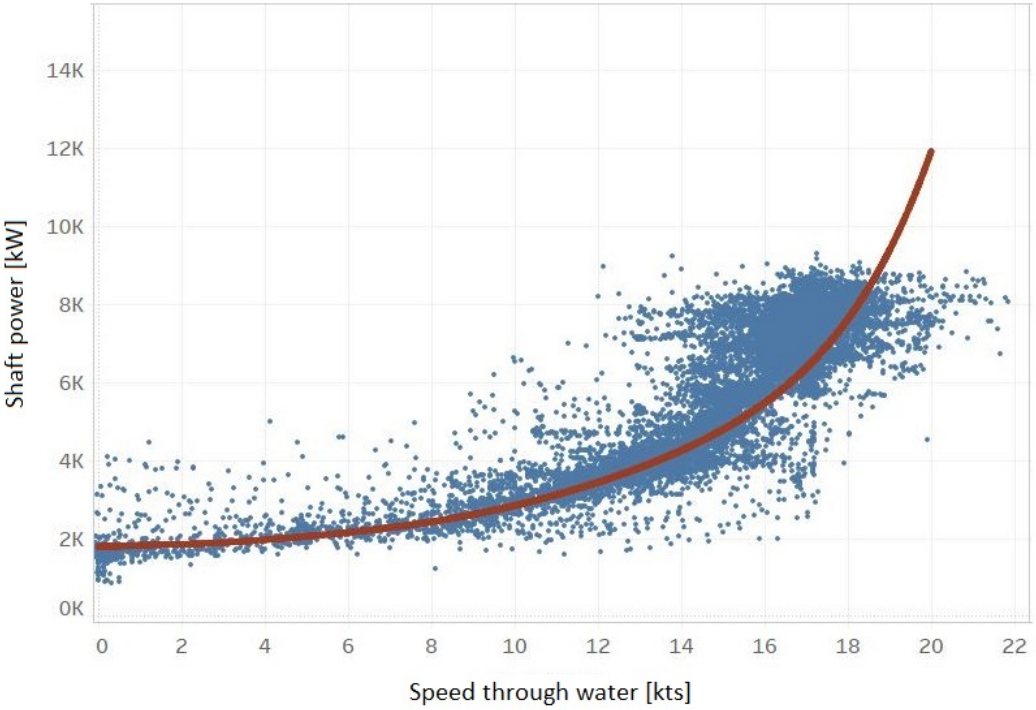

Figure 4.29: Shaft power estimated (based on extended curve) and measured values (draft 10 m)

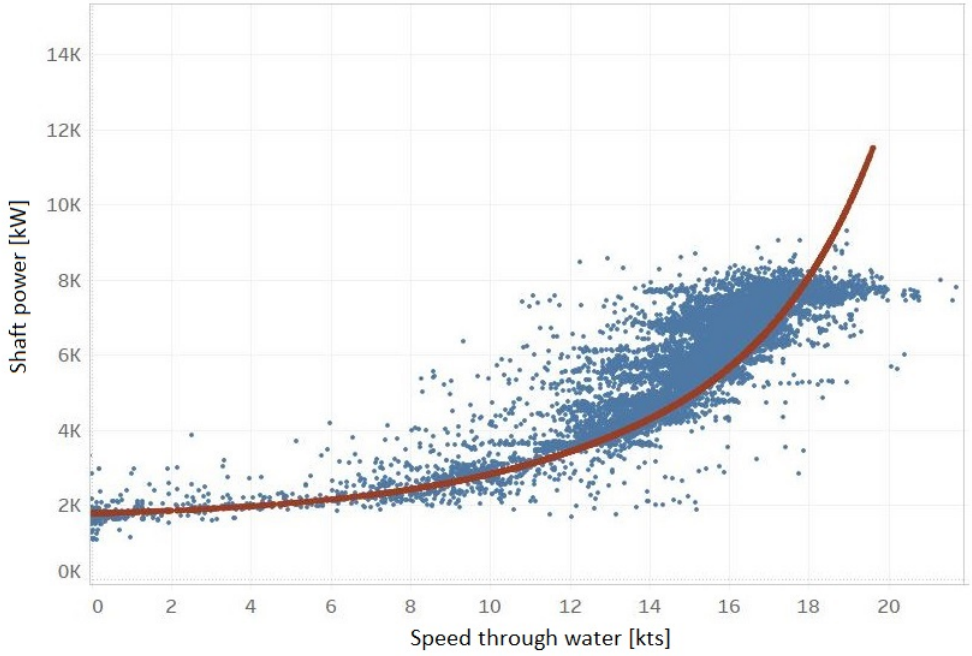

Figure 4.30: Shaft power estimated (based on extended curve) and measured values (draft 10.65 m)

Trim effect

As it was mentioned in the previous section the results from the model test at the draft of 6.75 m correspond to a 1.5 m trimmed by the stern condition. Thus, before the resistance model was extended in the full range

of draft, the resistance curve of 6.75 m draft at zero trim condition had to be derived first. For this reason, the model which enables the calculation of the resistance under any trim condition was developed first.

In order to develop this model, the information from the CFD, which was performed in order to offer to the company an insight about the influence of the trim on the power demand, were used. The S-type vessels, due to limitations which arise from the design of the vessels are limited to operate with trim values from 1.5 m by the stern to 0.5 m by the bow. Therefore, the trim model will also follow this limitation. Usually trim is defined as positive when the vessel is trimmed by the bow (draft at aft part higher than the draft of the bow part). However, within Spliethoff the opposite definition is used. The definition according to Spliethoff will be used in this report. Thus, positive trim corresponds to a trimmed by the stern condition. As it was presented in the previous section the CFD test reported higher values regarding the calm water resistance compared to the model tests. Therefore, it is questioned if we can rely on the results of the CFD regarding the influence of the trim on the resistance. However, the CFD results is the only available information regarding the influence of trim, and thus it was decided to use it, but further research is suggested. In Figures 4.31-4.33, the results from the CFD are presented. In z axis the difference in resistance is plotted, based on the Equation 4.2. The contours of these plots are presented in Appendix B.

$$Dif = \frac{Resistance((speed, trim) - Resistance(speed, trim(0))}{Resistance(speed, trim(0))} \tag{4.2}$$

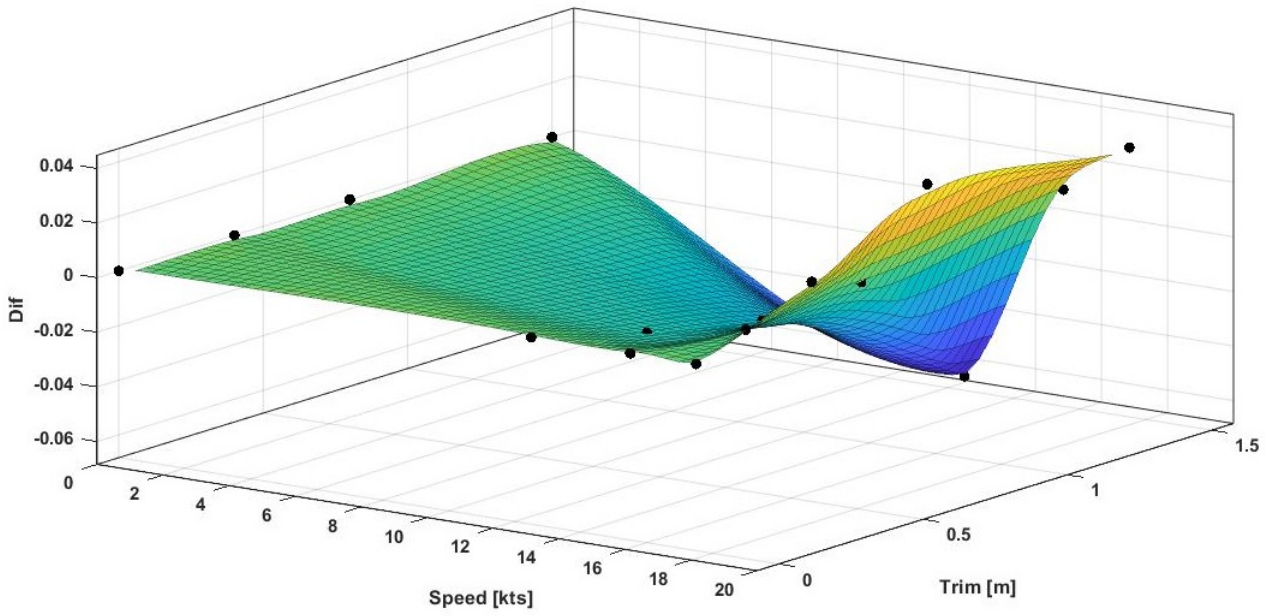

Figure 4.31: dif versus speed versus delta trim at 6.7 m Draft

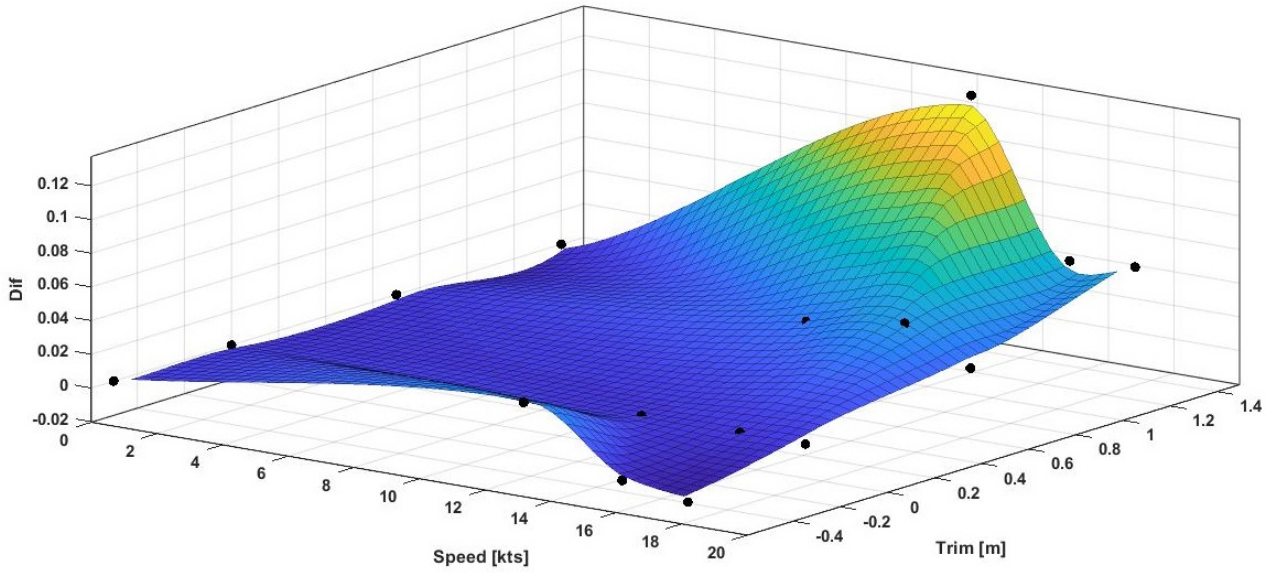

Figure 4.32: dif versus speed versus delta trim at 9 m Draft

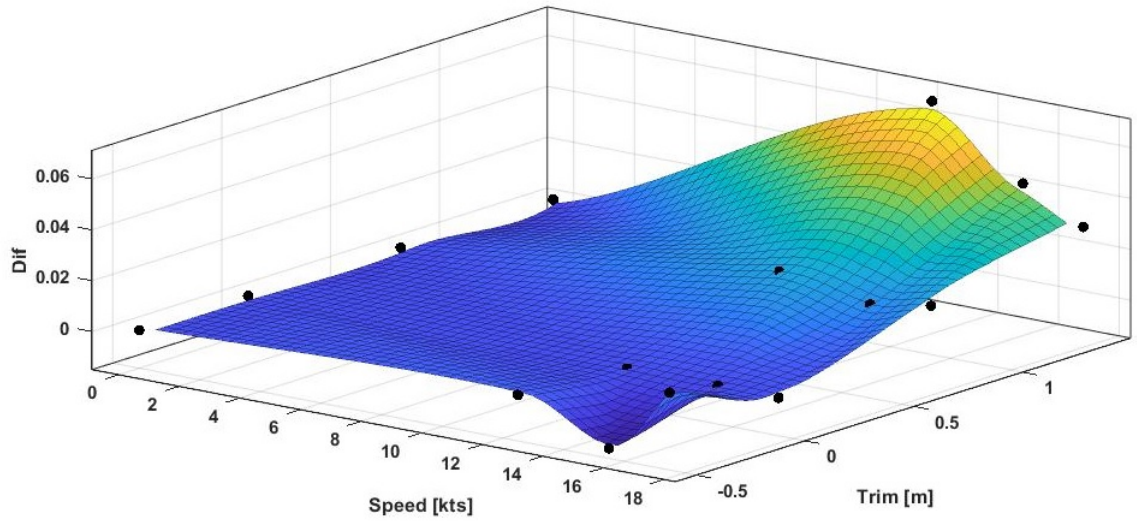

Figure 4.33: dif versus speed versus delta trim at 10.25 m Draft

The CFD test was performed only for three draft values (6.7 m, 9 m, 10.25 m) and three speed values (12.5, 15.5, 17.5 kts) and thus a method should be found in order to extend the model in the entire range of speed and draft. The influence of the trim at zero speed is zero, and with these additional points, the intermediate speed values (0-12.5) can be handled with interpolations. Regarding the draft, the required information will be calculated as well based on interpolation. In the following example it is presented how does the Dif value be calculated for the intermediate drafts, in this case the speed of 15 kts and 1 m trim were used.

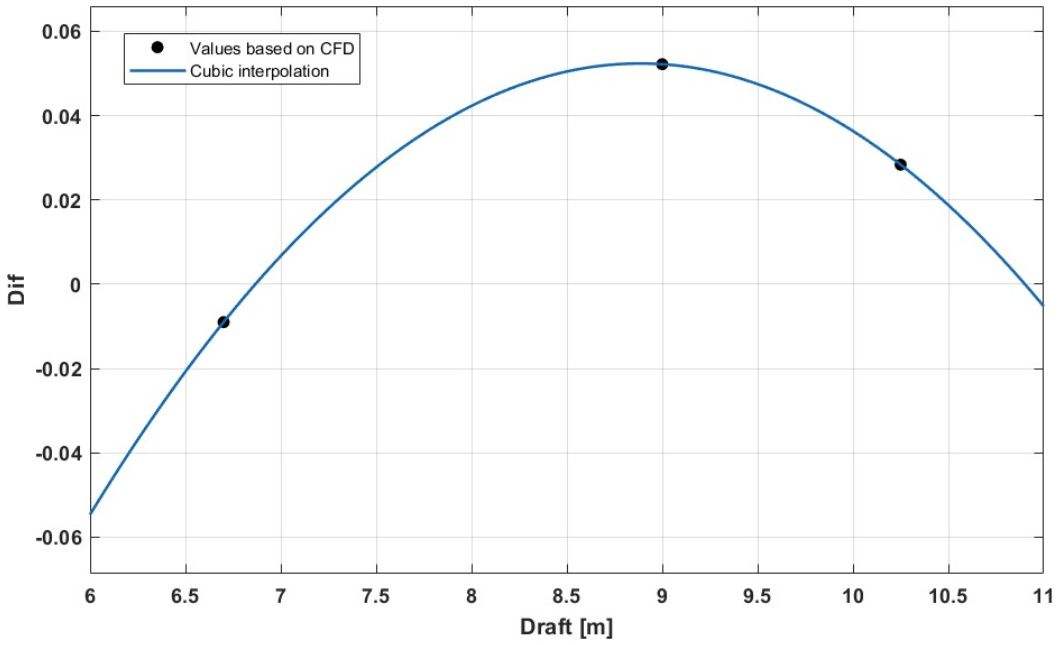

Figure 4.34: calculation of dif value at intermediate drafts (example for 15 knots and 1 m trim)

It should be noted here that the trim correction method is based on limited information. As it can be seen from Table 4.1, the CFD test was performed for 3 drafts and in each case 3 speeds were examined and 4 trim conditions. This information is not enough to create a model for trim correction for the entire operating profile of the vessel. For example, the lower speed that was tested in the CFD was 12.5 kts, which creates a big information gap for the speed range 0-12.5 kts. It is known that at zero speed the value of Dif will be zero and thus, an interpolation was used to give an estimation for the intermediate speeds (0-12.5). However, it cannot be known if the interpolation leads to results which represent the reality for the speed range 0-12.5 kts. On the other hand, the highest speed that was tested in the CFD was 17.5 kts which is lower than the maximum speed of the vessel (20 kts). Thus, we have an information gap for the speed range [17.5-20] as well. It is decided not to extrapolate to extend the model for higher speeds. An extrapolation without having an indication for the expected value at the speed of 20 kts can lead to unrealistic results. Thus, for all speed values higher than 17.5, the values that correspond to the speed of 17.5 kts will be used.

The same situation holds for draft values which do not coincide with the drafts that were tested. In Figure 4.34, it is shown how the calculation is performed, but again due to the lacking of enough information the reliability of the result is questioned. However apart from the issues caused due to lack of sufficient information which may lead to results far from reality (due to the interpolations), the quality of the information provided from the CFD should be questioned. In Figure 4.32 and 4.33 which correspond to 9 and 10.25 m draft we observe that for the case of 1.4 m trim, the dependency to the speed is not linear. There is a peak value at the speed of 12.5 kts in both Figures. This means that at the speed of 12.5 kts, a trim of 1.5 m by the stern has more impact on the resistance compared to higher speeds. Such a phenomenon may can be explained from the influence of this trimmed condition to the wave patterns. On the other hand, in the case of 9 m draft, we can see from the graph that the additional resistance for 1.5m ,trim by the stern, will be about 10%, which is considered a significant change to be caused only due to trim variations. Regarding the same speed and trim values at the draft of 6.75 m 4.31, it is observed the opposite situation. According to the CFD results there will be a resistance reduction of about 6% if the vessel is trimmed 1.5m by the stern when it is sailing with 12.5 kts at 6.7 m draft. In contrast, for higher speeds (higher than 16 kts) an additional resistance about 3% is expected according to the CFD results.

Some of the trends that the CFD results follow cannot be fully understood and thus the results should be treated with criticism. Due to the fact that the CFD results is the only available information regarding the effect of the trim on the resistance, it was decided to use them in this study. Despite, the lack of reliability

that is observed in the CFD results, it is worth mentioning that the CFD was intentionally performed for these draft and speed values. The 6.7 m draft correspond to the ballast condition, while the 10.25 at the full load. If the 3 speeds (12.5, 15.5, 17.5) are treated as a range (12.5-17.5 kts), they account for almost the entire speed operating profile if the port time is excluded, this is also illustrated in Figure 3.2. Thus despite the lacking of enough information to create a model for the full draft and speed range, the conditions (draft and speed values) under which the S-type vessels are mainly sailing were tested by the CFD test.

Extension of Calm water resistance for intermediate drafts

Since the model for the trim effect was developed, the calm water resistance curve of the 6.75 m draft can be created based on resistance curve corresponding to 1.5 m trim by the stern condition (which is presented in Figure 4.27). The calm water resistance curves which were derived based on the results of the model tests, and the zero trim resistance curve at the draft of 6.75 m, are presented in Figure 4.35.

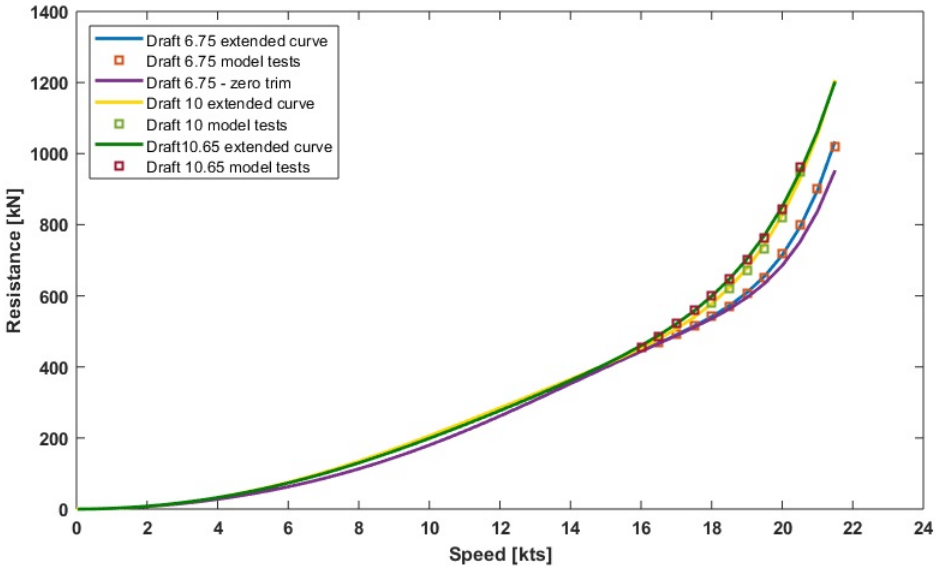

Figure 4.35: Proposed resistance curves

In order to create the resistance curves for the intermediate drafts, information from the Holtrop and Mennen method [20] were used. Despite the fact that the resistance based on the Holtrop and Mennen method [20] did not converge with the results of the model tests, it was decided to use this method to extract information about the resistance-draft dependency. The main reason for that decision was that the only available alternative was a simple interpolation between the three derived resistance curves. Thus, instead of using a simple linear interpolation based on the three resistance curves, the trend that is observed in the results of the Holtrop and Mennen method (resistance-draft dependency) will be used to interpolate between the three resistance curves.

As it can be seen in Figure 4.36, for the speeds 1-6 kts the resistance stays almost constant versus the draft. However, in higher speeds where the increase of the resistance versus the draft is clear, it is observed that the curves have a hump at the draft of 8 m. Fact which seems reasonable because the bulbous bow is just below the water at the draft of 8.75 m. Thus, from the draft of 8 m the additional resistance due to the fact that the bulbous bow is not submerged starts decreasing. Additional proof for that is provided in the Figure **??**, presented in the Appendix G. The trend observed in the results of the Holtrop and Mennen method was used in combination with the three resistance curves, as presented in the 4.35, in order to extend the resistance model in the intermediate drafts. Thus, with starting point the available resistance curves for the three drafts (Draft 6.75, 10, 10.65) the same pattern was reproduced for the resistance-draft dependency. The final results about the resistance model can be seen in the Figure 4.37.

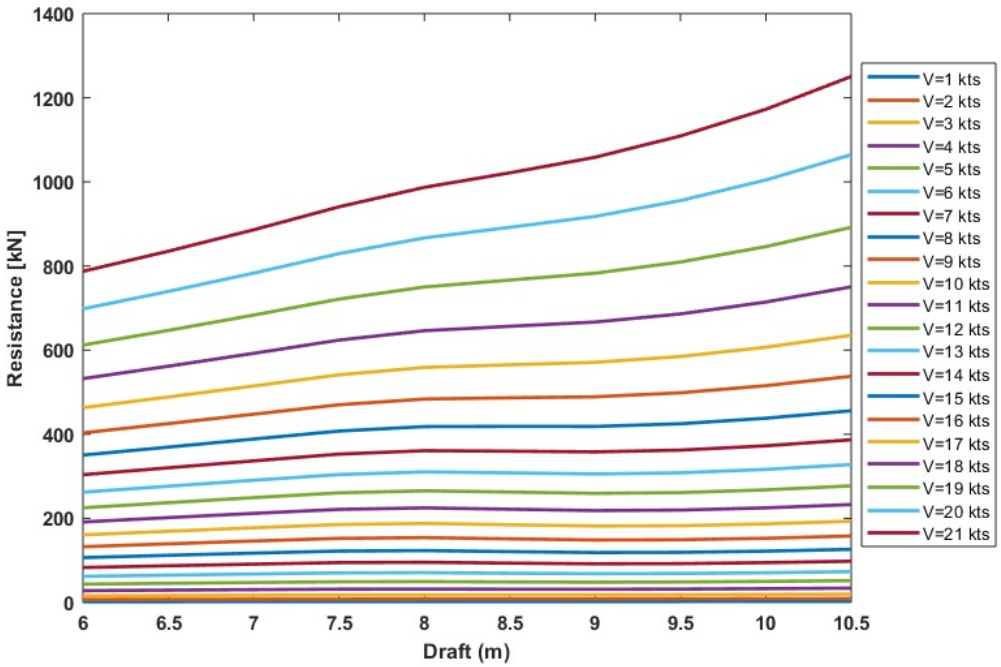

Figure 4.36: Resistance versus draft according to Holtrop and Mennen

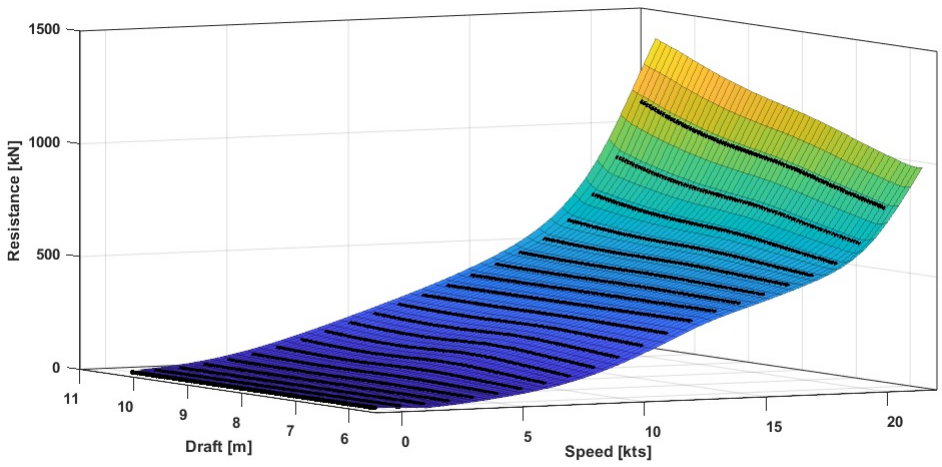

Figure 4.37: Proposed resistance model

Hull roughness influence

The developed resistance model was based on the results of the resistance model tests (the extension in intermediate draft was done by the trend observed in the results of Holtrop Mennen). However, the vessel is operating for almost 20 years, and as a result of the deterioration and corrosion, the hull's roughness will be higher than that of a newly built vessel. In addition the vessel is quite often sailing in ice conditions, which acts negatively regarding the hull's paint and resulting as well in increase of the hull's roughness. According to Townsin et al. [47] the initial hull's roughness is . An annual increase of 10 µm is reasonable for the first 4-5 years of operation, while for the rest of the vessel's lifetime, the roughness stays stable. In addition, Townsin et al. [47] estimates that 10 µm higher roughness will cause an increase to the power demand by 1%. Thus, based on the data reported from Townsin et al. an additional power demand of about 5% is reasonable due to the higher hull's roughness, after the first years of operation.

Thus, in the resistance model we have to take into account that after almost 20 years of operation the resistance of the vessel will be higher compared to the initial condition. However, there are not available measurements for the roughness of the hull and so we cannot perform a calculation to quantify the influence. In order to make an estimation about the additional resistance caused by the alteration of the hull's surface, the components of the WBM will be used. The resistance curves will be tested again, this time an additional resistance will be assumed. The estimated shaft power from the WBM for the present hull's condition will be compared both with the shaft power results from WBM for the initial hull's condition (shaft power results as presented in Figures 4.28-4.30), and with the measurements from the PMS. The resulted shaft power curves will be evaluated both for the agreement with the measurements from the PMS and for their deviation from the results of the initial resistance curves (based on model tests). After this iterative process, it seems reasonable to take into account an additional resistance of 5% compared to the resistance of the initial hull's condition (as presented in Figure 4.35). The final estimation of 5% additional resistance due to higher hull roughness results in an increase of 4% in the shaft power curve, which is in agreement with the results reported by Townsin et.al. [47]. The figures comparing the calculated shaft power curves (from the WBM), as estimated from the WBM, for both the initial resistance curves and the updated ones (considering 5% additional resistance) and the shaft power measurements from the PMS can be seen in the Figures 4.38-4.40.

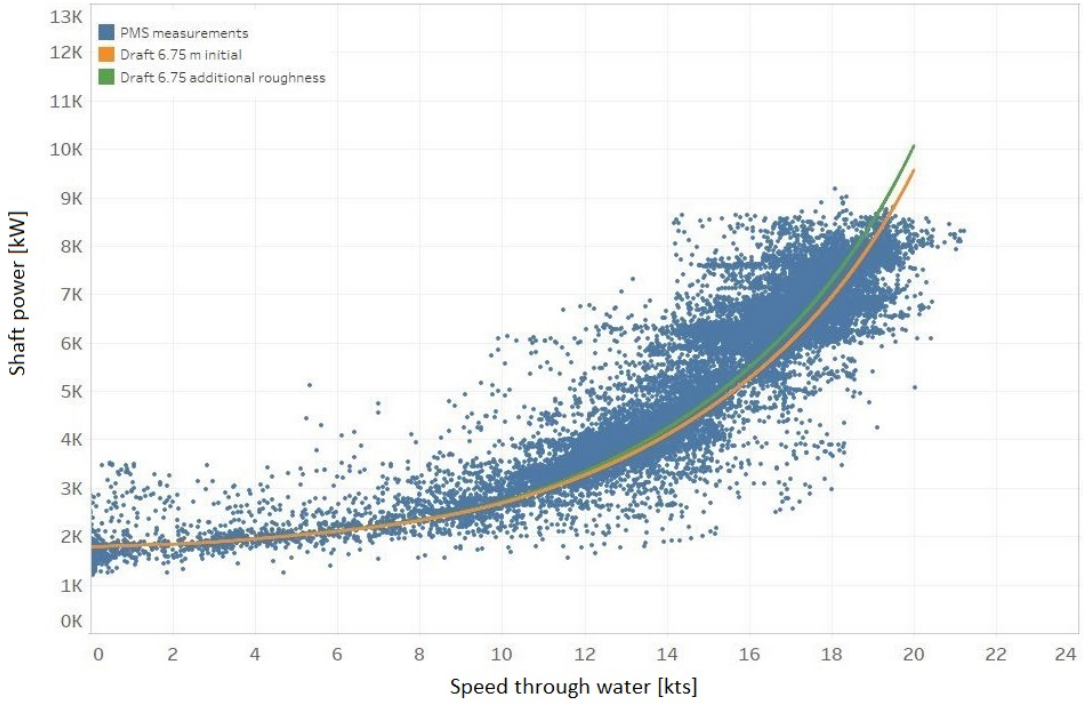

Figure 4.38: Shaft power curve from WBM for initial resistance curve and for higher roughness (6.75 m draft)

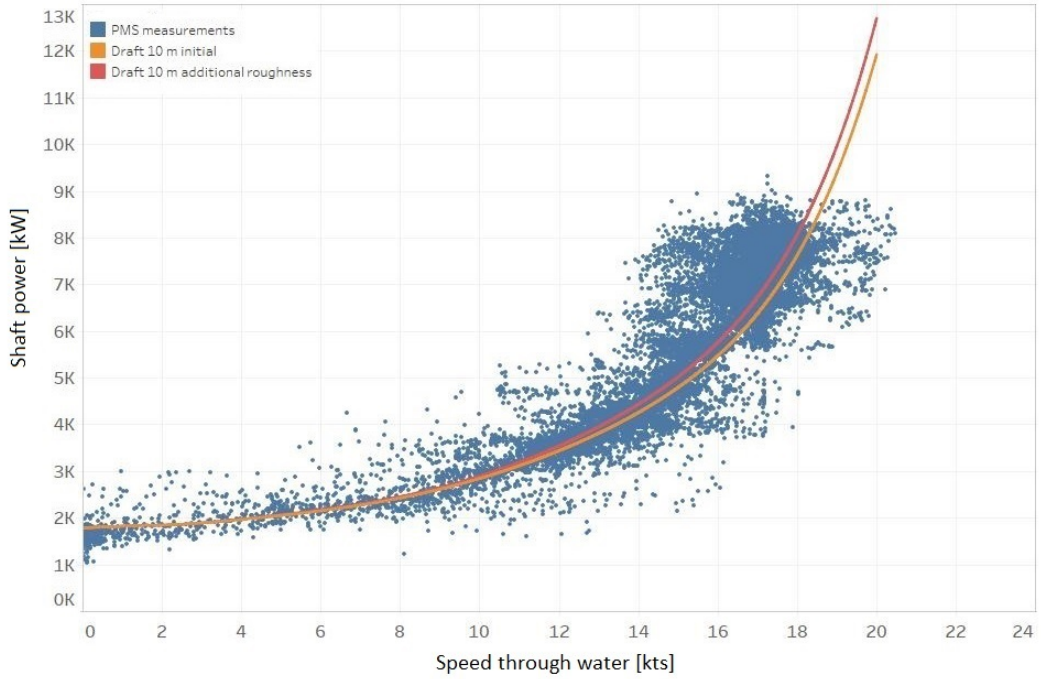

Figure 4.39: Shaft power curve from WBM for initial resistance curve and for higher roughness (10 m draft)

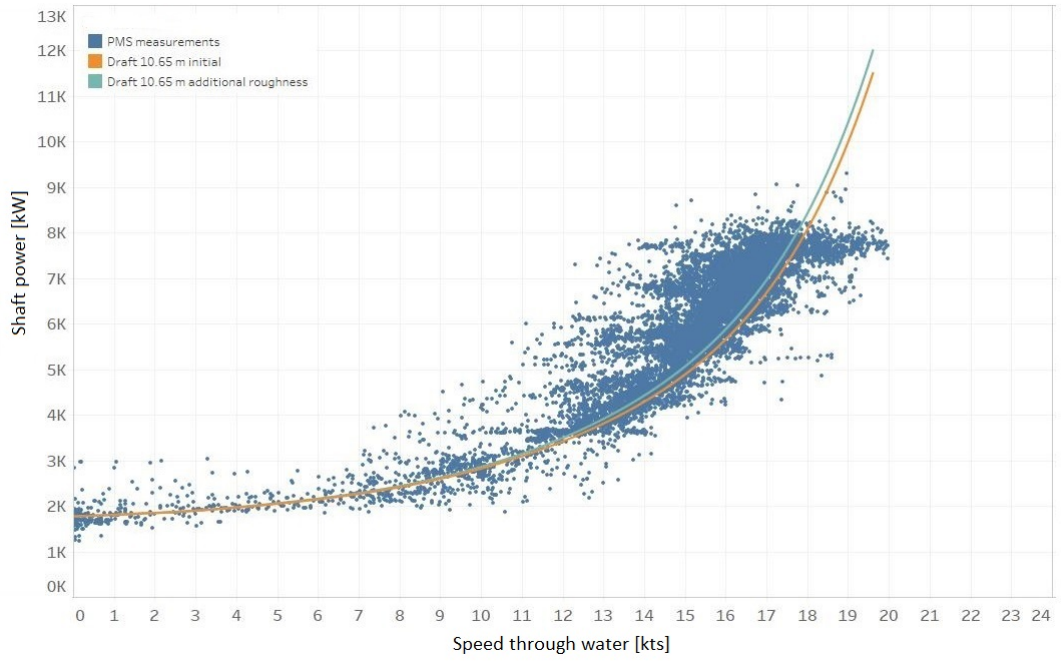

Figure 4.40: Shaft power curve from WBM for initial resistance curves and for higher roughness(10.65 m draft)

Verification of Calm water resistance model

The agreement between the calculated shaft power curves by the WBM and the measured values from the PMS was not examined in depth in the previous section. In the figures where the estimated curve is plotted against the measurements from the PMS the density of the data-points was not represented. Thus a visual comparison is not adequate to examine the agreement between the calculated (by the WBM) shaft power curves and the measurements from the PMS. For this reason the graphs presented in Figures 4.41-4.43 were

created.

The shaft power measurements from the PMS were plotted versus the speed through water (filters were applied to present data only ±0.25 m from the examined draft in each case). In addition the data are filtered to include only calm water conditions (wave height less than 1 m). The PMS data were separated in classes based on the speed through water (with a step of 0.5 kts), then for each class the mean shaft power value was calculated and plotted in the graph. The ±5 % from the mean value were plotted as well. In addition, for each draft which was examined the shaft power curve calculated from the WBM and was plotted in the same graph.

It is observed that the calculated by the WBM shaft power curves are in good agreement with the mean values calculated for each class. The deviations observed in the high speeds, are a result of the way that the mean value is calculated. The classes were created based on the speed. Thus the high speed classes contain only outliers. For the high speed, it would be more practical to create classes based on the shaft power. In that case, in the high speed values it is clear that the mean value of the shaft power measurements would be close to the one calculated by the WBM, but now in the low speeds a calculation of the mean value would not make sense (if classes were made based on the shaft power). To further prove that there is agreement between the measurement from the PMS and the calculated shaft power curve from the WBM, additional graphs are presented in Appendix H , where the density of the PMS measurements is also depicted.

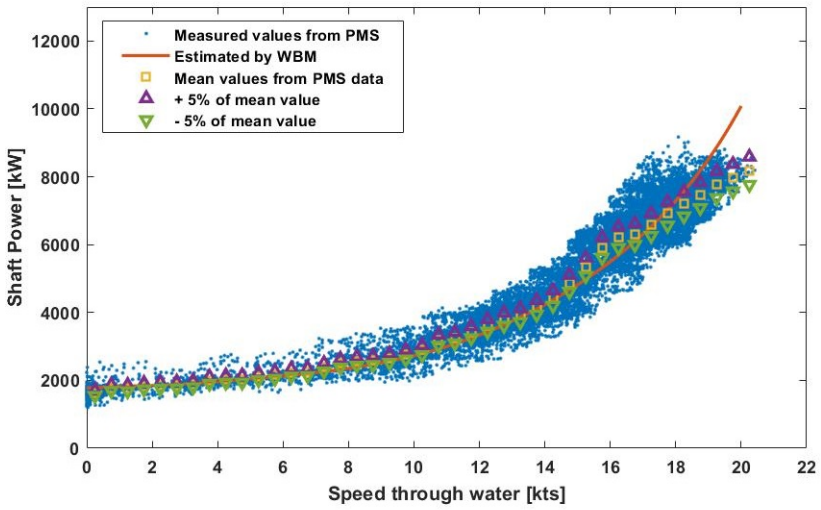

Figure 4.41: Comparison between estimated shaft power curve and PMS data (draft 6.75 m)

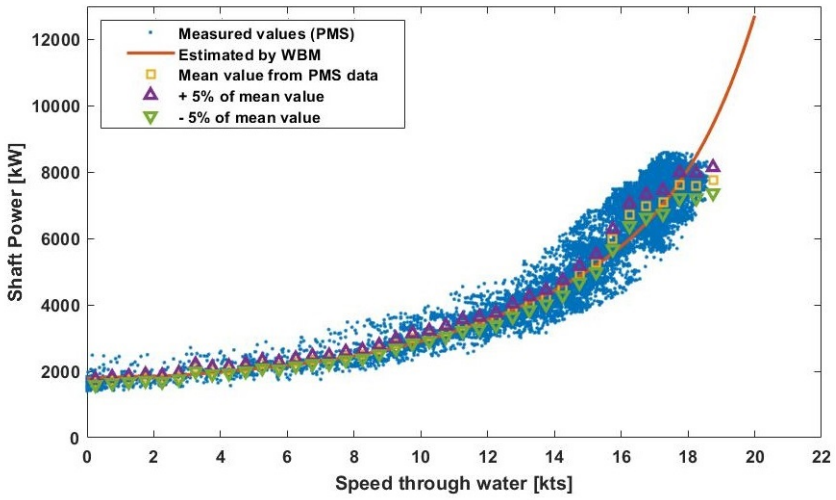

Figure 4.42: Comparison between estimated shaft power curve and PMS data (draft 10 m)

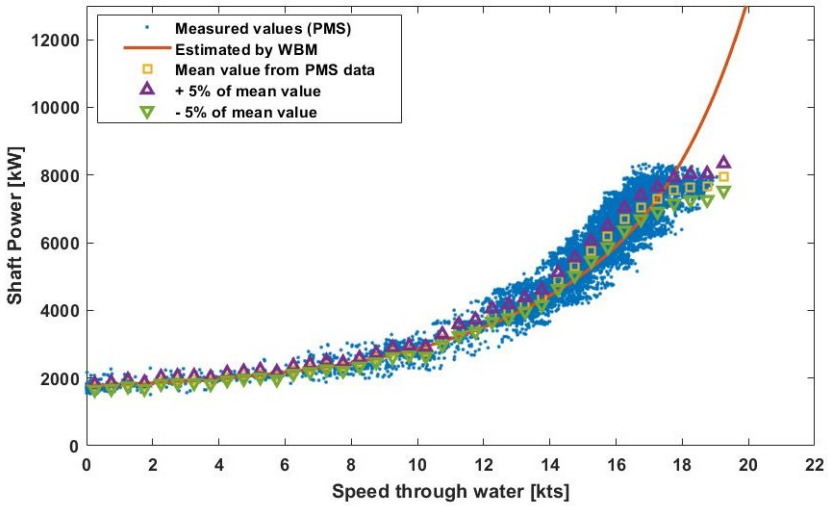

Figure 4.43: Comparison between estimated shaft power curve and PMS data (draft 10.65 m)

The same diagram is created for the draft of 8.5 m, as it is important to examine whether the resistance model is reliable for drafts which were not tested in the model tests. The results are presented in Figure 4.44. It is clear that in the case of the 8.5 m draft, the measurements and the estimated values are in close agreement. The classes' mean values present higher fluctuations in the case of the 8.5 m draft, compared to the situations examined before, but this is caused due to the smaller number of measurements.

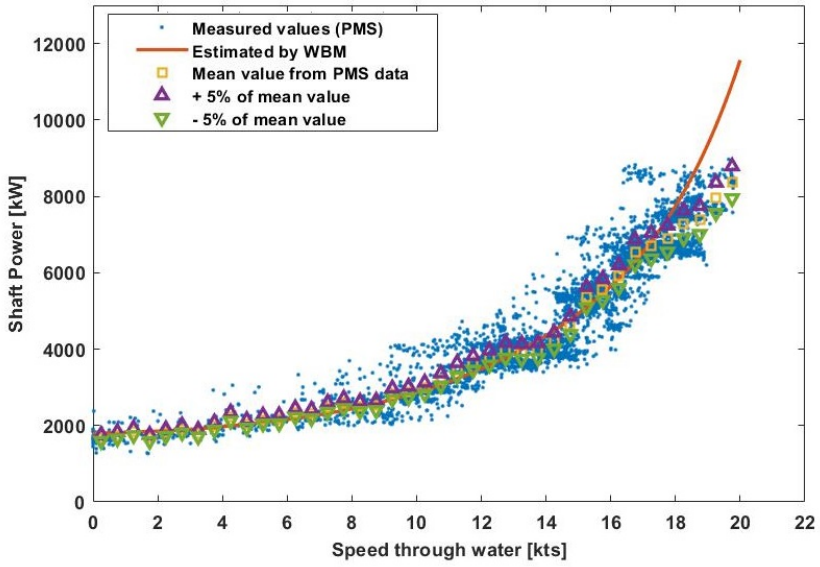

Figure 4.44: Comparison between estimated shaft power curve and PMS data (draft 8.5 m)

4.3.6. Added resistance

Shallow water

When the vessel is sailing in shallow water, the resistance increases compared to the calm water resistance in deep water. This is caused by the following reasons.

- Added resistance due to increase in water velocity along the ship's hull. This effect will cause an added sinkage (squat) to the hull and thereby an increased wetted surface which will lead to changed frictional resistance and wave making resistance.
- Added resistance due to change of the wave pattern. In deep waters the wave velocity for the ship induced diverging waves is dependent on the wave length only where as in shallow waters the wave velocity is dependent on the water depth. The changed wave velocity will change the wave pattern and thereby the wave resistance.

In this study the model of Lackenby [28] will be used to take into account the influence of the shallow water.The semi-empirical formula proposed by Lackenby [28] (Equation 4.3) will be used to calculate the speed loss due to shallow water.

$$\frac{\partial V}{V} = 0.1242\left(\frac{A_m}{h^2} - 0.05\right) + 1 - \left(\tanh\frac{gh}{V^2}\right)^{1/2} \tag{4.3}$$

with $\frac{A_m}{h^2} > 0.05$ and

- V the speed of the vessel in shallow water $[m/s]$
- ∂V the speed loss when the vessel is sailing in shallow water $[m/s]$
- A_m the area of the underwater midship section $[m^2]$
- h the depth of water $[m]$
- g acceleration of gravity $[m/s^2)]$

The underwater midship section area is taken as a function of the draft based on the information from the stability booklets. The component $\frac{A_m}{h^2} > 0.05$ indicates the water depth for which the effect of shallow water starts to take place. In figure 4.45 the water depth for which according to Lackenby the effect of the shallow water initiates, is presented versus draft.

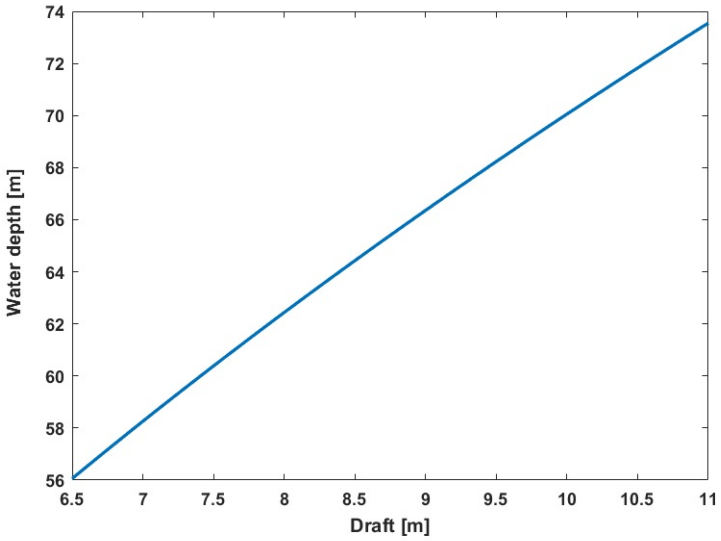

Figure 4.45: Initiation water depth of shallow water effect

In Figure 4.46 the calm water resistance curve at the draft of 6.75 m and deep water is compared with the resistance curves for equivalent draft and water depth of 40 and 20 meters. It is clear that the influence of the shallow water is quite significant when the water depth is very low and especially at the high speeds. In order to examine whether Lackenby's model gives reliable results the resistance curves plotted in Figure 4.46 will be used as input to the theoretical model and the results will be compared with the real measurements from the PMS. In Figure 4.47 the results are presented. The colorbar is divided in two main parts, the red colour corresponds to deep water (higher than 57 m where the influence of the shallow water initiates for the draft of 6.75 m) while the green to shallow water (lower than 57 m). The data from the PMS are filtered so that only drafts of 6.75±0.25 m are presented and only calm water conditions.

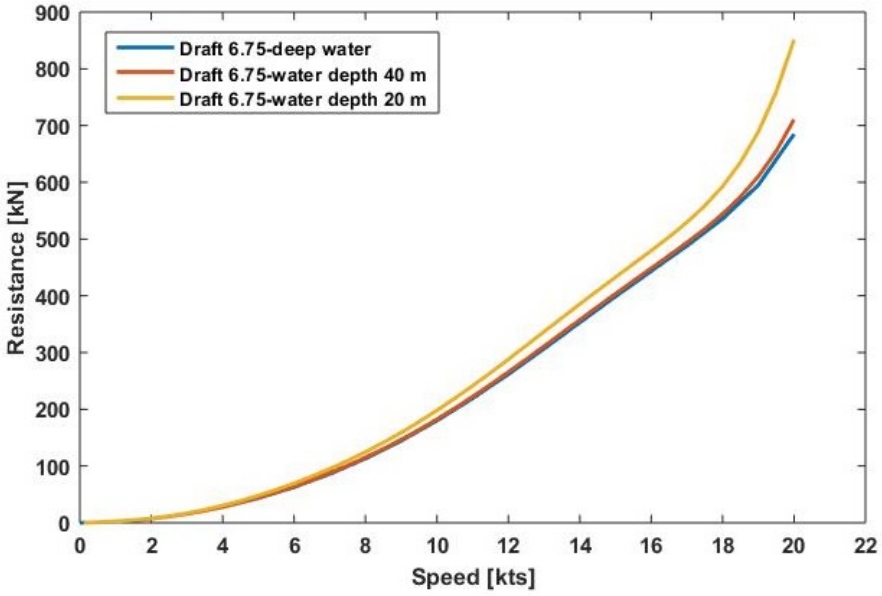

Figure 4.46: Resistance curves at 6.75m draft, variable water depth

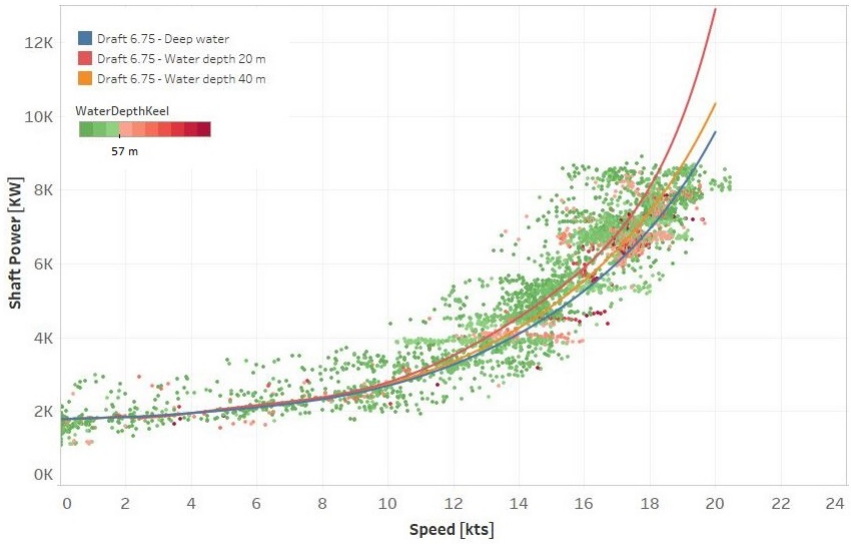

Figure 4.47: Shaft power estimated from the theoretical model for variable water depth and measured (PMS)

Wind resistance

The additional resistance due to the effect of wind can be calculated by the following formula.

$$R = \frac{1}{2}\rho_A V_{WR}^2 C_X(\Psi_{WR}) A_{XV} \tag{4.4}$$

where,

- ρ_A mass density of air
- V_{WR} the relative wind speed
- C_X wind resistance coefficient
- Ψ_{WR} relative wind angle
- A_{XV} area of maximum transverse section exposed to the wind

In the S-type vessels the anemometer which is installed on-board is not used and the wind predictions are prefered as a source for the wind speed and wind direction at the sailing area of the vessel.
The area of the maximum transverse section exposed to the wind can be calculated based on the drawings of the vessel. The results for variable draft can be seen in Appendix C.
Unfortunately, there are not available wind tunnel tests for the S-type vessels. Thus the estimation of the wind resistance coefficient will be based on Blendermann's [7] study where wind tunnel tests were performed for 18 ship types and variants of them. In the vessel's that were tested by Blendermann [7], there is a general cargo vessel with design similar to the S-type vessel and thus the wind force coefficient (as presented in Figure 4.48) of this vessel will be used. It is important here to mention that the values of the wind force coefficient correspond to empty deck. The relative wind angle is the angle between the ship's heading and the wind, with angle 0 defined as headwind. The relative wind speed is calculated based on the relative wind direction.

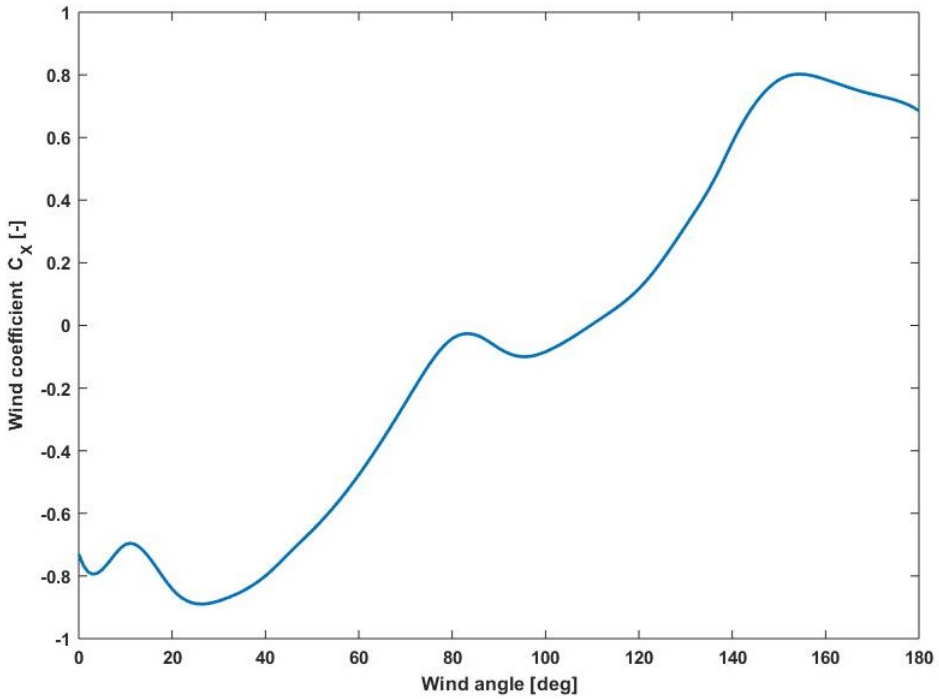

Figure 4.48: Wind force coefficient C_x based on Blendermann [7].

In Figure 4.49 the calm water resistance curve at the draft of 10 m and is compared with the resistance curves for equivalent draft and headwind of 10 kts. It is clear that the wind can influence significantly the resistance of the vessel. In order to examine whether the model gives reliable results the resistance curves plotted in Figure 4.46 will be used as input to the theoretical model and the results will be compared with the real measurements from the PMS. In Figure 4.50 the results are presented. In the colobar, it can be seen in what wind speed each colour corresponds. The data from the PMS are filtered so that only drafts of 10 ± 0.25 m are presented. In addition, the relative wind angle is filtered so that only values in the range 0 ± 25 deg are plotted.

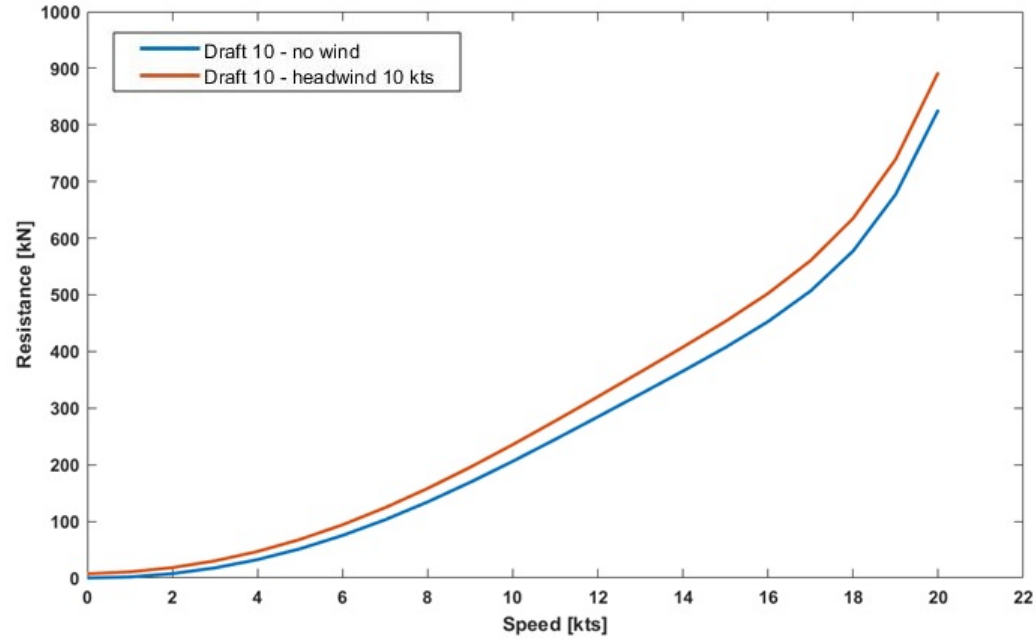

Figure 4.49: Resistance curves at 10 m draft, for no wind condition and 10 kts head wind

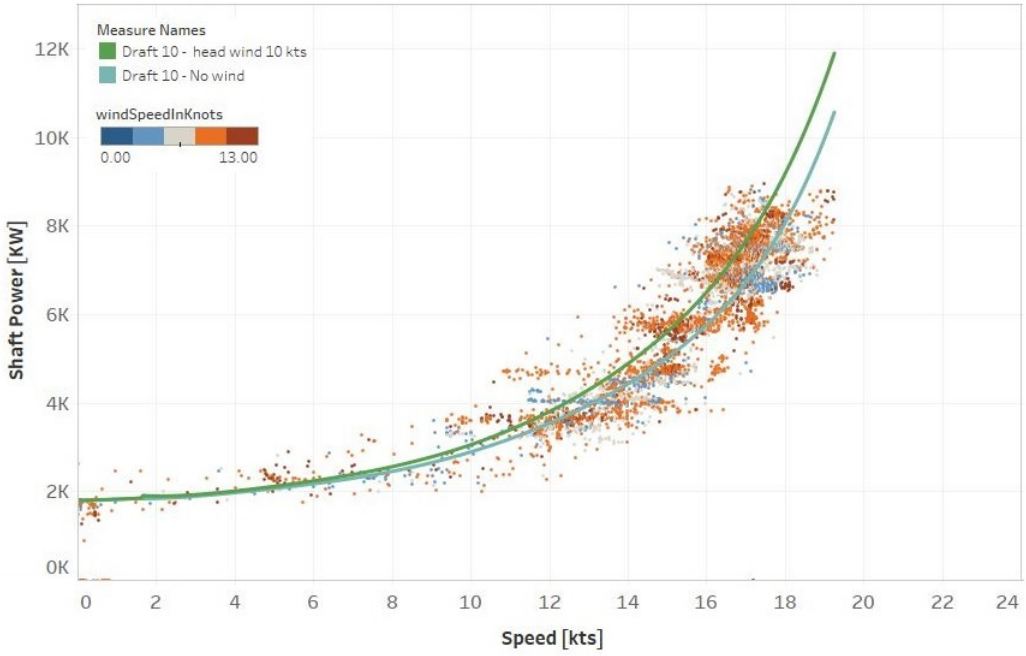

Figure 4.50: Shaft power measured and estimated for no wind condition and 10 kts headwind

Wave added resistance

The added resistance in short-crested irregular waves is calculated with the following equation.

$$\Delta R_{wave}(H,T,\theta;V) = 2\int_0^{2\pi}\int_0^{\infty} \frac{R_{AW}(\omega,\alpha;V)}{\zeta^2} E(\omega,\alpha;H,T,\theta)\,d\omega\,d\alpha \tag{4.5}$$

where,

- H significant wave height
- T wave period
- θ encounter angle between the ship's heading and the main component wave
- V vessel's speed through water
- R_{AW} mean resistance increase in regular waves
- ζ wave amplitude
- E direactional spectrum
- α encounter angle between the ship's heading and the component waves

As it is shown by the equation 4.5 the mean resistance increase due to waves is calculated by the superposition of the mean resistance increase in regular waves and the directional wave spectrum.

From the weather provider the significant wave height and the wave period of the main component wave, at the sailing area of the vessel are available both for the swell and the wind waves. Thus, the added resistance due to swell and wind waves will be calculated separately. The two components summed up give the total added resistance due to waves [39]. The standard form of the directional spectrum will be used as suggested by the ITTC[4] [22], the directional spectrum is calculated with the following relation.

$$R_{added-waves} = R_{wind-waves} + R_{swell} \tag{4.6}$$

$$E = S_f(\omega)G(\alpha) \tag{4.7}$$

where,

- S_f frequency spectrum
- G angular distribution function

For wind waves the modified Pierson-Moskowitz frequency spectrum is used, which is described from the following equations.

$$S_f(\omega) = \frac{A_f}{\omega^5}\exp\frac{-B_f}{\omega^4} \tag{4.8}$$

$$A_f = \frac{1}{4\pi}(\frac{2\pi}{T_{02}})^4 H^2 \tag{4.9}$$

$$B_f = \frac{1}{\pi}(\frac{2\pi}{T_{02}})^4 \tag{4.10}$$

$$T_{02} = \frac{\Gamma(3/4)}{\pi^{(1/4)}}T \tag{4.11}$$

While for swell , the JONSWAP frequency spectrum is used, described by the following equations.

$$S_f(\omega) = \frac{A_f}{\omega^5}\exp\frac{-B_f}{\omega^4}\gamma^{\exp\left\{\frac{1}{-2\sigma_f^2}(1.3T\frac{\omega}{2\pi}-1)^2\right\}} \tag{4.12}$$

$$A_f = 0.072(\frac{2\pi}{T})^4 H^2 \tag{4.13}$$

[4] International Towing Tank Conference

$$B_f = 0.44\left(\frac{2\pi}{T}^4\right) \tag{4.14}$$

$$\sigma_f = \begin{cases} 0.07 & \text{if } \omega \leq \frac{2\pi}{1.3T} \\ 0.09 & \text{if } \omega > \frac{2\pi}{1.3T} \end{cases}$$

As angular distribution a cosine-squared type is used as shown in equation 4.15. For wind waves the spreading parameter $s = 1$ is used, while for the swell $s = 75$ is used.

$$G(\alpha) = \frac{2^{2s}\Gamma^2(s+1)}{2\pi\Gamma(2s+1)} cos\left(\frac{\theta-\alpha}{2}\right) \tag{4.15}$$

In order to calculate the mean resistance increase in regular waves (R_{AW}), the methods for the added wave resistance proposed by MARIN are used, mainly due to the combination of accuracy and practicality. STAwave-2 was developed within the Sea trial Analysis Joint Industry Project (STA-JIP). This empirical method is publicly available and can be applied for head waves (±45 deg from the bow) covering both the motion-induced and the reflection induced added resistance [16]. The STAwave-2 method was further developed within the Service Performance Analysis Joint Industry Project (SPA-JIP) and resulted to the SPAwave method, which can be applied for all wave directions [16]. However SPAwave method is not public and thus the STAwave-2 method was used with the advantage that MARIN offered an indication for the resistance calculation of waves with encounter angle out of the STAwave-2 limits. The mean added resistance due to regular waves (R_{AW}) is calculated as shown in the following equation. The way that waves out of the (±45 deg (to the bow) is presented in Appendix D.

$$R_{AW} = R_{AWM} + R_{AWR} \tag{4.16}$$

$$R_{AM} = 4\rho g\zeta_A^2 \frac{B^2}{L_{pp}} \overline{raw}(\omega) \tag{4.17}$$

$$raw(\omega) = \overline{\omega}_1^b \exp\left\{\frac{b_1}{d_1}(1-\overline{\omega}^{d_1})\right\} \alpha_1 Fr^{1.5} \exp(-3.5Fr) \tag{4.18}$$

$$\overline{\omega} = \frac{\sqrt{\frac{L_{pp}}{g}}\sqrt[3]{k_{yy}}}{1.17Fr^{-0.143}}\omega \tag{4.19}$$

$$\alpha_1 = 60.3C_B^{1.34} \tag{4.20}$$

$$b_1 = \begin{cases} 11 & \text{for } \omega < 1 \\ -8.5 & \text{elsewhere} \end{cases}$$

$$d_1 = \begin{cases} 14 & \text{for } \omega < 1 \\ -566\left(\frac{L_{pp}}{B}\right)^{-2.66} & \text{elsewhere} \end{cases}$$

$$R_{AWR} = \frac{1}{2}\rho g\zeta_A^2 B\alpha_1(\omega) \tag{4.21}$$

$$\alpha_1(\omega) = \frac{\pi^2 I_1^2(1.5kT_M)}{\pi^2 I_1^2(1.5kT_M) + K_1^2(1.5kT_M)} f_1 \tag{4.22}$$

$$f_1 = 0.692\left(\frac{V_s}{\sqrt{T_M g}}\right)^{0.769} + 1.81C_B^{6.95} \tag{4.23}$$

where,

- ρ density of water
- ζ_A wave amplitude
- B Beam
- L_{pp} length between perpendiculars
- ω angular wave frequency
- Fr froude number
- k_{yy} non dimensional radius of gyration in lateral direction
- CB block coefficient
- T_M draught at midship
- I_1 modified Bessel function of the first kind of order one
- K_1 modified Bessel function of the second kind of order one

In Figure 4.51 the calm water resistance curve at the draft of 6.75 m is compared with the resistance curves for 2 m and 3 m head waves. In both cases it was considered that both the swell and the wind waves had the same height (thus what is represented as 2m wave corresponds to 2m swell and 2m wind wave). Regarding the wave period, reference values which correspond to that weather condition were used from the available database. The resistance curves for 2m and 3m head waves were used as input in the WBM and the estimated shaft power curve is compared to the real measurements from the PMS in Figure 4.52. The data from the PMS were filtered so that only data points which correspond to draft of 6.75±0.25 m and head waves ±30 deg are presented. In addition, it should be noted that the plotted data from the PMS correspond to total wave height calculated with the relation $\sqrt{{H_{wave}}^2 + {H_{swell}}^2}$.

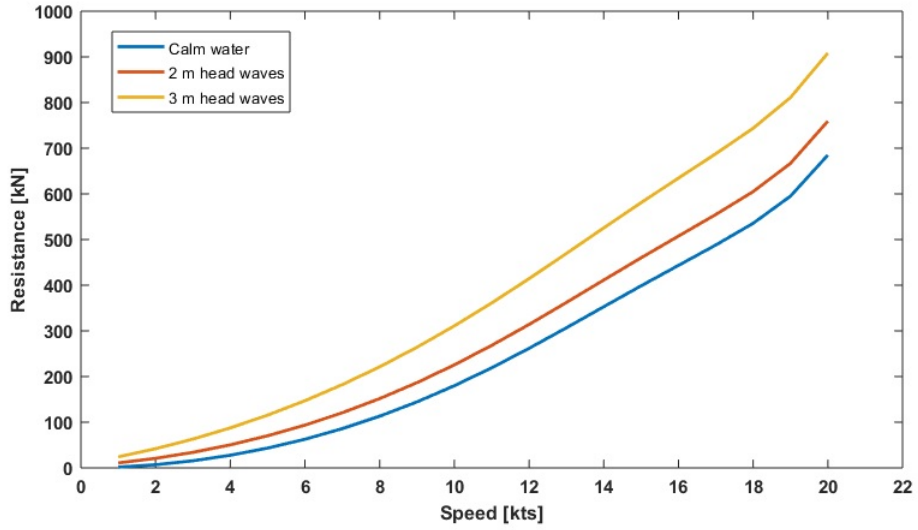

Figure 4.51: Resistance curves at 6.75 m draft, for calm water, 2m and 3m head waves

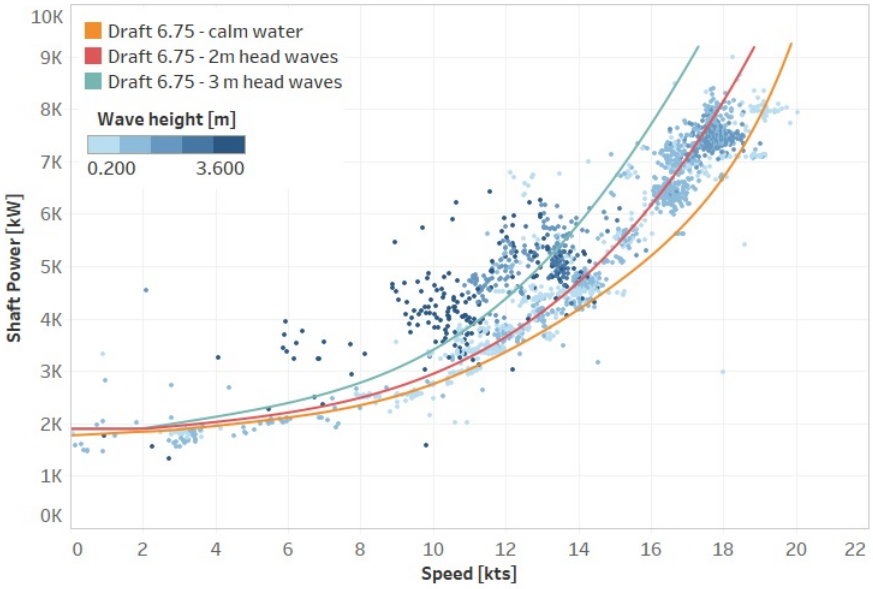

Figure 4.52: Shaft power measured and estimated for calm water, 2m and 3m head waves

4.3.7. Power losses in Gearbox, shaft and shaft generator

With the models developed in the previous sections, the required power that should be provided to the propeller in order the vessel to sail with a certain speed under any weather conditions can be determined. Before we continue with the calculation of the fuel consumption the power losses of the gearbox, the shaft and the shaft generator should be examined. Unfortunately, there is no information available (nominal values from the manufacturer or measurements) regarding the efficiency of these systems. Thus some reference values available in the literature will be used.

Gearbox

According to Godjevac et.al [15] the power loss model which was initially proposed by Stapersma was validated with a thermal network by their study. In this model the power losses of the gearbox are dependent on the gearbox's operating speed and load. However, the coefficients that are used in the power-loss model are derived based on technical information of the gearbox which is not available for the gearbox used in the S-type vessels. Thus it is decided to use the results from a conventional gearbox as reported from Godjevac et.al [15]. As, the S-type vessels are operating in constant rpm, the dependency of the losses to the operating speed can be neglected. In addition, the operating load will never be lower than 15% of the maximum, since the combination of CPP with fixed rpm (due to the shaft generator) has the drawback that in very low speeds a power of around 1600-1700 kW is required. The values that will be used for the efficiency of the gearbox can be seen in Figure 4.53.

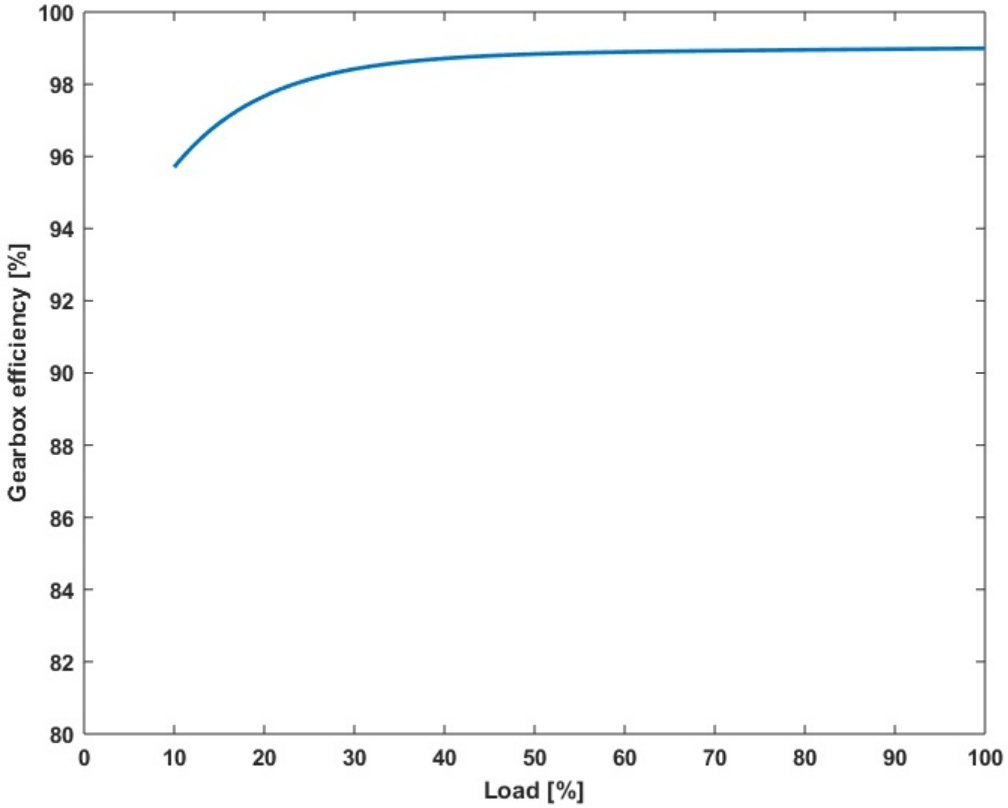

Figure 4.53: Gearbox efficiency versus load

Shaft generator

According to Stapersma [26], the efficiency of the shaft generators/ PTO (Power take off) which are used on ships varies depending the size, with reference values 92%-98% when operating in the design load. The efficiency for lower loads is lower with significant reduction for loads below 20% of the maximum. Based on the literature findings [54], the efficiency curve as presented in Figure 4.54 will be used.

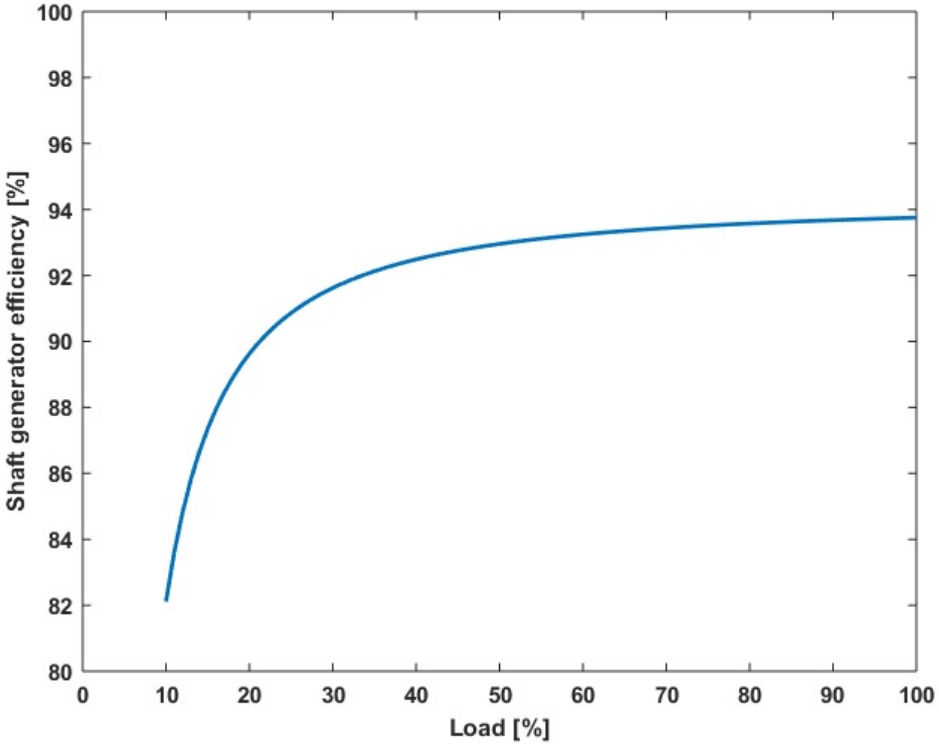

Figure 4.54: Shaft generator efficiency versus load

Shaft

The main source of power losses in the shaft system is caused by the shaft bearings [26]. However, the efficiency oh the shaft system is quite high (around 99%) and in contradiction with the gearbox and the PTO, the dependency on the load and the speed is insignificant (according to Shi et al. [43]) .Thus a constant efficiency of 99% for the shaft system will be used in this study.

4.3.8. Fuel Consumption

As it was mentioned in section 3.1, the S-type's propulsion plant operates fixed at 105 rpm. The reason for that is that the PTO should be rotating at constant rpm and more specifically at the speed which will result in generated electric power with frequency of 60 Hz. Thus in the fuel consumption model, the engine's speed will be ignored and only the load dependency will be taken into account. From the technical documentation of the vessel, the diagram of the specific fuel consumption versus the engine load is available. However, this diagram correspond to the ideal conditions, and thus it is expected that the consumption of the engine will always be higher than that. The comparison of the calculated specific fuel oil consumption (based on the measurements of the PMS), versus the nominal curve as provided from the manufacturer can be seen in Figure 4.55. In addition, a curve is fitted to the calculated specific fuel consumption and it is also plotted in Figure 4.55.

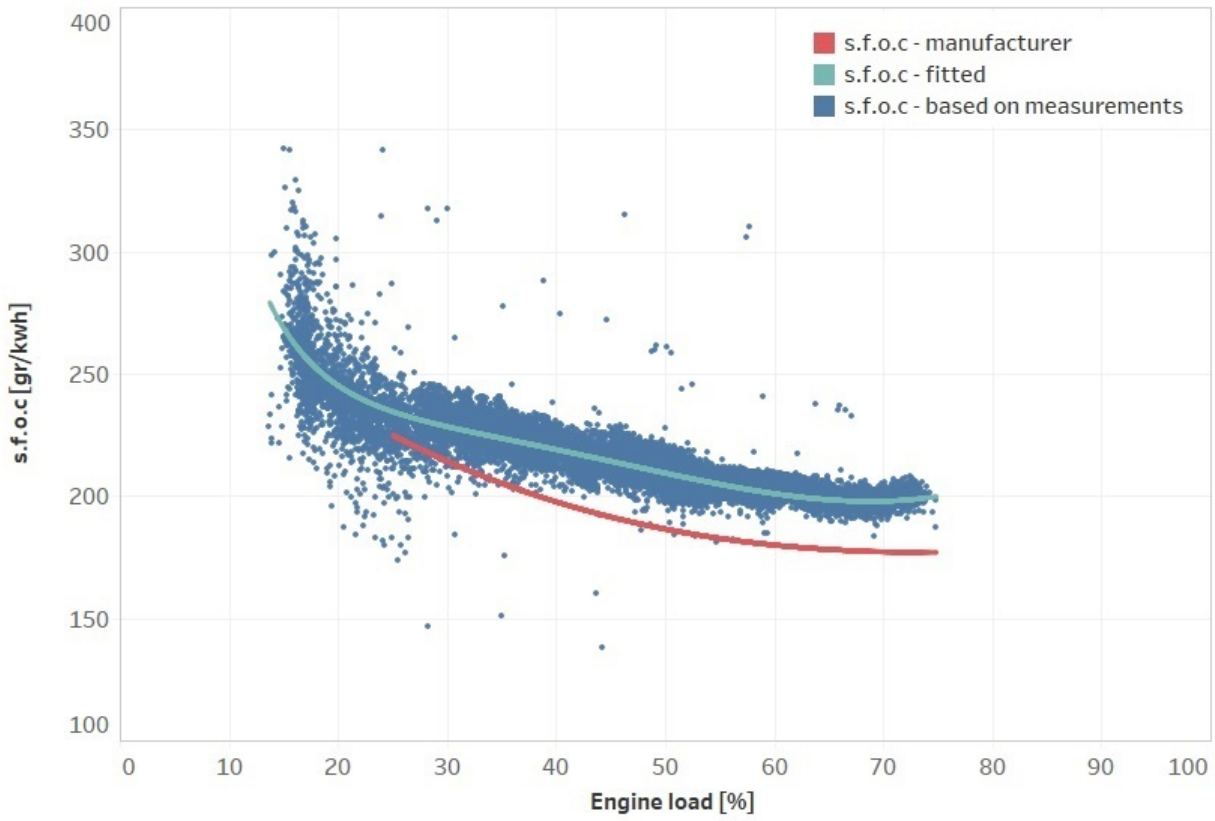

Figure 4.55: specific fuel oil consumption (s.f.o.c) versus engine load

In Figure 4.55 it is proven that the s.f.o.c in reality is higher (around 10 %) than the nominal value provided by the manufacturer. Thus it is decided to use the available measurements to create a simple model for the calculation of the fuel oil consumption. In this model the fuel consumption is dependent only to the engine load. In Figure 4.56 the measured fuel oil consumption versus the engine load is presented. The fitted curve to the measured values which is used for the calculation of the fuel consumption is also presented in Figure 4.56. It is important to mention that the engine load in Figure 4.56 ranges from 1,700 kW to 9,000 kW. The down limit is explained from from the combination of CPP and fixed rpm as it was explained previously. The upper limit of 9,000 kW is caused due to the fact that the S-type vessels do not sail in higher load the last years (so there are not available measurements for higher loads in the PMS). Thus in order to calculate the fuel consumption for an engine load higher than 9,000 a linear extrapolation to the fitted curve will be used.

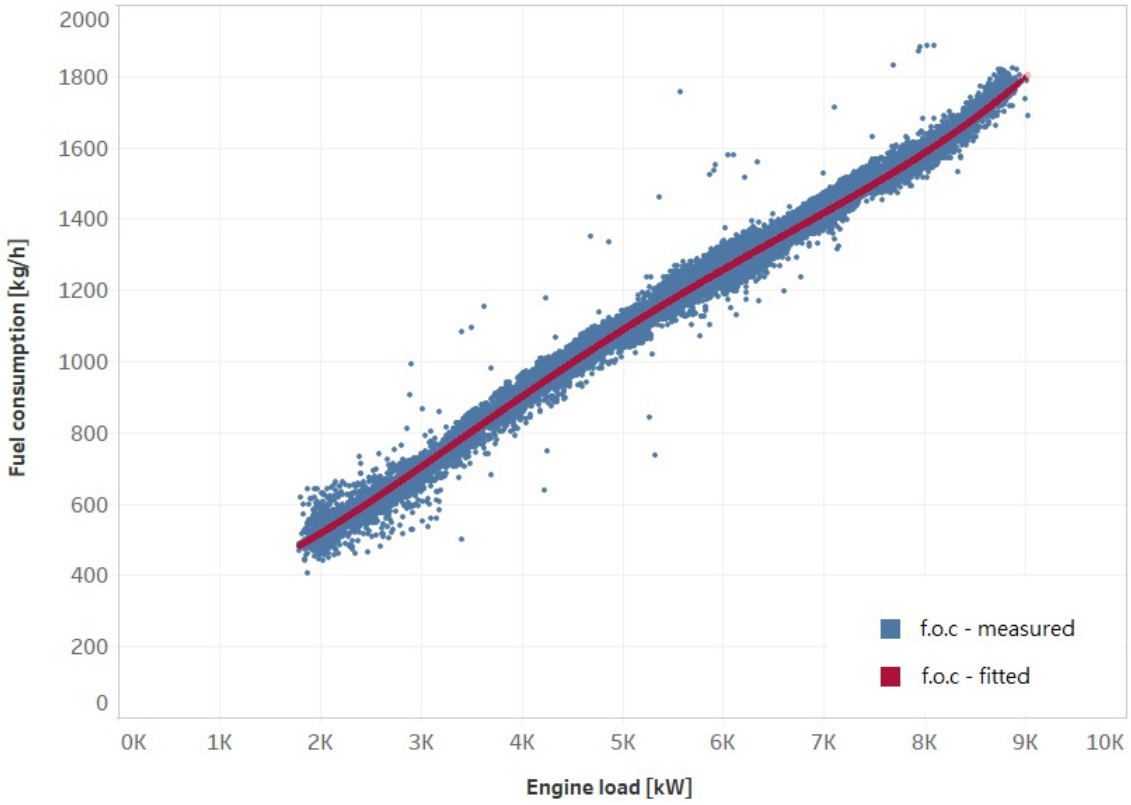

Figure 4.56: fuel oil consumption (f.o.c) versus engine load

4.3.9. Results of WBM

In order to examine the accuracy of the WBM, the historical data from the PMS will be used. As it was mentioned in Chapter 3, the PMS is recording data for the operating conditions of the vessels (speed, draft, trim, weather conditions) and the energy demand (shaft power, fuel consumption) with a frequency of 5 minutes. Thus every datapoint stored in the PMS contains information for the variables presented in Table 3.1. For every examined datapoint a calculation will be performed from the WBM for the shaft power and the fuel consumption. The required inputs of the WBM will be taken from the PMS and the calculated output will be compared to the measured value, stored as well in the PMS. However, it should be decided first which data for the speed through water will be used. As it was aforementioned, within Spliethoff the calculated speed through water is preferred, however both signals (calculated and measured from speed logger) are available in the PMS. The selection of which one will be used in the examination of the WBM accuracy will be done in the following section.

Speed through water signal selection

As it was aforementioned, the data from the speed logger is not used within Spliethoff due to the fact that the sensor is not very accurate. However, it is stored in the PMS. Thus, the speed through water that is used is calculated based on the speed over ground (taken from the GPS) and the speed of the currents (provided from the weather provider). In the report, the terms logger speed and calculated speed through water will be used for simplicity. Errors and inaccuracies can be identified in both speed signals. In order to decide which speed data had to be used, two datasets were created from the available data of the PMS, the difference between them was only be the speed input. The calculated speed signal was used as the speed data in the first dataset and the speed from the logger was used for the second dataset. Both datasets were given as input to the WBM and since the only difference between the two datasets was the speed through water data, based on the agreement between the calculated shaft power/fuel consumption from the model and the measured shaft power/fuel consumption from the PMS, we can evaluate which speed input is of better quality.

First the case of the speed logger is presented. In Figure 4.57, the speed logger signal, the speed over ground

and the calculated speed through water is presented for the vessel Slotergracht. Within Spliethoff it is known that the speed loggers of the vessels are not well calibrated and thus there is error in the measurement. This is what is observed in Figure 4.57, where the measurement of the speed logger is always higher than the calculated speed through water. Thus, it was examined whether a correction factor can be used for the speed logger signal. It should be mentioned that the situation is different in every vessel, which means that the correction method should be applied for every vessel. In addition, as it can be seen in Figure 4.58 a correction of the signal is not possible for the vessel Schippersgracht due to the high fluctuations. In Figure 4.59, it is shown how the equation for the correction of the speed logger signal for the vessel Slotergracht was determined. It is known within Spliethoff that in general the calculated speed through water is more accurate than the speed logger despite some issues which occur due to the bad predictions of the currents (more information are provided in the next paragraph). Thus, the calculated speed through water was used to derive a correction factor for the speed logger signal. The dataset, which was given as input to the WBM, concerning the speed logger case, contained the corrected speed through water signal. It should be noted that in Figure 4.59, the outliers have already been removed.

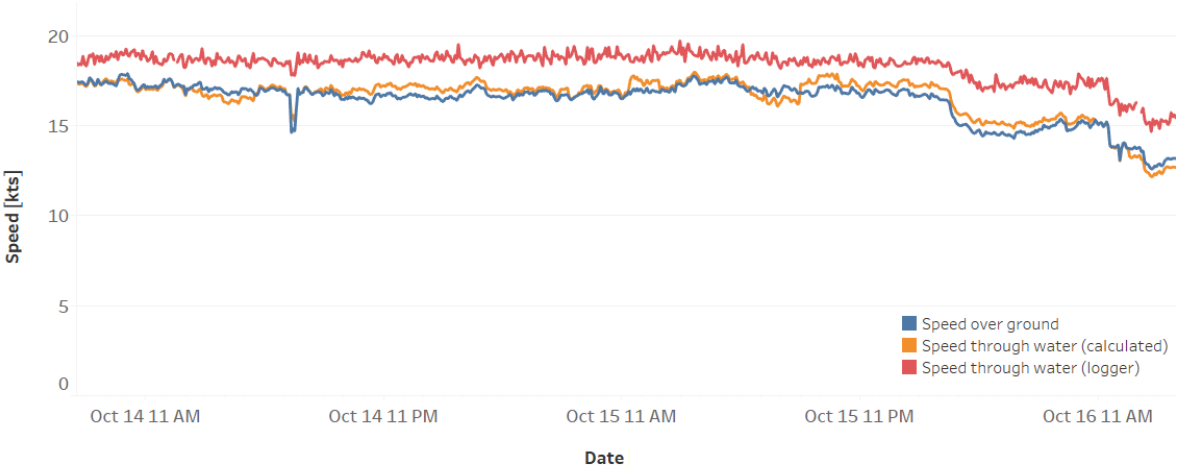

Figure 4.57: Speed through water and speed over ground for Slotergracht

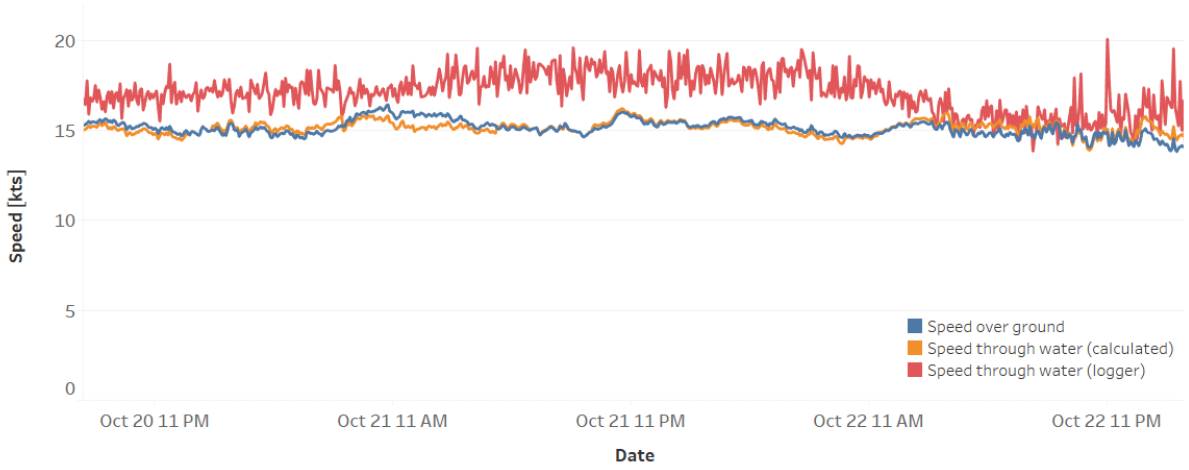

Figure 4.58: Speed through water and speed over ground for Schippersgracht

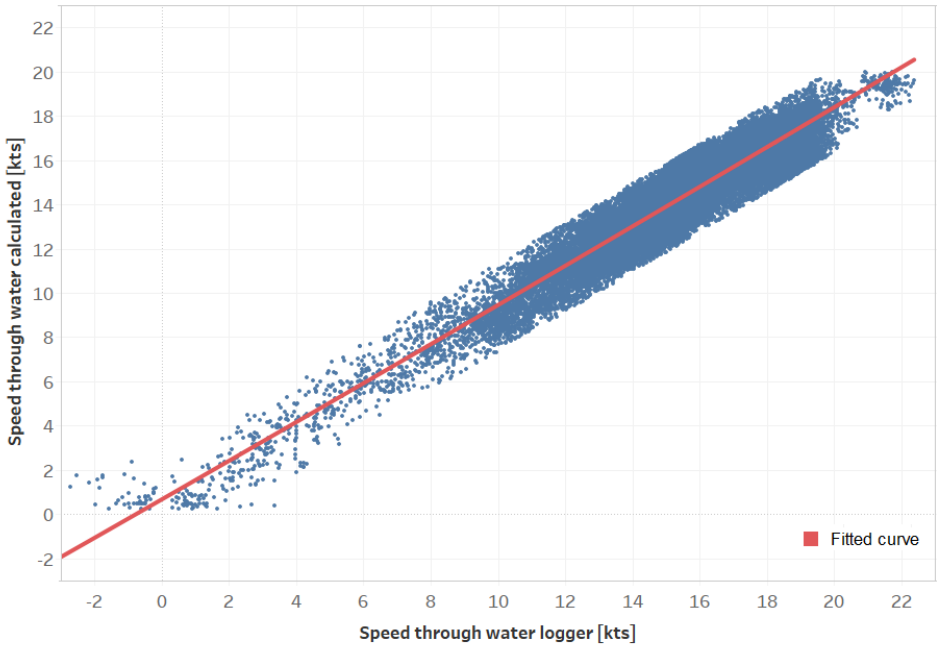

Figure 4.59: Speed through water logger signal correction method

Regarding the calculated speed through water, the accuracy is mainly influenced from bad prediction of the currents. It is known within Spliethoff that the currents are bad predicted mainly at areas close to the shore, in areas which are enclosed by land (i.e English Channel) and the east coast of North America (due to the Gulf stream). An example of such a situation is presented in Figure 4.60, where it can be seen that the calculated speed through water suddenly dropped from approximatelly 15 knots to almost 10 while the speed over ground was stable and a more moderate decrease was observed in the speed through water from the logger. This resulted from wrong data about the currents. However, the calculated speed though water is preferred within Spliethoff and it is believed that the accuracy is sufficient despite the issues that occur occasionally due to the bad predictions of the currents. The dataset was filtered manually and data where the calculated speed through water seem to be wrong were filtered out.

Figure 4.60: Speed through water and speed over ground for Slotergracht

Both datasets were filtered, to eliminate datapoints in which an error could easily be identified. Datapoints which included missing values were excluded as well. In Figures 4.61 and 4.62, the fuel oil consumption data from the PMS versus the speed through water is plotted for both the calculated and the logger's speed through water (for the vessel Slotergracht). It is clear that the spread in Figure 4.61 is smaller. However, this does not necessarily mean that the speed signal from the logger is more accurate.

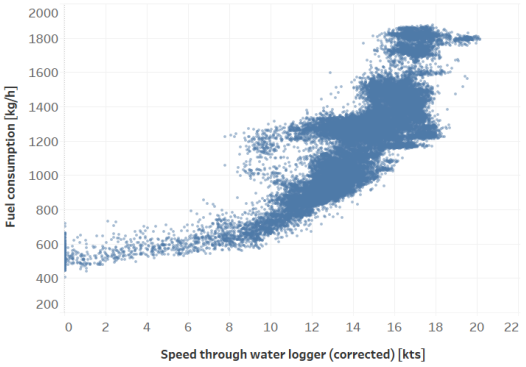

Figure 4.61: Fuel consumption versus speed through water from logger (corrected and filtered)

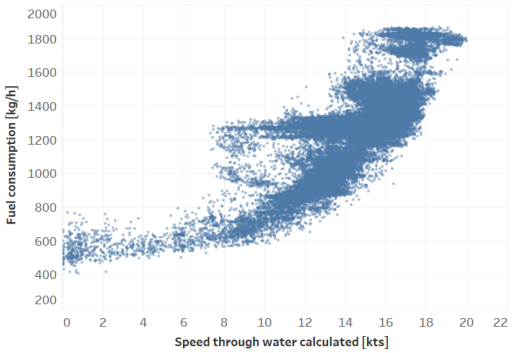

Figure 4.62: Fuel consumption versus speed through water calculated (filtered)

The procedure was applied for the vessels Slotergracht and Singelgracht. Thus, four datasets were created in total, two for each vessel. The datasets were given as input to the WBM which for every datapoint performed a calculation about the fuel consumption. Afterwards, the calculated fuel consumption (by the WBM) was compared to the measured fuel consumption which is stored in the PMS. To evaluate which dataset is of better quality, the R^2 value and the $RMSE$ value were calculated between the measured fuel consumption and the estimated by the WBM. The results are presented in Table 4.4.

	Calculated speed (filtered)		Speed from logger (corrected and filtered)	
	Slotergracht	Singelgracht	Slotergracht	Singelgracht
R^2	0.8313	0.7692	0.765	0.584
RMSE [kg/h]	109	119.5	127.9	157.2

Table 4.4: Evaluation of speed input

It is clear from the results presented in the Table 4.4 that the datasets in which the calculated speed through water was used resulted in better agreement between the measured fuel consumption and the calculated one (by the WBM). The conclusion is that despite the attempt to correct the speed though water signal from the speed logger, the calculated speed through water signal is of better quality and thus this data will be used for the rest of the work.

Results

The historical data regarding Schippersgracht's last year of operation (around 45000 data points), were used to further examine the accuracy of the model. The input values that should be given to the WBM were taken from the database, and after the WBM performed the calculation for every data point, the fuel consumption/shaft power that was calculated from the WBM was compared with the measured fuel consumption/shaft power stored in the PMS. It should be noted that for the Schippersgracht the water depth data are not available, and thus, the shallow water added resistance component of the WBM was neglected (influence from shallow water was not taken into account).

In Figure 4.63 the comparison between the measured and the predicted shaft power value is presented. The green line corresponds to the situation where the predicted value is equal with the measured, while the two lines are the ±10% error bounds. It is clear that there is a high concentration of data points within the ±10% area (within the red lines). It is calculated that for the prediction of the shaft power 68.77% of the dataset lies within the area of ±10% whereas if the limit is increased to ±15% the same percentage rise to 83.83% (further information is presented in Table 4.5). It should be noted that the error was calculated with the following formula. The absolute value of the error was mainly used.

$$ErrorFuelCons = \frac{FuelConsCalculated - FuelConsMeasured}{FuelConsumptionMeasured} \tag{4.24}$$

Since the relation that is used for the calculation of the fuel consumption is quite simple and involves only the shaft power it was expected that the same situation will hold in the comparison between the measured and the predicted fuel consumption (Figure 4.64). Regarding the fuel consumption, 78% of the dataset lies within the ±10% whereas 89.39% lies within the ±15%. More information are presented in Table 4.5. As it can be seen the fuel consumption is predicted with higher accuracy compared to the shaft power. This can be explained due to the fact that the shaft power sensor gives a signal with high fluctuations (especially in harsh weather conditions). In order to calculate the mean value for the time-window (5 min) an average is taken from 5 measurements and this value is stored to the PMS. Thus it clear that the average value that is used might be overestimated or underestimated in some cases due to the small sample. On the other hand, the fuel sensor gives a more stable signal which is not affected by the environmental conditions. Therefore, since the fuel's flow sensor gives data of better quality it is decided to continue the comparison on the basis of the fuel consumption data from the PMS instead of the shaft power data.

Error band	Percentage of datapoints within the error band for shaft power prediction	Percentage of datapoints within the error band for fuel consumption prediction
5%	40.22%	49.25%
10%	68.77%	78%
15%	83.83%	89.39%
20%	90.54%	94.48%
25%	94.21%	97.32%

Table 4.5: Percentage of datapoints within the given error bands for WBM

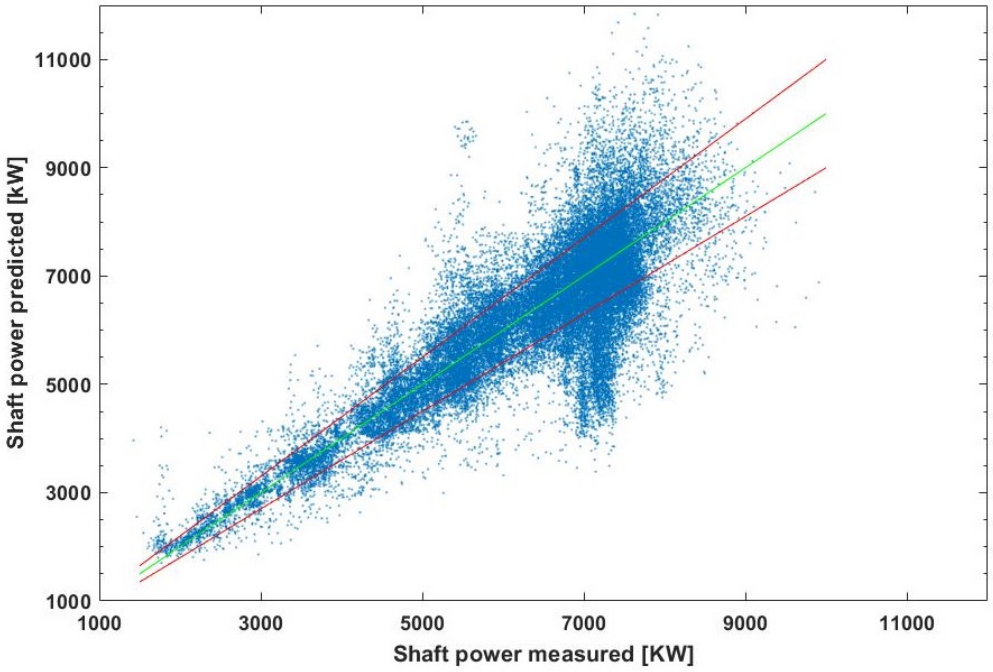

Figure 4.63: Predicted shaft power from WBM versus measured shaft power (47398 datapoints)

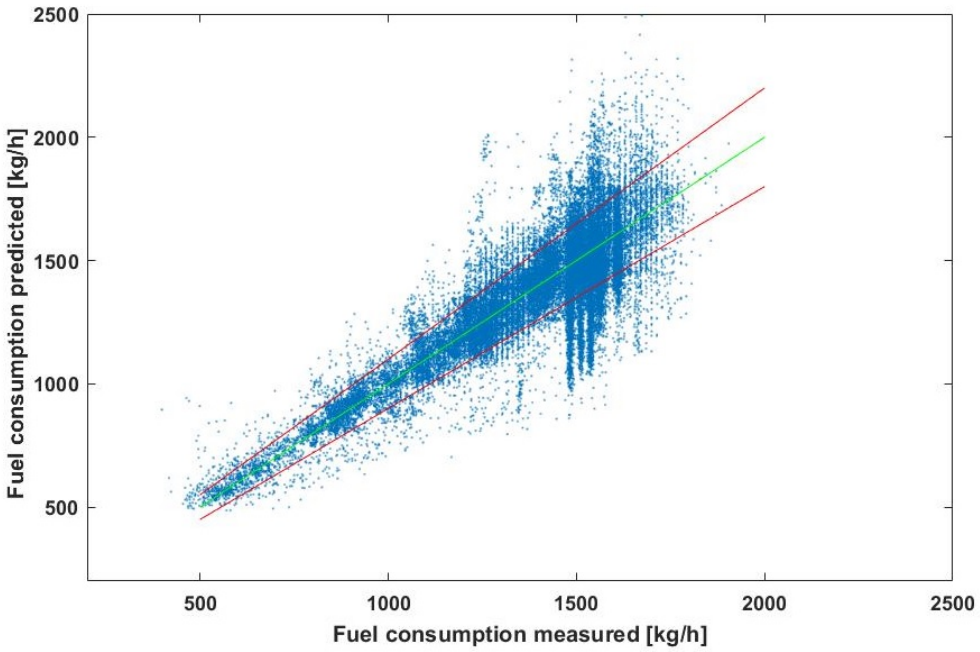

Figure 4.64: Predicted fuel consumption from WBM versus measured fuel consumption (47398 datapoints)

As it can be seen in Figures 4.63-4.64 in some cases the deviation between the predicted and the measured value is quite large. Due to the fact that the data from the PMS are not free of errors, part of these outliers can be explained from wrong values in the PMS (speed, weather conditions heading etc, or wrong measured values from the shaft/fuel sensor due to technical issues). On the other hand, it is reasonable that the theoretical model has weak points. Sub-models of the theoretical model were derived with limited information (i.e resistance curves, propeller curves, trim effect) while the added resistance sub-models that were used, are well established models but their accuracy is also not perfect (i.e wind force coefficient from Blendermann

[7], STA-wave 2 [16]).

Thus it should be examined if the large errors between the measured value and the predicted from the PMS are caused due to poor accuracy of the WBM or are mainly a result of wrong input values which are stored in the PMS. The routes followed from the vessel the last 12 months are plotted in the map. The colour indicates the error between the measured fuel consumption and the predicted one (by the WBM) expressed in percentage. In that way areas where the predicted value and the measured fall far from each other can be selected for further investigation. Figure 4.65 gives a missleading impression due to the high amount of the data points, which are overlaping with each other and thus conclusions cannot be extracted. Thus, the data points are separated in classes based on the error (in percentage) between the predicted and the measured value and are plotted separately (Figures 4.66-4.71). It should be noted that the absolute error is plotted.

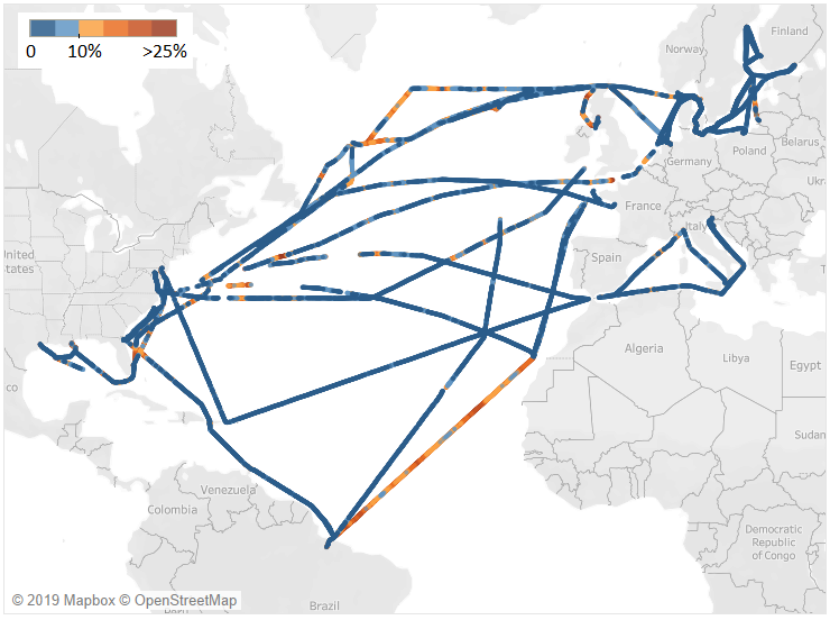

Figure 4.65: Error (%) between predicted (by WBM) and measured fuel consumption

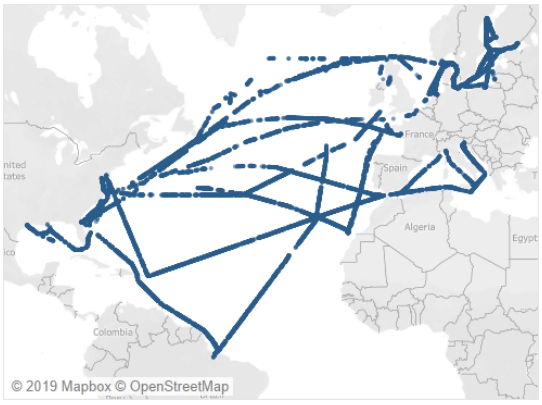

Figure 4.66: Error(%) between predicted (by WBM) and measured fuel consumption, class 0-5%

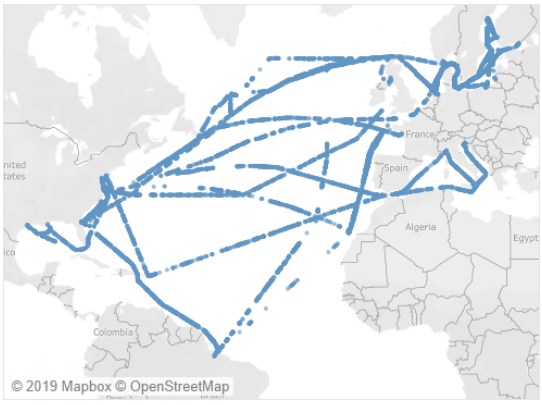

Figure 4.67: Error(%) between predicted (by WBM) and measured fuel consumption, class 5-10%

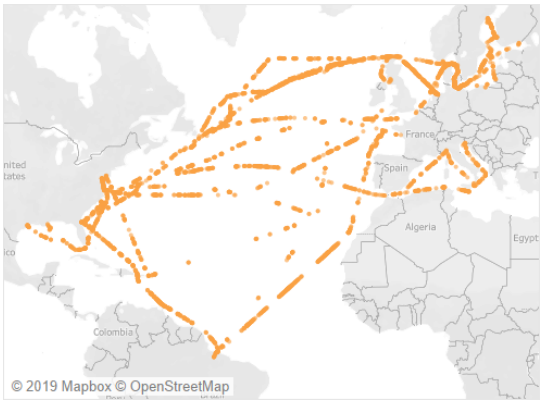

Figure 4.68: Error(%) between predicted (by WBM) and measured fuel consumption, class 10-15%

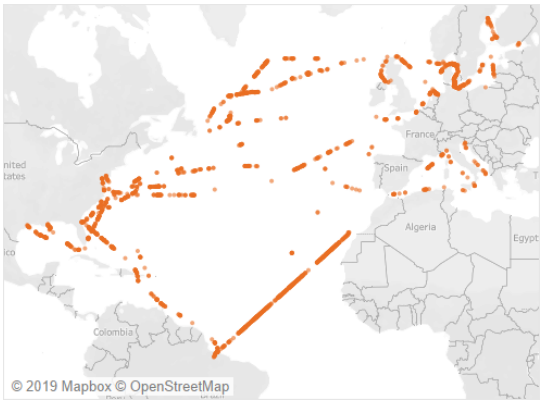

Figure 4.69: Error(%) between predicted (by WBM) and measured fuel consumption, class 15-20%

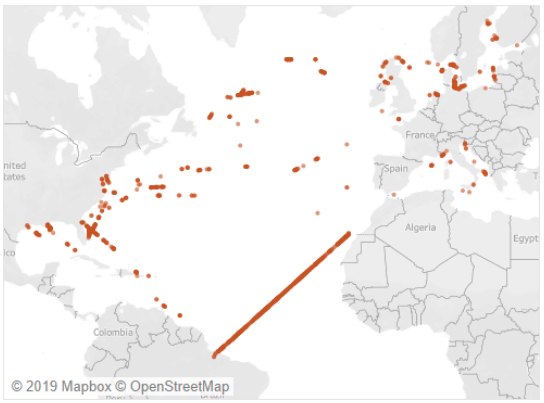

Figure 4.70: Error(%) between predicted (by WBM) and measured fuel consumption, class 20-25%

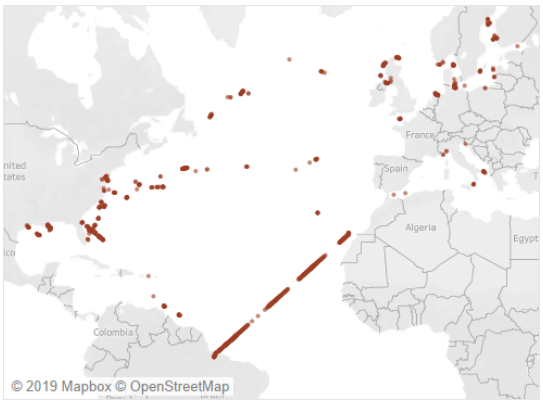

Figure 4.71: Error(%) between predicted (by WBM) and measured fuel consumption, class >25%

A general observation is that in almost all voyages the density of the predictions which lie in the classes of 0-5% and 5-10% outweighs the remaining classes. An exemption is the voyage from Brazil to the Canary islands, which will be discussed separately in a later stage. From the whole dataset a percentage of 78% lies within the first two classes, meaning that 78% was predicted with an error less that 10%. In Figures 4.69-4.71 it is observed a high frequency of occurrence in areas close to the shore, fact which indicates that the prediction of the currents is worst at areas close to the shore (as it is believed within Spliethoff). Regarding the voyage from Brazil to the Canary islands, due to the fact that the prediction is bad for the entire voyage it is expected that the input values from the PMS were wrong. Most likely, the draft (which is reported by the crew) or the speed over ground (technical problem with GPS) was reported wrongly. The case that the shaft power sensor or the fuel flow sensor was faulty cannot be true since their measurements match with each other. At this voyage the vessel's draft was reported to be 10.99 m which is almost the upper limit of the attainable drafts. Thus, the case that the model is not performing well at high drafts was also considered, but after examination this case was proven wrong due to the fact that the model is accurate at the draft of 10.8 m and thus such a large difference does not seem reasonable for the draft of 10.99 m.

As it was mentioned above, part of the large deviations between the predicted and the measured values are caused by wrong inputs from the PMS while the rest from the performance of WBM. After taking a closer look to the data some cases where the PMS data were wrong or the WBM could not predict well, were identified and will be discussed briefly. Afterwards, the accuracy of the WBM will be further examined by examining separately every component with a strong influence on the energy demand (speed, draft, wind, waves, swell).

- The most common error observed in the data of the PMS is related with the data of the currents. As it was explained in the beginning of this Chapter, the calculated speed through water that is used is not perfect (however the speed through water from the logger is worse). It is also known within Spliethoff

that in the case of the calculated speed through water, inaccuracies are mainly observed in areas close to the shore, areas enclosed by the shore (i.e. English channel) and the East coast of North America (due to bad predictions of the currents). As it can be seen in Figure 4.70-4.71 the frequency of occurrence of bad estimated values is high at the regions mentioned above. It is important to mention that an inaccuracy of (±0.5 kts) in the speed through water can result in difference between the calculated and the estimated shaft power in the order of 10-15%. Thus for the case that a wrong speed through water is recorded for a datapoint and is stored in the PMS, if this speed input is given as input to the WBM then it is clear that the calculated fuel consumption from the WBM will not match with the measured value stored in the PMS. In the regions mentioned above, the difference between the measured and the predicted shaft power is up to 30-40% when the currents' prediction is not correct and in some cases difference of up to 90% was observed in situations where the direction of the currents was wrong. It is worth mentioning here that if the areas where it is known that the current predictions are often not accurate, and the voyage from Brazil to Canary islands are not evaluated, only 0.6% of the data are predicted with a difference of 20% or higher compared to the measured values.

- Another reason of wrong input data is related with the weather prediction (wind, waves, swell). It was observed that in some cases the wave height was not predicted correctly. A second observation was that in other cases although the wave height was predicted correctly, the corresponding time of occurrence was not correct.

- The data from the PMS are not filtered which means that except from errors (from sensors) they also contain data from situations for which the model does not account for. An example is when the vessel is in port and maneuvering assisted by tugs, in that case the shaft power/fuel consumption cannot be predicted. In addition, difference between the measured and the calculated values is observed when the vessel is accelerating or decelerating. When the vessel accelerates, the power is rising instantly, however the speed takes some time until it stabilizes again. The same applies when the vessel is decelerating. In the meanwhile, due to this dynamic phenomenon (which is not taken into account by the model) the power/fuel consumption is not well predicted. Indicatively the resulted error lies within 10-15 %.

In order to further examine the performance of the WBM, every component with strong influence on the vessel's energy demand was examined separately with the following procedure. The amplitude was divided in classes (i.e waveheight [0-1m], [1-2m]) and then for each class the distribution of the errors (in percentage) between the measured and the predicted fuel consumption was plotted. A high percentage of bad predicted values will give us an indication the examined component is no taken into account properly in the WBM. In addition, a similar distribution is expected between the different amplitude classes (i.e between distributions for wave height 0-1 and 2-3) in order to prove that the errors are mainly caused from random factors and not the model itself. The results are presented below (Figures 4.79-4.92).

Error distribution based on the speed

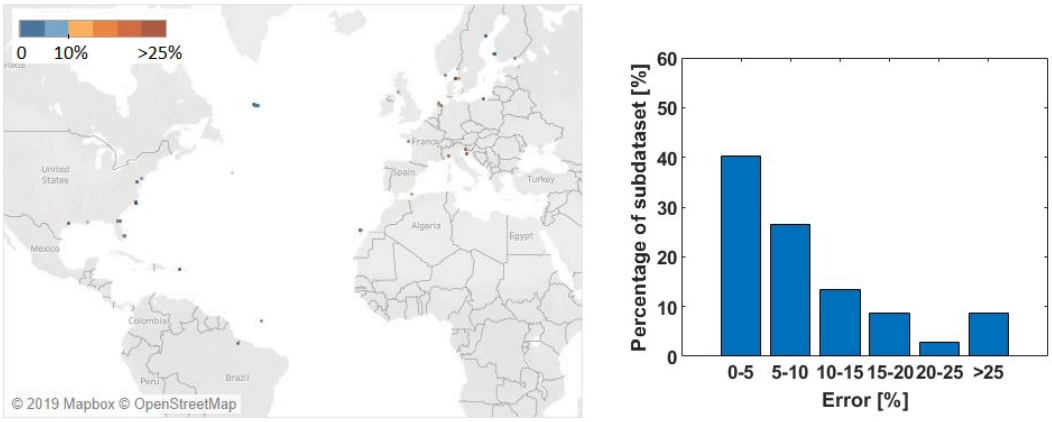

Figure 4.72: Error distribution (by WBM) for the subdataset (321 datapoints) of speed 0-5 kts

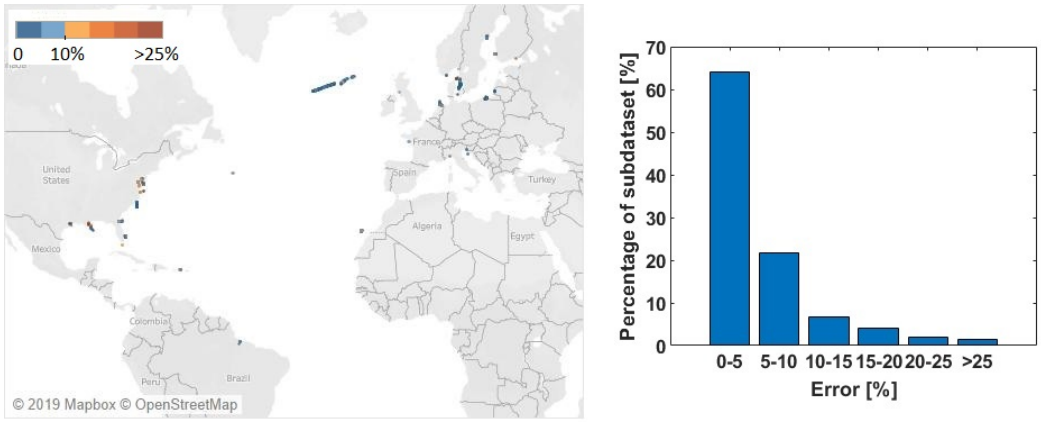

Figure 4.73: Error distribution (by WBM) for the subdataset (1299 datapoints) of speed 5-10 kts

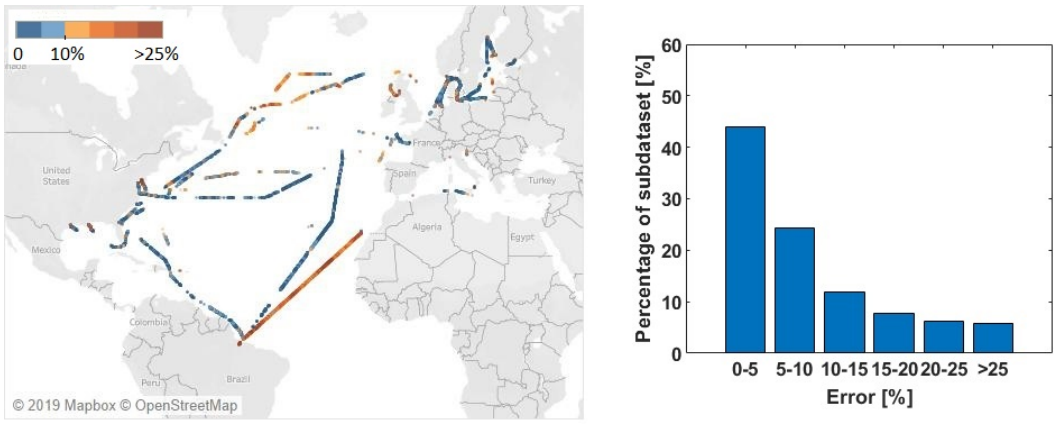

Figure 4.74: Error distribution (by WBM) for the subdataset (13797 datapoints) of speed 10-15 kts

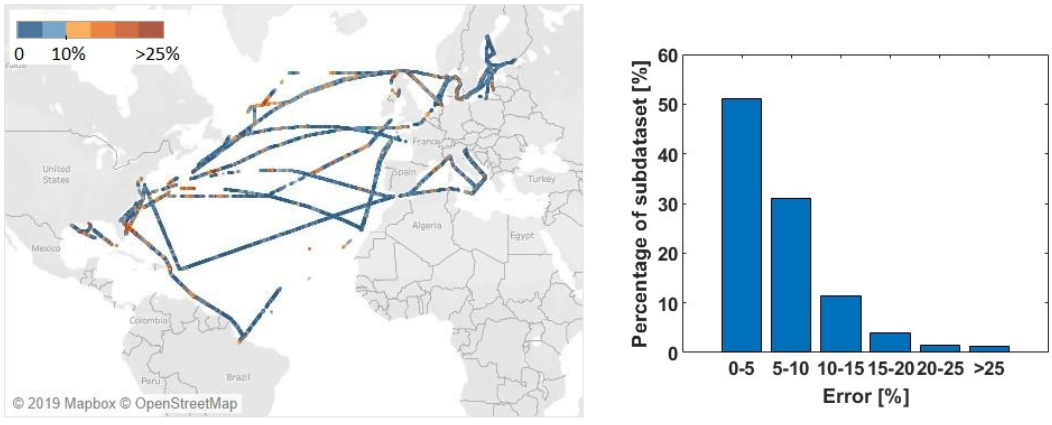

Figure 4.75: Error distribution (by WBM) for the subdataset (32361 datapoints) of speed 15-20 kts

Error distribution (by WBM) based on the draft

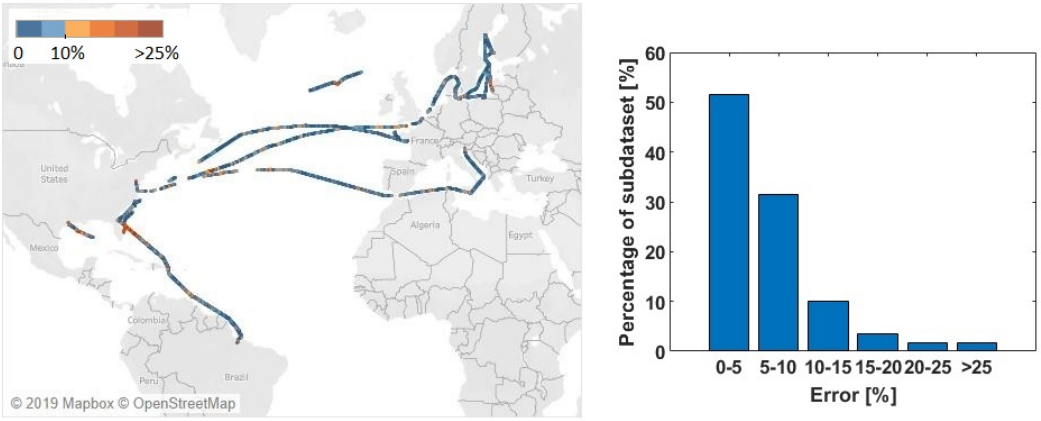

Figure 4.76: Error distribution (by WBM) for the subdataset (15355 datapoints) of draft 6-7.5 m

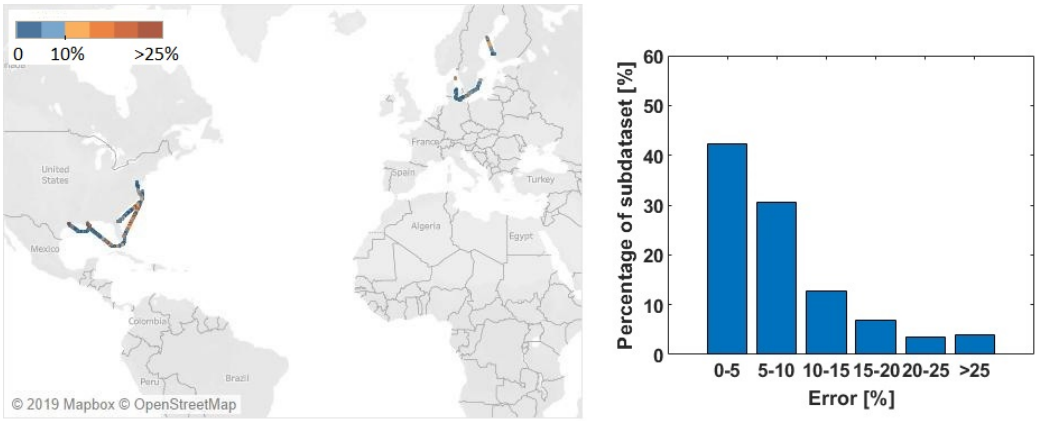

Figure 4.77: Error distribution (by WBM) for the subdataset (2814 datapoints) of draft 7.5-9 m

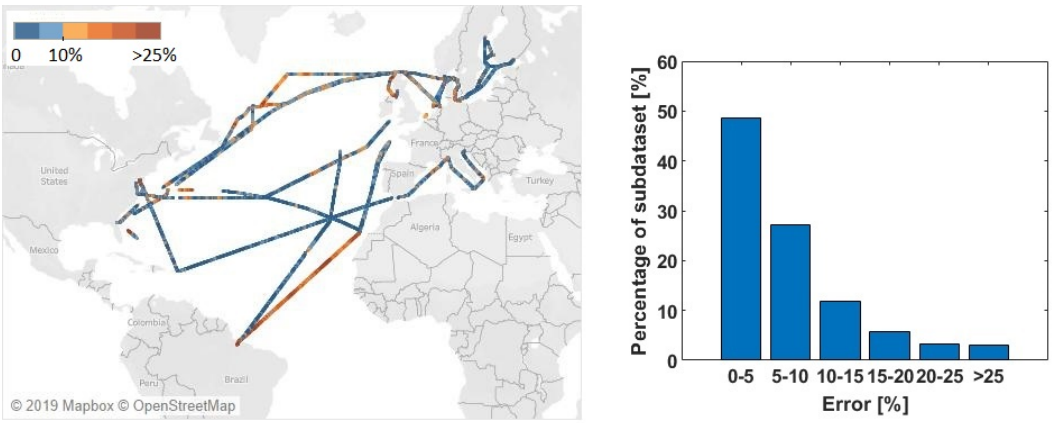

Figure 4.78: Error distribution (by WBM) for the subdataset (29607 datapoints) of draft 9-11 m

Error distribution based on the wave height

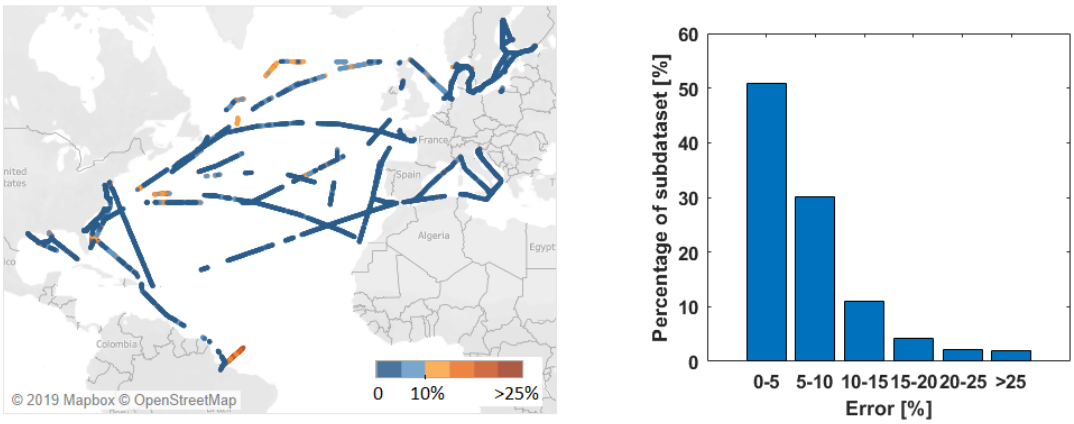

Figure 4.79: Error distribution (by WBM) for the subdataset (25523 datapoints) of wave height 0-1 m

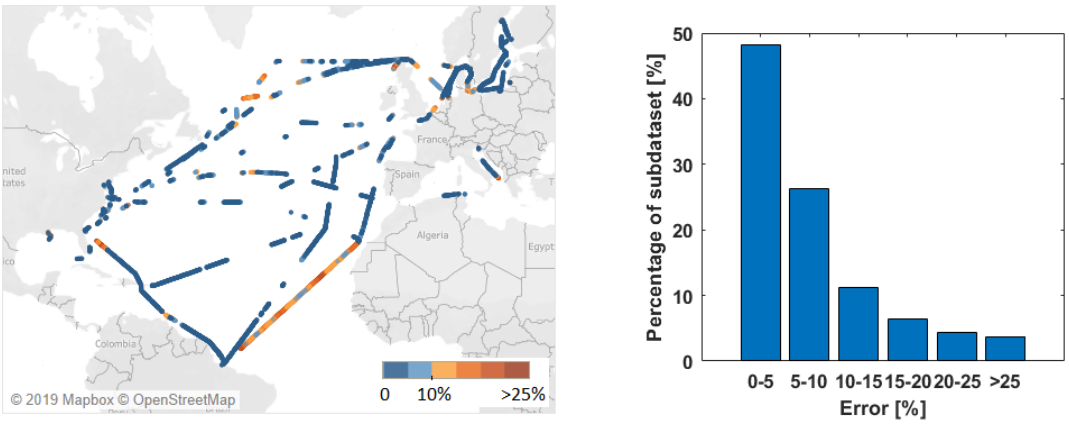

Figure 4.80: Error distribution (by WBM) for the subdataset (16021 datapoints) of wave height 1-2 m

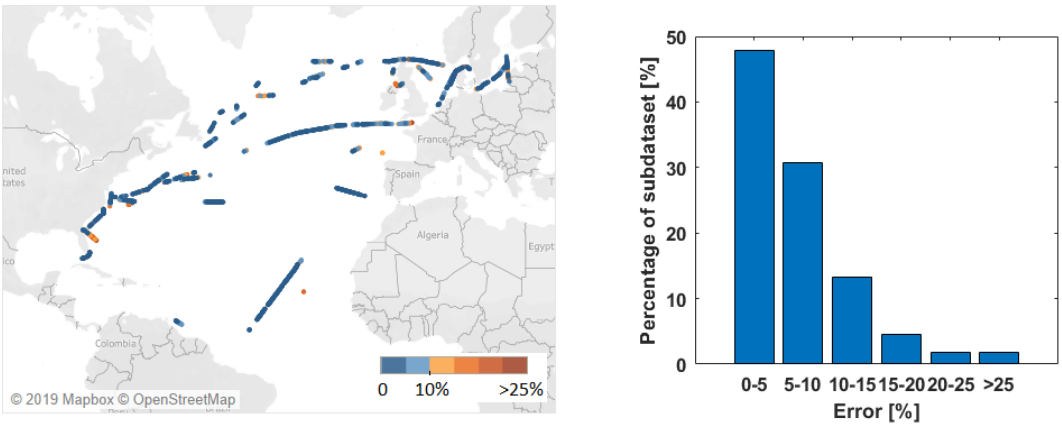

Figure 4.81: Error distribution (by WBM) for the subdataset (5680 datapoints) of wave height 2-3 m

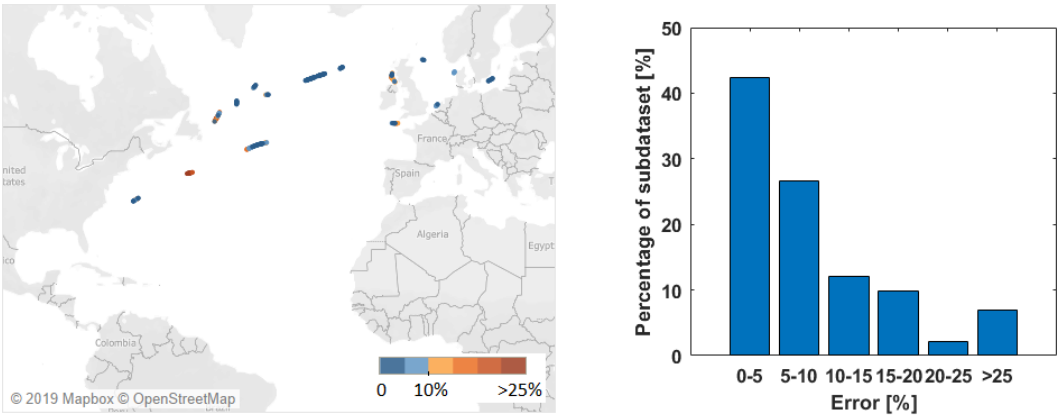

Figure 4.82: Error distribution (by WBM) for the subdataset (789 datapoints) of wave height 3-4 m

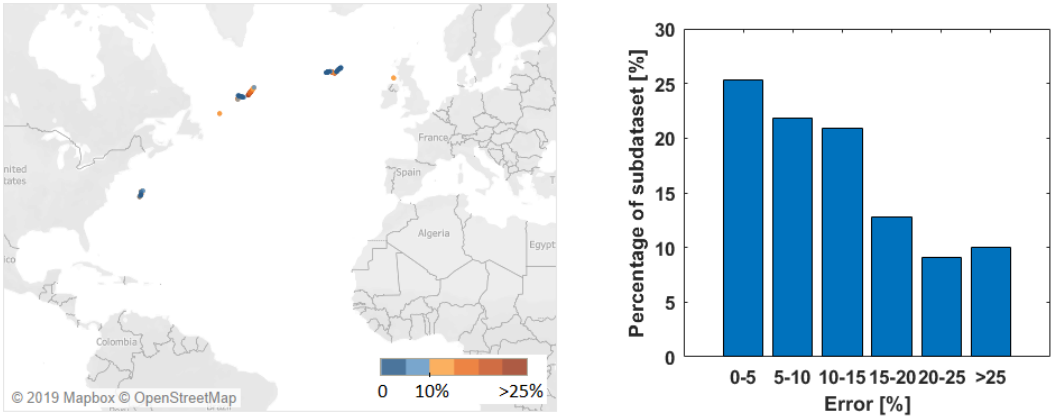

Figure 4.83: Error distribution (by WBM) for the subdataset (320 datapoints) of wave height 4-6 m

Error distribution based on the swell height

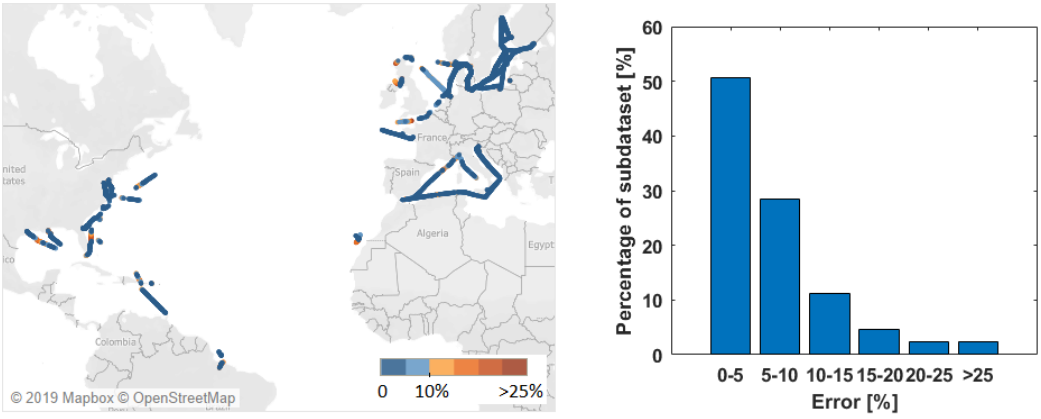

Figure 4.84: Error distribution (by WBM) for the subdataset (15773 datapoints) of swell height 0-1 m

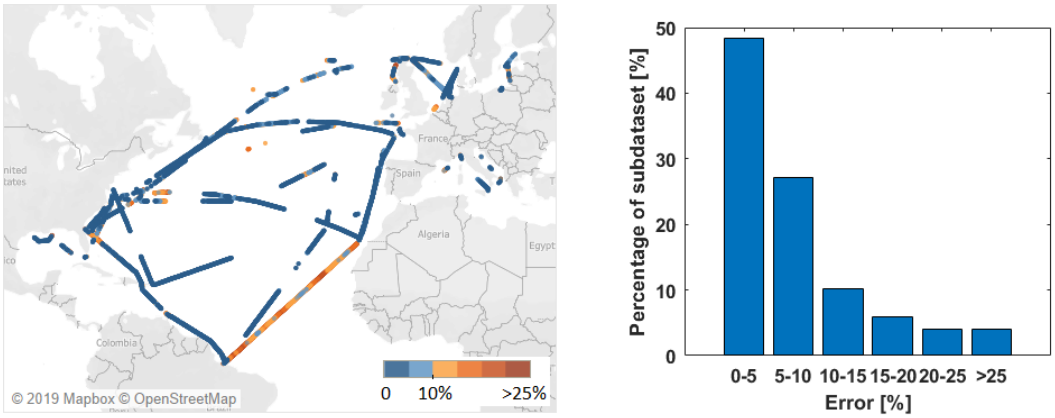

Figure 4.85: Error distribution (by WBM) for the subdataset (19746 datapoints) of swell height 1-2 m

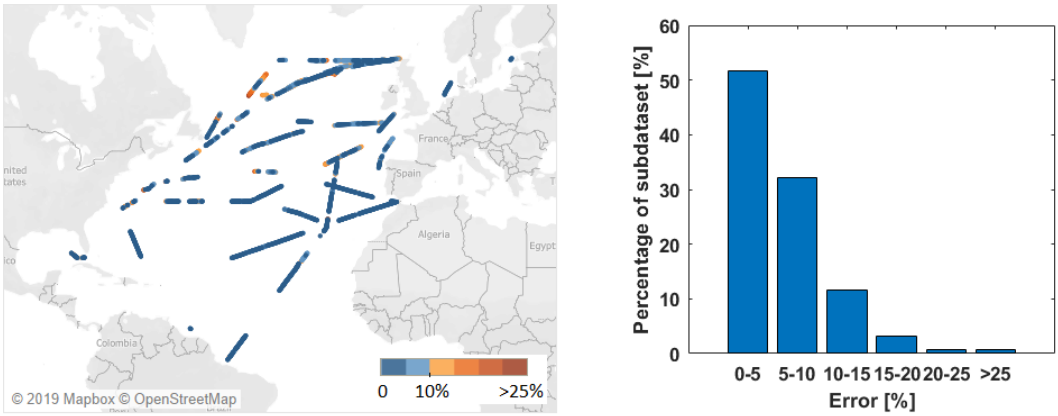

Figure 4.86: Error distribution (by WBM) for the subdataset (9289 datapoints) of swell height 2-3 m

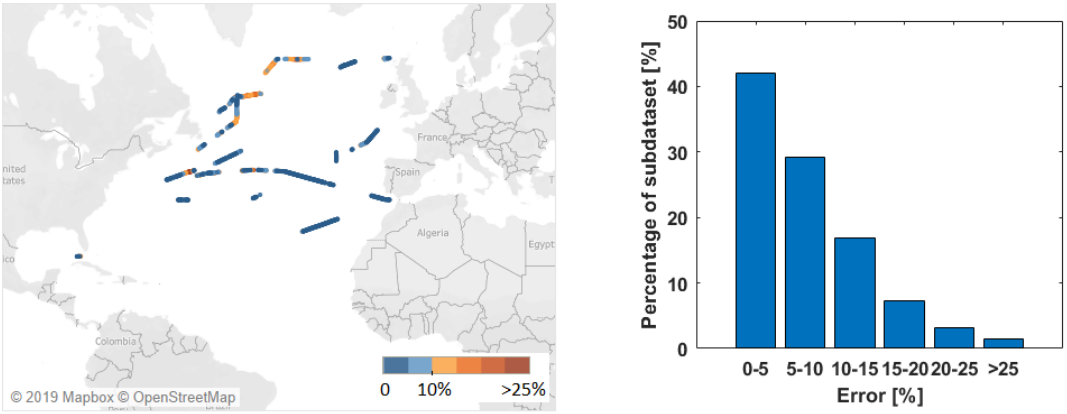

Figure 4.87: Error distribution (by WBM) for the subdataset (3342 datapoints) of swell height 3-4 m

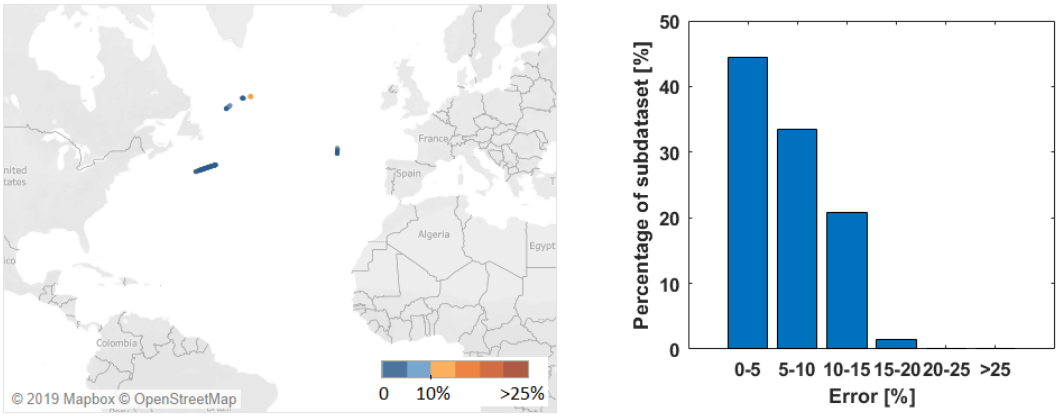

Figure 4.88: Eror distribution (by WBM) for the subdataset (284 datapoints) of swell height 4-6 m

Error distribution based on the wind speed

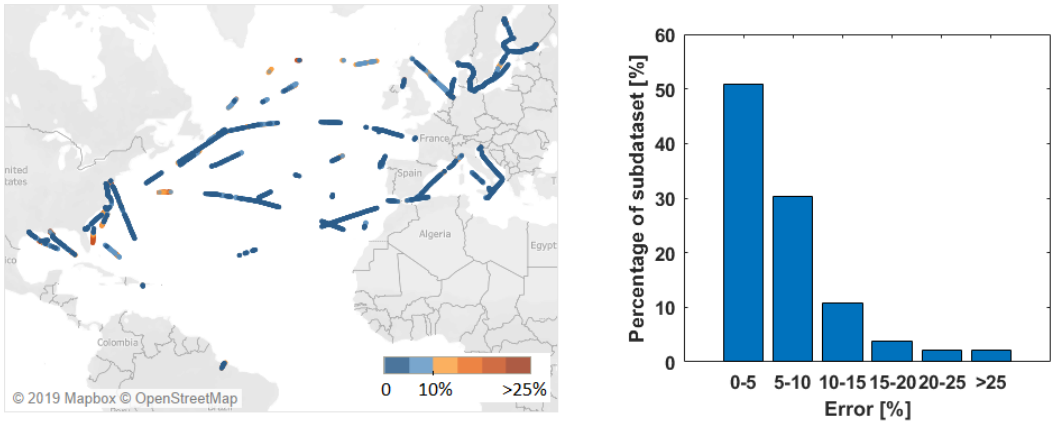

Figure 4.89: Error distribution (by WBM) for the subdataset (11213 datapoints) of wind speed 0-10 kts

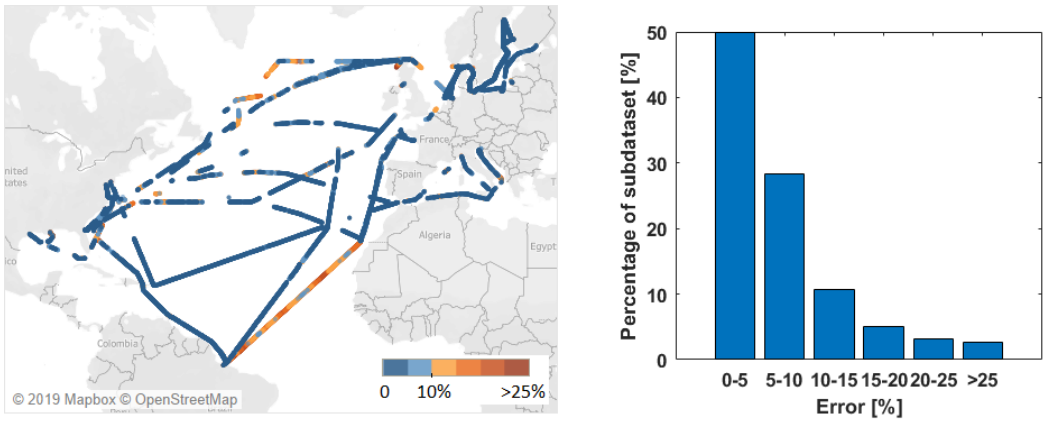

Figure 4.90: Error distribution (by WBM) for the subdataset (30716 datapoints) of wind speed 10-20 kts

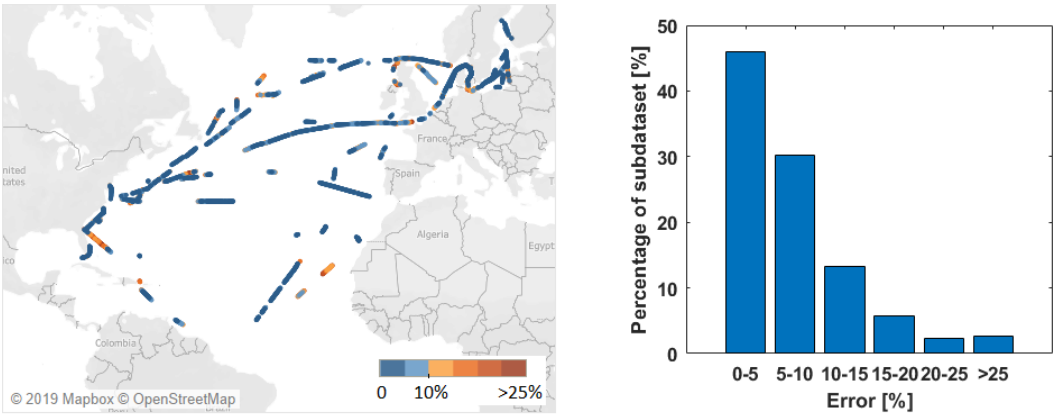

Figure 4.91: Error distribution (by WBM) for the subdataset (10279 datapoints) of wind speed 20-30 kts

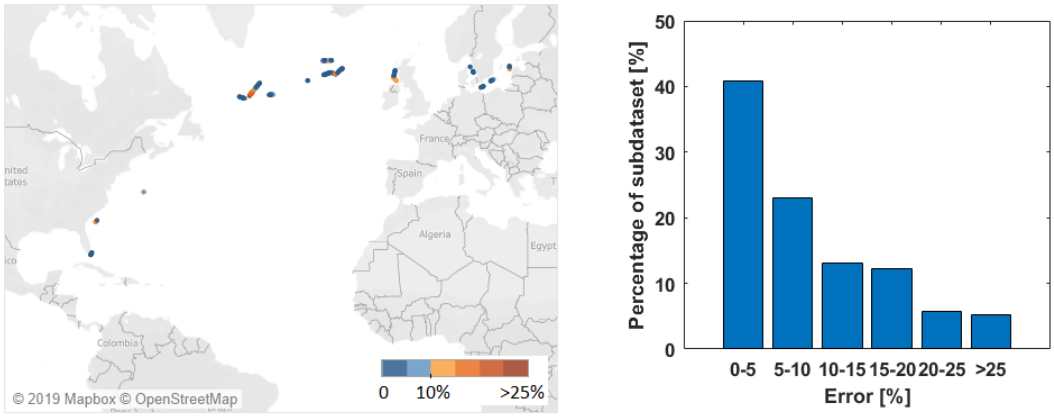

Figure 4.92: Error distribution (by WBM) for the subdataset (649 datapoints) of wind speed 30-40 kts

In Figures 4.79-4.92, it was proven that there is not a parameter for which large errors were observed. It is observed a higher concentration of errors higher that 25% in the cases of waveheight 3-4 m and 4-6 m however this fact is not enough to make the conclusion that the model for the added resistance of the waves is not performing well. The fact that the cases of the 3-4m and 4-6m waveheight were observed in areas where the prediction of the currents is not good in combination with the low number of observations in these classes, leads to the question if these data can be trusted. In addition, in Figure 4.87 we observe that for the 3-4m swell, where the position of occurrence is more widely distributed, the model performs good. The fact that the models of the added resistance due to swell and added resistance due to waves are based on the same method, leads to the conclusion that the situation observed in Figures 4.82-4.83 is not due to the bad performance of the wave model but due to data of bad quality.

5

Data-driven model

In this chapter it will be investigated whether the available data from the Performance Monitoring System (PMS) can be used to develop a model for the fuel consumption prediction of the S-type vessels (completely based on the data without using the knowledge of the physical system). Since, the development will be based solely on the historical data from the PMS, the model will be a Black Box Model. In addition, it will be attempted to combine the WBM and the BBM to examine whether better results can be achieved in this way. Finally, the accuracy of the aforementioned models will be compared.

5.1. Introduction to supervised learning

Supervised learning involves building a model for predicting an output based on one or more inputs. In a more mathematical definition the supervised learning can be described as the problem of approximating a mapping function (h) from input variables (X) to output variables (Y) [51]. The goal is to find the best mapping function (h) given the available time and resources. In this thesis the goal is to create a model for the fuel consumption of the vessel (Y), the input is limited to data which are stored in the Performance monitoring system (X) (speed, weather conditions, etc). More information about the data which are collected and stored from the Performance monitoring system was given in Chapter 3. Supervised learning problems are categorised in regression problems and classifications problems [51]. The difference between the two categories is that regression is the problem of predicting a continuous quantity output, while classification is the problem of predicting a discrete class label. In a different way, regression is the problem where the value of a continuous quantity is predicted based on the inputs, while classification is the problem of predicting the category/label based on the inputs. Therefore, it is clear that in this thesis a regression model will be developed.

The development of Machine learning (ML) models relies on the availability of data. The existence of a large dataset where both the input variables and the output variables are known, is necessary. The development of a ML model consists of two phases, the training phase and the validation phase. The available dataset is separated in two smaller, with one being assigned to each phase. The training dataset, consists of 70-85% of the initial dataset, while the validation dataset accounts for the remaining 15-30%. The purpose of the training phase is to find the best approximating function $h(x)$. Thus, the training phase is an iterative process where many approximating functions h are tested in order to find the one leading to the best result. In order to select the final model (approximating function h) the average error is calculated for every candidate model, as shown in the following equation.

$$L_n(h) = \frac{1}{n}\sum_{i=1}^{n} l(h(x_i), y_i)$$

where $l(h(x), y)$, is a loss function calculating the discrepancy between the true value y and the estimated value $h(x)$ [29]. One strategy, could be to select the model which leads to the lower average error [51], however this approach is usually avoided since sometimes leads to over-fitting of the model to the training dataset. A more effective approach is to modify the selection process by employing a function where both the average error and the over-fitting of the model are taken into account [46]. This can be done by employing a measure

for the complexity of the model $C(h)$. Therefore, the selection of the final model is made by the following equation.

$$h : min\{L_n(h) + \lambda C(h)\}$$

where, λ is a hyperparameter that is used to regulate the trade-off between the overfitting tendency, caused by the minimization of the average error and the underfitting tendency caused by the minimization of the complexity measure. The complexity measure depends on the ML approach that is followed, while λ must be set a priori.

In this study the Support Vector (SV) regression algorithm will be used. In the following paragraphs more information will be presented about the method of SV regression, both regarding the mathematical formulation but also about the methods that were used in this research to develop the model. In the case of SV regression the goal is to find the function h that has at most ϵ deviation from the actual value, for the entire dataset and at the same time is as flat as possible [44]. The case of a linear function h will be described first. In that case the approximating fuction takes the form

$$h(x) = \langle w, x \rangle + b$$

where $w \in R^d, b \in R$ and $\langle \cdot, \cdot \rangle$ the dot product in X.
In the case of SV regression is derived from the solution of the following optimization problem.

$$minimize \quad \frac{1}{2}\|w\|^2 + C\sum_{i=1}^{n}(\xi_i + {\xi_i}^*)$$

subject to

$$y_i - \langle w, x_i \rangle - b \leq \epsilon + \xi_i$$

$$\langle w, x_i \rangle + b - y_i \leq \epsilon + {\xi_i}^*$$

$$\xi, \xi^* \geq 0$$

where $\|w\|^2 = \langle w, w \rangle$, the minimization of which leads to more flat functions. Variables $\xi_i, {\xi_i}^*$ are slack variables which allow for errors higher than ϵ. The constant C determines the trade-off between the flatness of h (introduced by the minimization of $\|w\|^2$) and the amount up to which deviations larger than ϵ are tolerated. In comparison with the general case presented in the beggining of this section, in the SV regression the complexity measure $C(h)$ is replaced by $\|w\|^2$ and C is the constant which is used instead of λ.

If Lagranze multipliers used, then the dual problem is as follows.

$$maximize \begin{cases} -\frac{1}{2}\sum_{i,j=1}^{n}(\alpha_i - {\alpha_i}^*)(a_j - (\alpha_j)^*)\langle x_i, x_j \rangle \\ -\epsilon\sum_{i=1}^{n}(\alpha_i + {\alpha_i}^*) + \sum_{i=1}^{n} y_i(\alpha_i - {\alpha_i}^*) \end{cases} \tag{5.1}$$

subject to

$$\sum_{i=1}^{n}(\alpha_i + {\alpha_i}^*) = 0 \quad , \alpha_i, {\alpha_i}^* \in [0, C]$$

from the dual formulation it is also derived that

$$w = \sum_{i=1}^{n}(\alpha_i - {\alpha_i}^*)x_i$$

and thus,

$$h(x) = \sum_{i=1}^{n}(\alpha_i - {\alpha_i}^*)\langle x_i, x \rangle + b$$

The case of nonlinear functions can be handled easily with the Kernel trick [41], since it is possible to reformulate the problem as follows

$$maximize \begin{cases} -\frac{1}{2}\sum_{i,j=1}^{n}(\alpha_i - {\alpha_i}^*)(a_j - (\alpha_j)^*)\kappa(x_i, x_j) \\ -\epsilon\sum_{i=1}^{n}(\alpha_i + {\alpha_i}^*) + \sum_{i=1}^{n} y_i(\alpha_i i {\alpha_i}^*) \end{cases} \tag{5.2}$$

subject to

$$\sum_{i=1}^{n}(\alpha_i + {\alpha_i}^*) = 0 \quad , \alpha_i, {\alpha_i}^* \in [0, C]$$

which leads to

$$w = \sum_{i=1}^{n} \Phi(x_i)$$

and

$$h(x) = \sum_{i=1}^{n}(\alpha_i - {\alpha_i}^*)\kappa(x_i, x) + b$$

This transformation is feasible since for the SV algorithm is sufficient to know the $\kappa(x, x') := \langle \Phi(x), \Phi(x') \rangle$, rather than Φ explicitly.

Various kernel functions are available in the literature, in this study the Gaussian kernel [25] will be used as it enables learning every possible function by adjusting coefficient γ.

$$\kappa(x_i, x_j) = e^{-\gamma \|x_i - x_j\|^2}$$

The solution of the optimization problem presented above lead to the development of the model. However, this process should be performed many times in order to find the model leading to the best results. It should be noted here that all programming languages offer packages which make the development of a model easier since the user should not formulate the mathematical problem or solve the optimization problem on his own.

The procedure that was followed for the development of the model can be seen in Figure 5.1. Different solutions for the model are taken by adjusting the values of C and γ. Thus, the coefficients C, γ can be seen as the way that the model is regulated. A second optimization problem is the selection of the values for the combination of C, γ which will result to the most accurate model. This problem is handled as well in the training phase. The procedure that is followed in this study is an exhaustive grid search. In this methodology a large amount of C, γ combinations is created and the model is trained for each of them. The performance of the trained models are benchmarked based on metrics and finally the one with the highest ranking is selected. In order to create the benchmarking framework, a part of the training set should be used to test the candidate model, and calculate the selected metrics (the testing dataset mentioned here is not the same with the validation dataset aforementioned). This part is handled by exploiting the K-Fold Cross Validation method. In this method the training set is splitted in k-Folds, then every model (every combination of C, γ) is trained k times in which the training set consists of $k-1$ folds and the testing set from the remaining. The average performance is taken as the final performance of the model. After the models are trained and their performance is benchmarked, the one leading to the best results is selected. As a final step the selected model will be tested on the validation dataset to examine the case of overfitting.

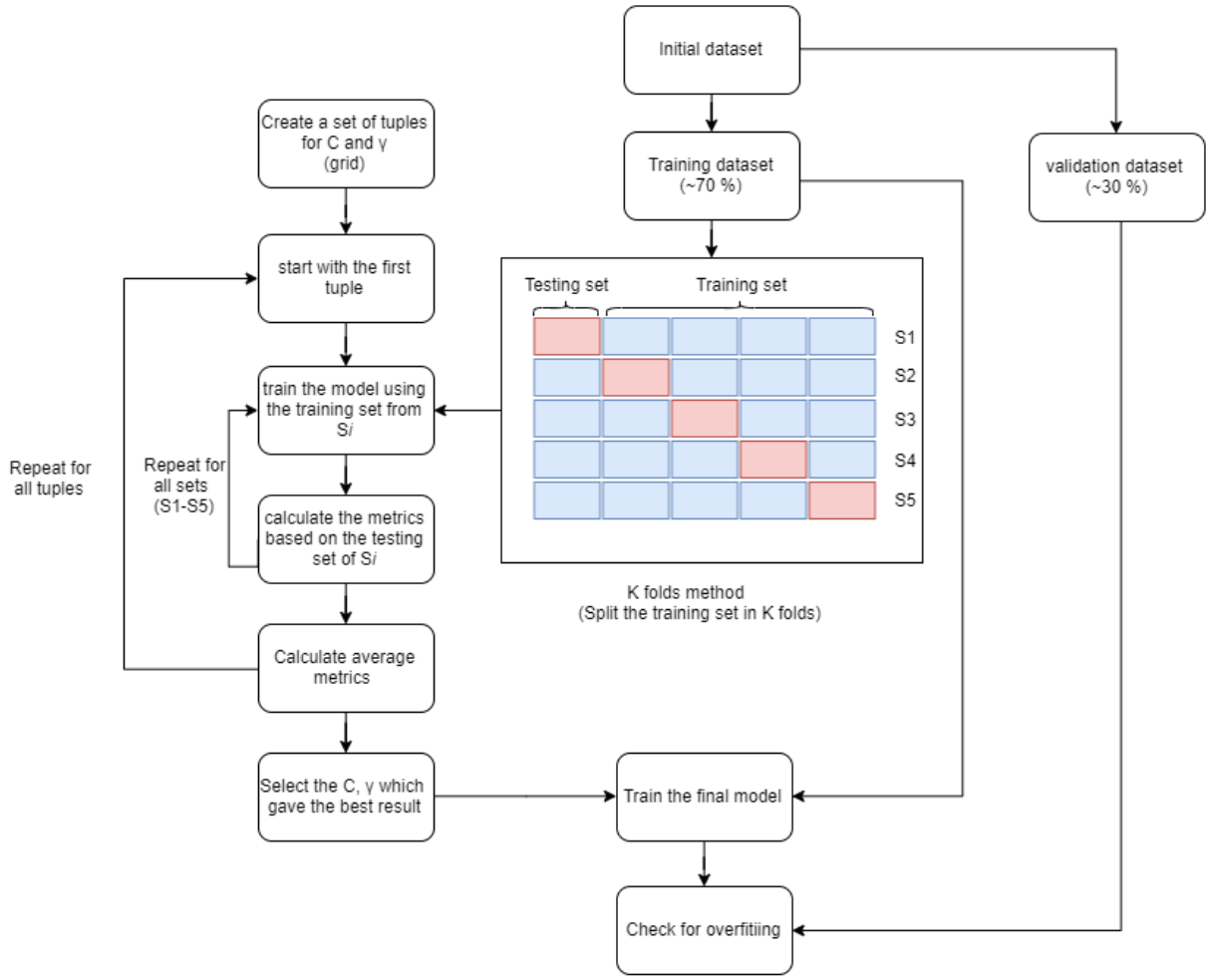

Figure 5.1: Procedure followed for the development of the BBM

5.2. Models' description

The variables that are used as input in the WBM were presented in the previous Chapter. It is important to decide whether the same inputs will be given in the statistical models or additional variables can be added. As it was also mentioned in during the development of the WBM, variable cannot be predicted for a future voyage, should not be a part of the model inputs. Regarding the water depth, due to the fact that there are no sufficient data in the PMS (since only a few vessel's were occasionally recording the water depth), it cannot be taken into account into the BBM and GBM.
Taking into account the data which are stored in the PMS and the restrictions which arise from the end goal of the model (to be used in the voyage simulation algorithm), the following variables can be used as inputs to the statistical models.

- Speed through water
- Speed over ground
- Draft
- Trim
- Heading
- Wave height
- Wave direction

- Wave frequency
- Swell height
- Swell direction
- Swell frequency
- Wind Speed
- Wind direction
- Electric power demand
- Sea water temperature

The only additional variable compared to the inputs of the theoretical model is the sea water temperature. In this case it was decided to include the seawater temperature as parameter of the model, since with the statistical approach it is possible that apart from the influence on the vessel's resistance, effects that cause drop in the efficiency of the systems (i.e. diesel engine) may be taken into account. It is already known that these variables have impact on the fuel consumption of a vessel. However, it should be examined whether the quality of the available data from the PMS is sufficient to capture the influence of all the aforementioned variables. There in no doubt that the speed-fuel consumption relation is captured in the data, however it is a question whether the data are sufficiently accurate in order the influence of less strong relations (i.e sea water temperature) to be identified.
The Pearson's [36] and Spearman's [45] correlation coefficients which are widely used to give an indication about the significance of the variables to the target variable cannot be used since both are based in assumptions which do not hold in that case. Pearson's correlation is based on the assumption that the data have a linear relationship, on the other hand in the Spearman's correlation a monotonic relationship is required. In addition in the examined dataset, there are interdependencies within the candidate features which is also a restriction to use the Pearson's or Spearman's correlation.

According to Guyon et.al [18] the feature selection can be based on the domain knowledge. In addition, in order to examine the significance of a feature the backward elimination method can be used [18]. In that case the model is trained with the entire set of features, then the model is trained again, but now the variable under examination is eliminated from the feature set. Based on the difference in performance between the two models, it is decided whether the variable should be used or not.

Therefore it is decided to use all the variables listed above as features and by applying the backward elimination method to decide whether to use or not the Sea water temperature and the Speed over ground. Regarding the speed over ground it is not questioned whether this variable is significant for the fuel consumption prediction, but it is examined whether it should be used taking into account that the speed through water is also a feature of the model.

Three different models will be developed. Their structure and the differences between them are described below.

- Model 1 - Black box model (BBM)
  This model is a pure Black box model. The inputs and the output of the model can be seen in Figure 5.2.
- Model 2 - Grey box model 1 (GBM1)
  The difference between the GBM1 and BBM is that the output of the WBM (developed in chapter 4), is used as an additional input to the model. The structure can be seen in Figure 5.3.
- Model 3 - Grey box model 2 (GBM2)
  In this case a Black box model is trained to predict the error of the output of the WBM. The working principle of the model can be seen in Figure 5.4.

In Figures 5.3-5.4, the inputs of the WBM model are not presented. The inputs of the WBM can be found in Chapter 4. The only difference compared to the inputs of the BBM is that the influence of the sea water temperature is not accounted in the WBM.

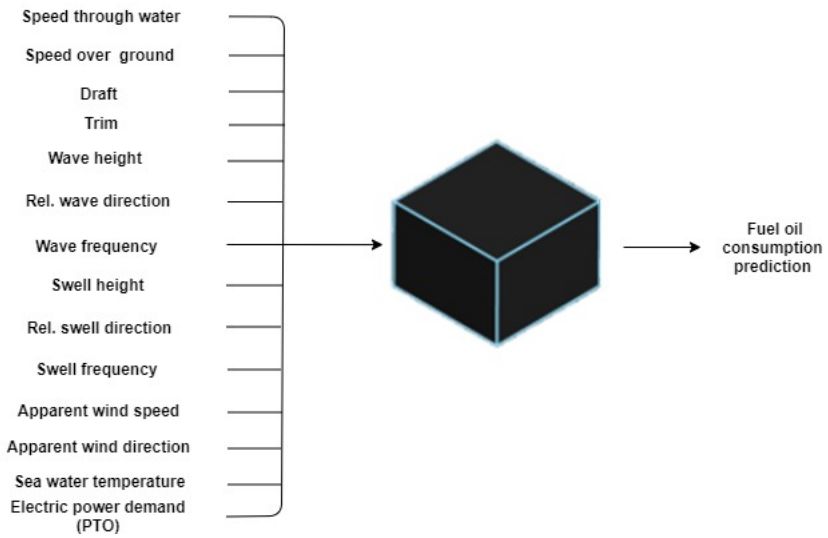

Figure 5.2: Structure of Black box model (BBM)

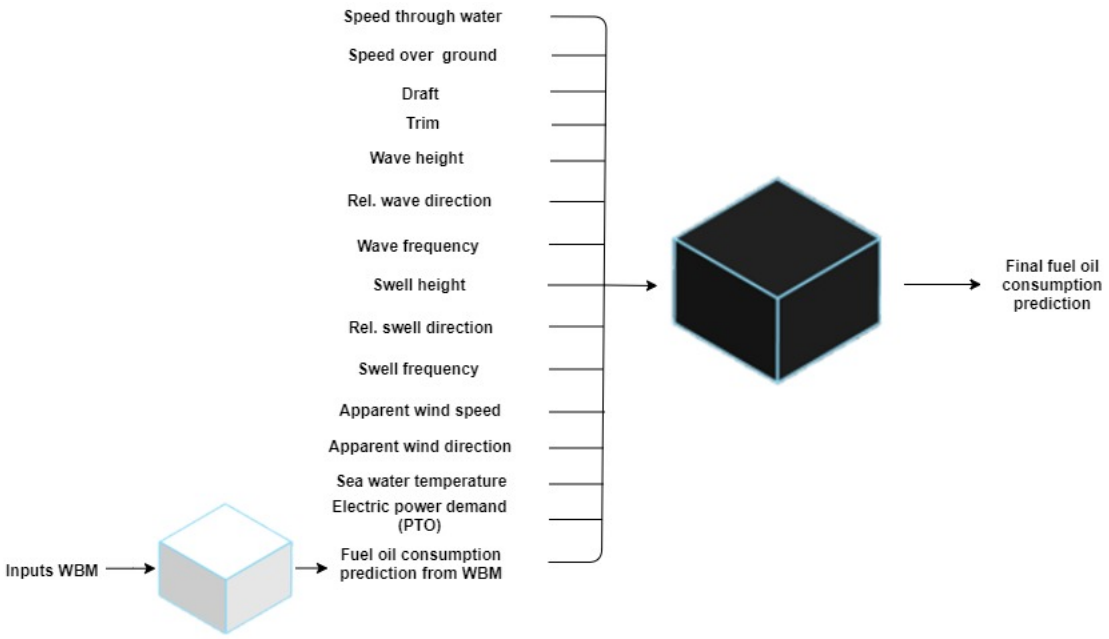

Figure 5.3: Structure of Grey box model 1 (GBM-1)

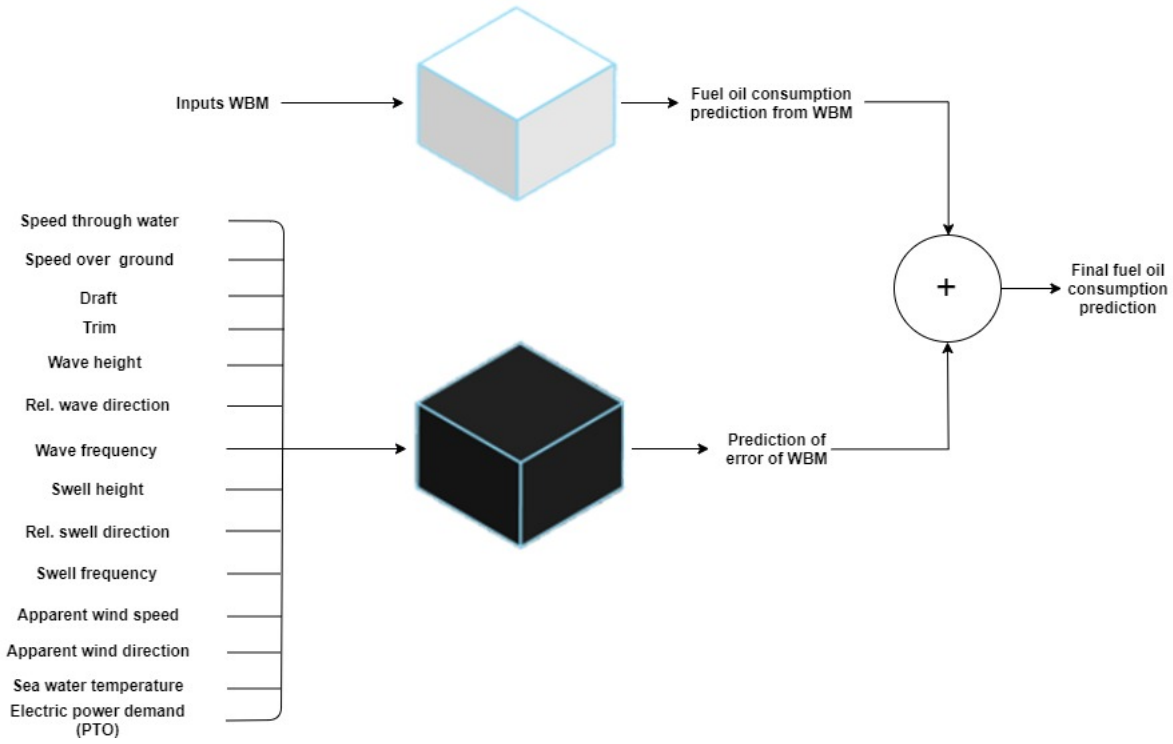

Figure 5.4: Structure of Grey box model 2 (GBM-2)

5.3. Results

As it was mentioned above the performance of the models will be tested with the same dataset that the WBM was tested (last year of operation of vessel Schippersgracht). Thus, comparisons between the models can be done on equal basis.

In Figures 5.5-5.7 the comparison between the predicted and the measured fuel oil consumption is presented for the three data-driven models. From the graphs it cannot be identified a difference regarding their performance. More information is given in Table 5.1, where it can be seen that the performance of the three models is comparable. It is only observed that the GBM-2 is slighlty less accurate in the error bandwidth 0-10%, but the difference compared to the BBM and GBM-1 is negligible.

Error band	Percentage of datapoints within the error band for BBM	Percentage of datapoints within the error band for GBM-1	Percentage of datapoints within the error band for GBM-2
5%	53.04%	53.24%	48.63%
10%	81.45%	81.34%	78.15%
15%	91.43%	91.50%	89.17%
20%	96.16%	96.24%	95.49%
25%	98.49%	98.68%	98.32%

Table 5.1: Percentage of datapoints within the given error bands for BBM, GBM-1 and GBM-2

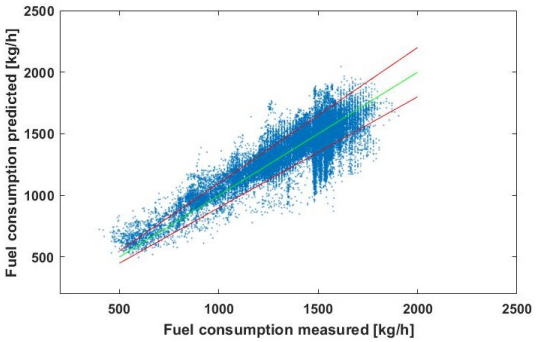

Figure 5.5: Predicted fuel consumption from BBM versus measured fuel consumption (47398 datapoints)

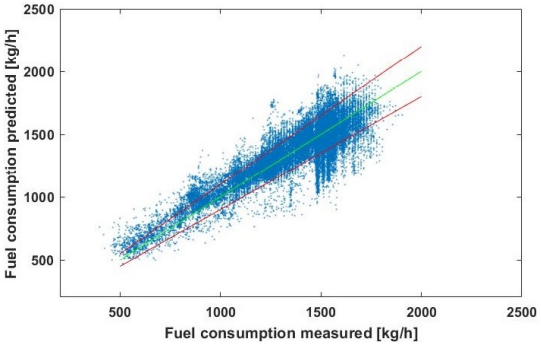

Figure 5.6: Predicted fuel consumption from GBM-1 versus measured fuel consumption (47398 datapoints)

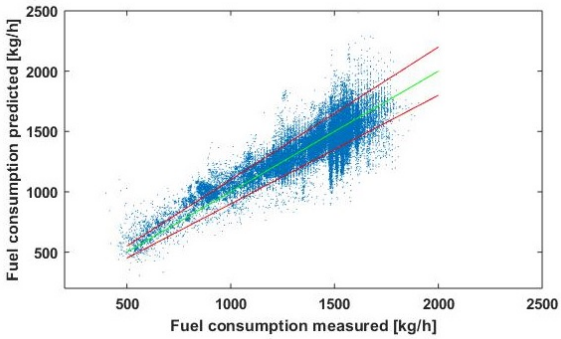

Figure 5.7: Predicted fuel consumption from GBM-2 versus measured fuel consumption (47398 datapoints)

In the previous Chapter, Figures 4.65-4.92 were presented to further examine the accuracy of the WBM. Thus the same procedure will be followed for the BBM, GBM-1 and GBM-2. The figures regarding the performance of the BBM are presented below (Figures 5.8-5.35). The graphs regarding the GBM-1 and GBM-2 in Appendix E since they do not differ significantly from those of the BBM.

In Figures 5.8-5.14 significant differences cannot be identified regarding the performance of the BBM compared to the WBM. It is observed that in both cases (WBM which is presented in Chapter 4 and BBM) there is a high concentration of errors higher that 20% close to the shore. In addition, the same applies with the voyage from Brazil to Canary islands which is not predicted with sufficient accuracy from any of the models (another indication that there is an issue with the data that were recorded in the PMS for that voyage, as discussed in the previous chapter). It is observed that the BBM is not performing well in the cases where the speed is lower than 10 kts as it is depicted in Figures 5.15-5.16. The corresponding diagrams regarding the WBM have shown that the WBM is performing better in that area. The reason behind that is that the training dataset does not contain a large number of datapoints in the speed range of 0-10 kts. This is due to the fact that the vessel sails in that speed range mainly when it is entering or leaving a port. In addition, the fact that the low speed data are mainly in areas close to the shore, affects the accuracy of the data. It is known that the currents' prediction is lacking in accuracy in areas close to the shore, meaning that there is higher possibility for faulty speed through water value in areas close to the shore. Thus the combination of small sample in which faulty data are included also, is the reason why the BBM is not performing well in that speed range.
A second case where the predictions of the BBM are not sufficiently accurate are in the case of 4-6 meters wave height, as it is presented in Figure 5.26. However the same situation was observed as well regarding the predictions of the WBM for the wave height 4-6 meters. The fact that both the WBM and the BBM (and GBM-1 and GBM-2) resulted in large errors in the case of wave height 4-6 meters, while all the cases of lower wave height were predicted significantly better, and taking into account that in the class of 4-6 meters wave height there are only 320 datapoints, indicates that the reason behind the poor predictions are associated with the input data and not with the performance of the models.

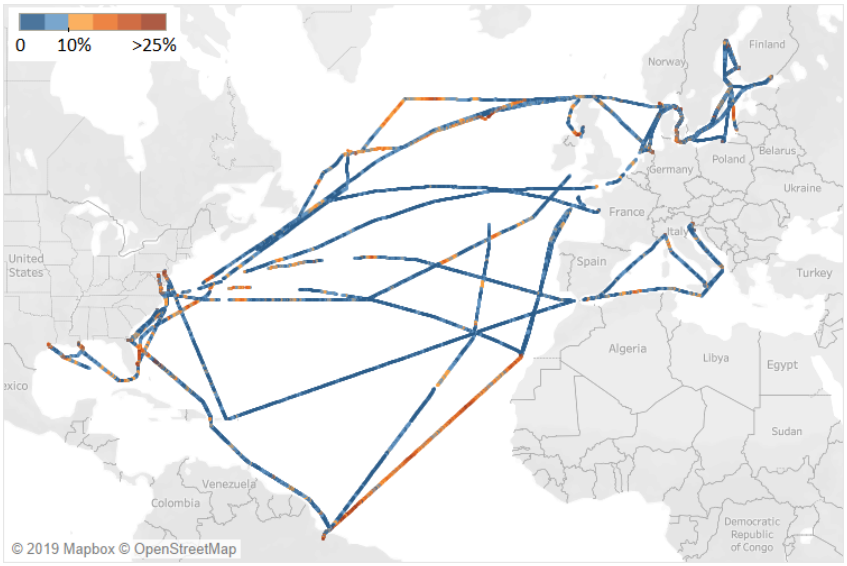

Figure 5.8: Error (%) between predicted (by BBM) and measured fuel consumption)

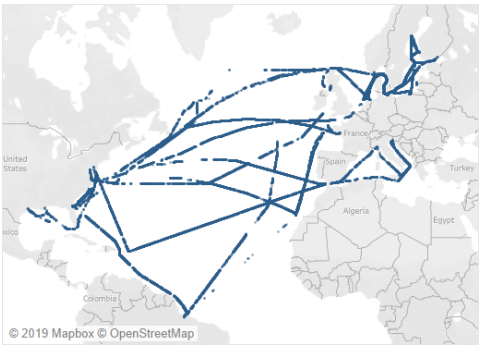

Figure 5.9: Error (%) between predicted (by BBM) and measured fuel consumption, class 0-5%

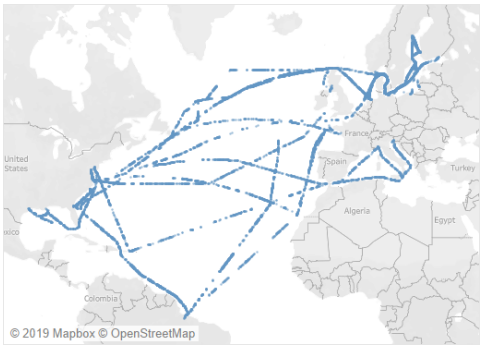

Figure 5.10: Error (%) between predicted (by BBM) and measured fuel consumption, class 5-10%

Figure 5.11: Error (%) between predicted (by BBM) and measured fuel consumption, class 10-15%

Figure 5.12: Error (%) between predicted (by BBM) and measured fuel consumption, class 15-20%

Figure 5.13: Error (%) between predicted (by BBM) and measured fuel consumption, class 20-25%

Figure 5.14: Error (%) between predicted (by BBM) and measured fuel consumption, class >25%

Error distribution based on the speed

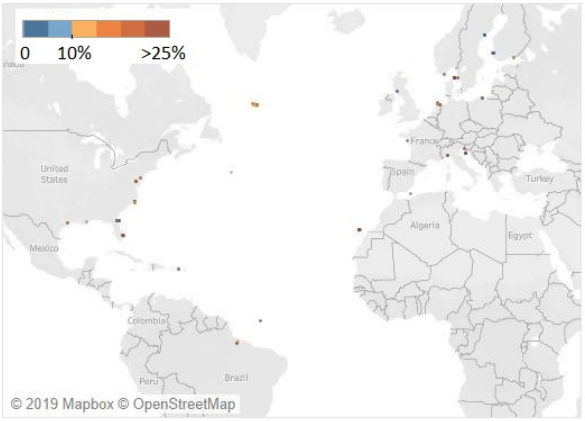

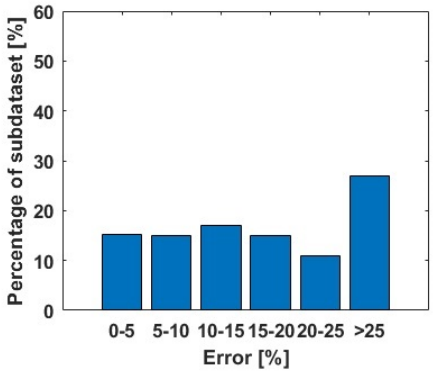

Figure 5.15: Error distribution (by BBM) for the subdataset (321 datapoints) of speed 0-5 kts

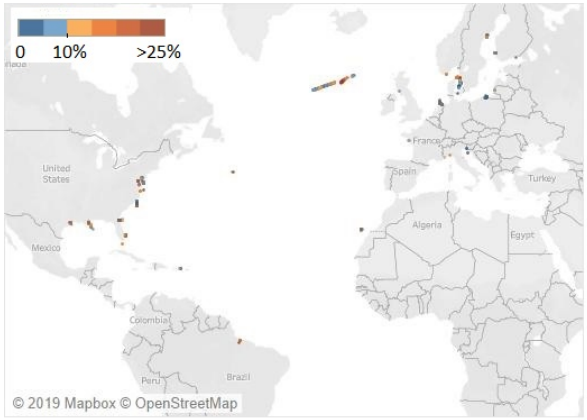

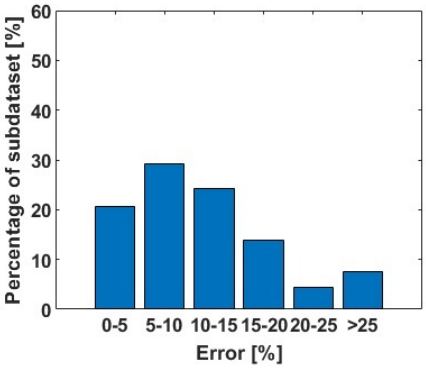

Figure 5.16: Error distribution (by BBM) for the subdataset (1299 datapoints) of speed 5-10 kts

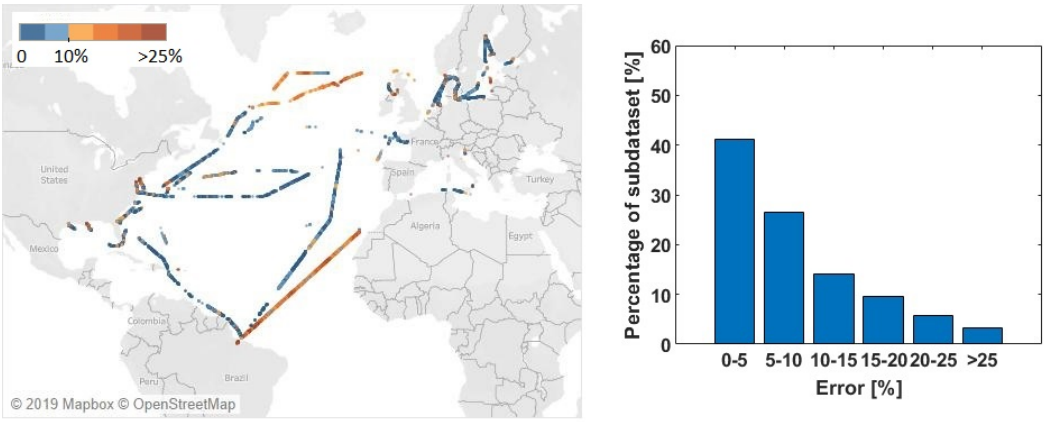

Figure 5.17: Error distribution (by BBM) for the subdataset (13797 datapoints) of speed 10-15 kts

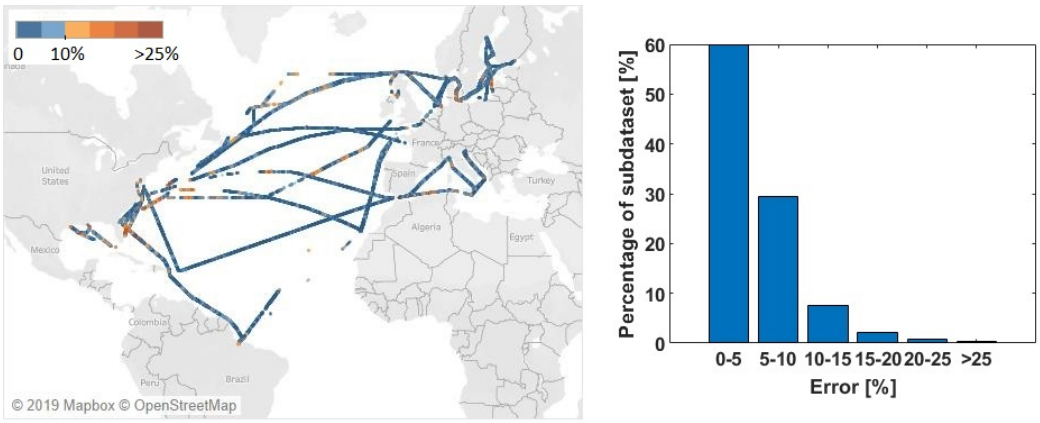

Figure 5.18: Error distribution (by BBM) for the subdataset (32361 datapoints) of speed 15-20 kts

Error distribution based on the draft

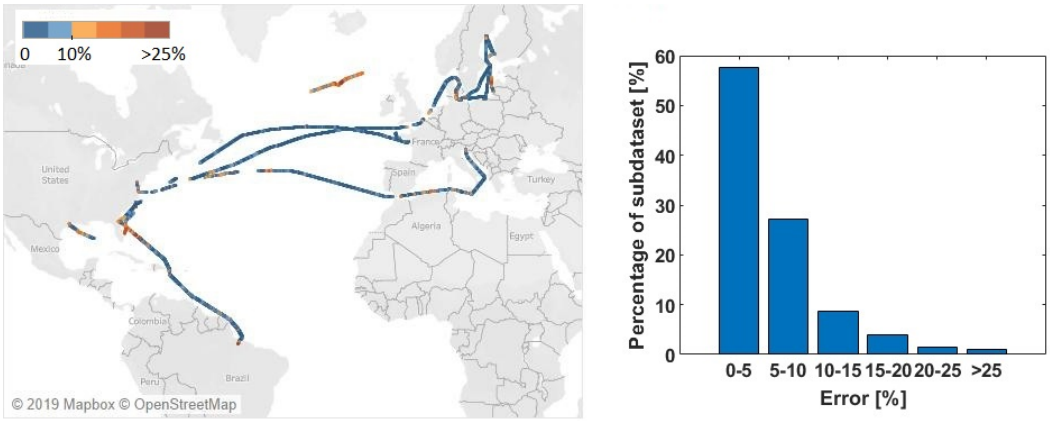

Figure 5.19: Error distribution (by BBM) for the subdataset (15355 datapoints) of draft 6-7.5 m

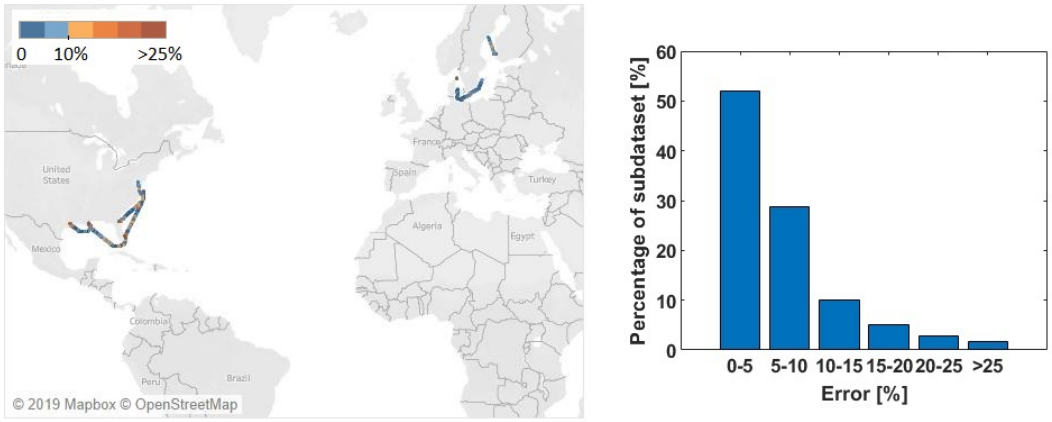

Figure 5.20: Error distribution (by BBM) for the subdataset (2814 datapoints) of draft 7.5-9 m

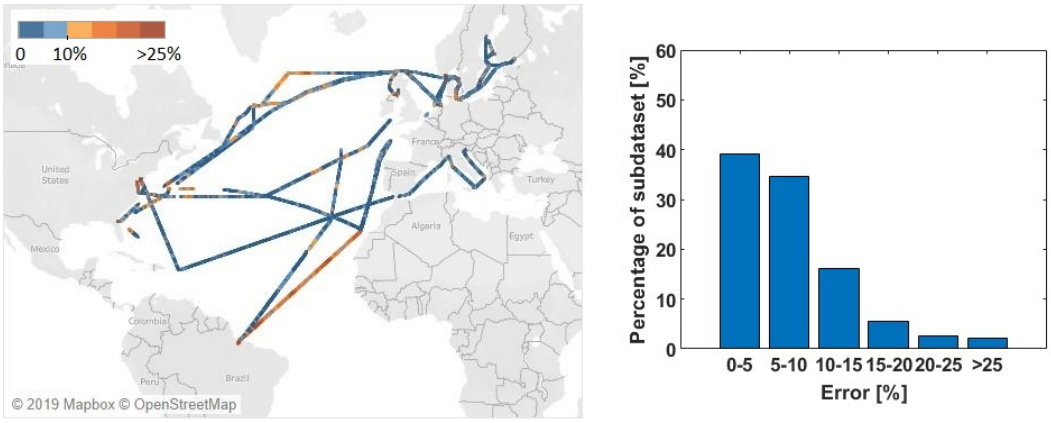

Figure 5.21: Error distribution (by BBM) for the subdataset (29607 datapoints) of draft 9-11 m

Error distribution based on the wave height

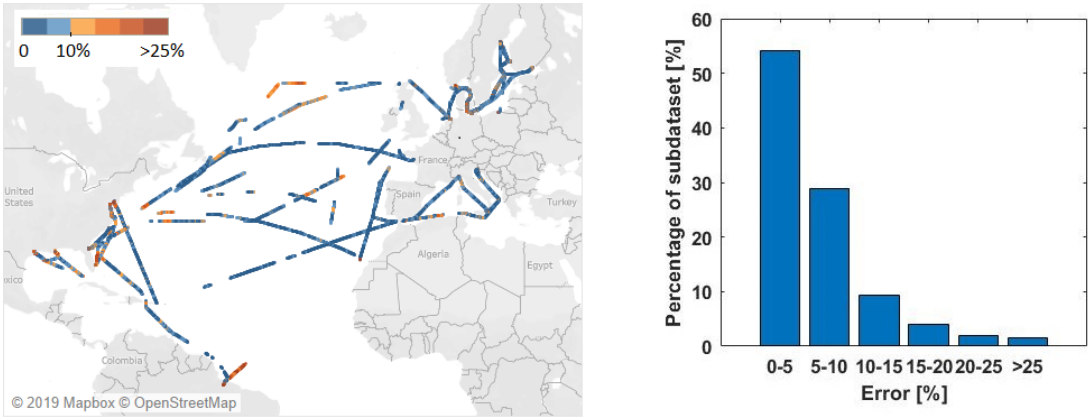

Figure 5.22: Error distribution (by BBM) for the subdataset (25523 datapoints) of wave height 0-1 m

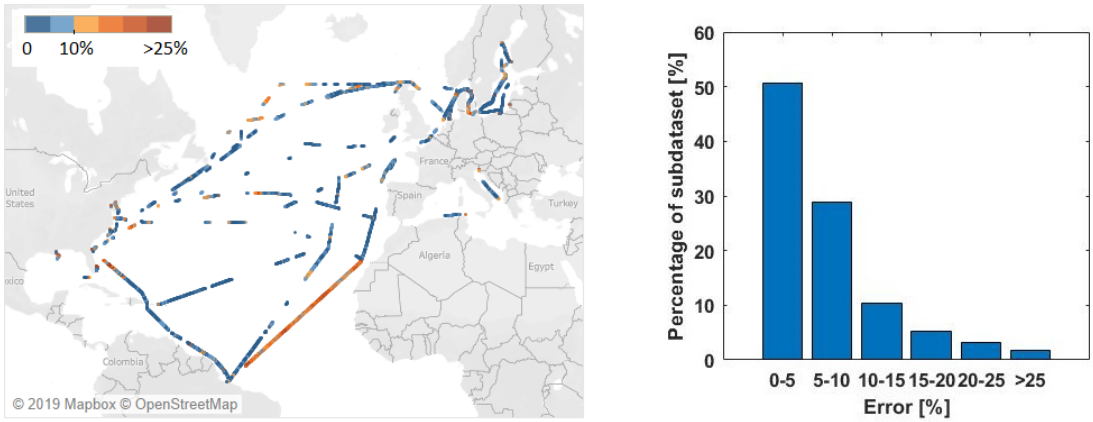

Figure 5.23: Error distribution (by BBM) for the subdataset (16021 datapoints) of wave height 1-2 m

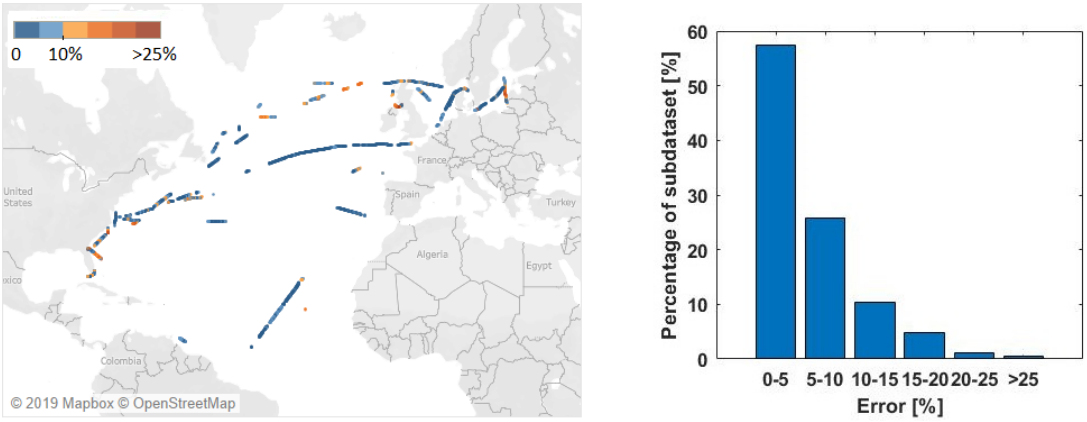

Figure 5.24: Error distribution (by BBM) for the subdataset (5680 datapoints) of wave height 2-3 m

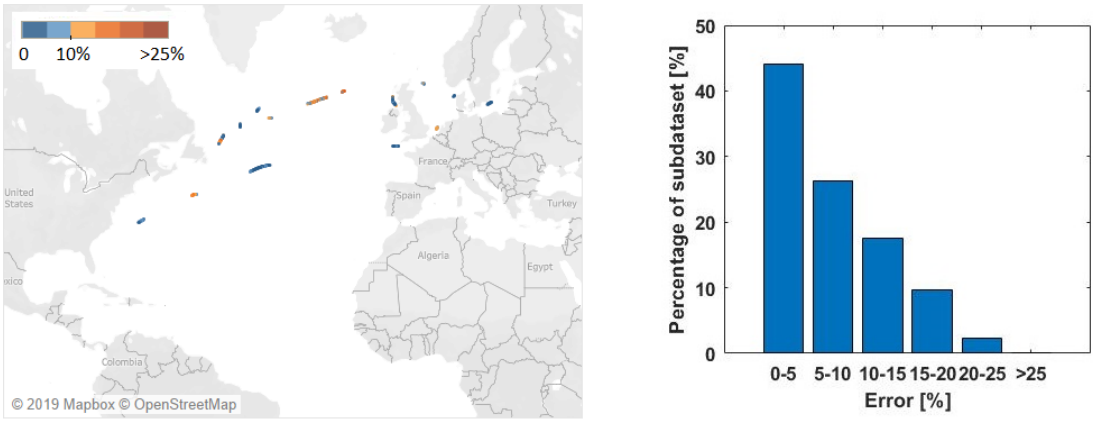

Figure 5.25: Error distribution (by BBM) for the subdataset (789 datapoints) of wave height 3-4 m

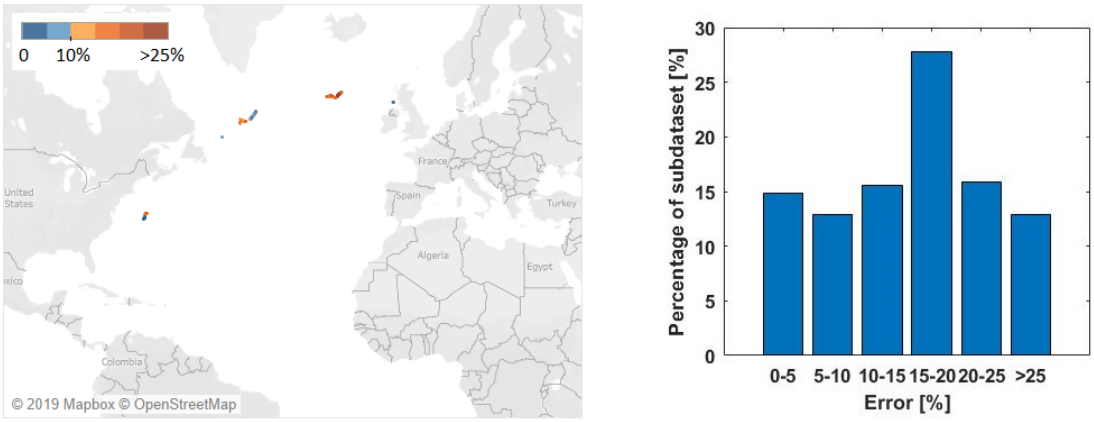

Figure 5.26: Error distribution (by BBM) for the subdataset (320 datapoints) of wave height 4-6 m

Error distribution based on the swell height

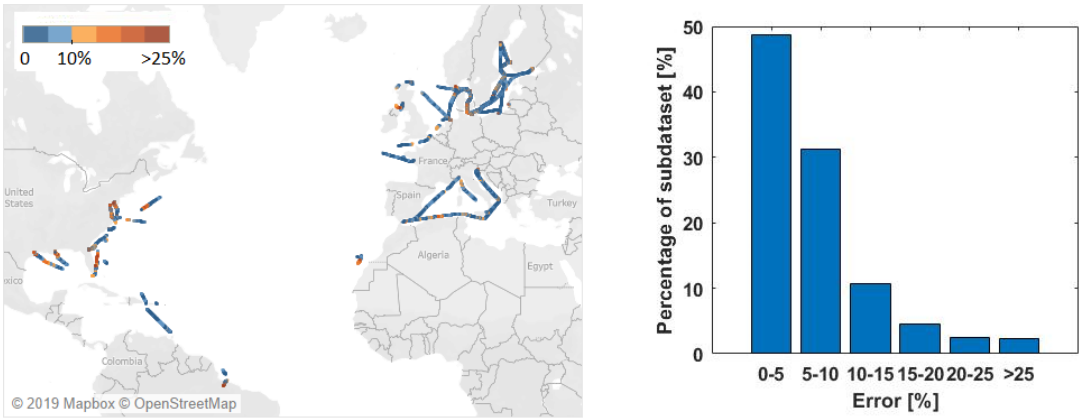

Figure 5.27: Error distribution (by BBM) for the subdataset (15773 datapoints) of swell height 0-1 m

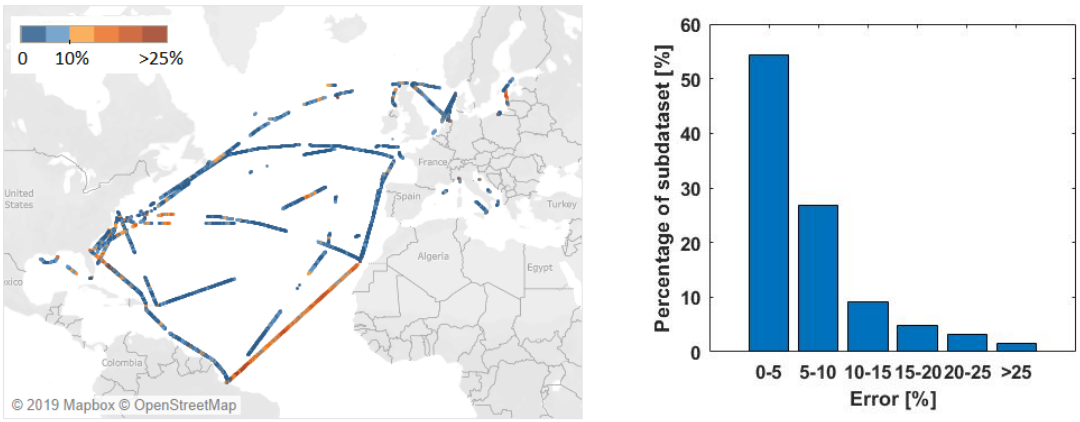

Figure 5.28: Error distribution (by BBM) for the subdataset (19746 datapoints) of swell height 1-2 m

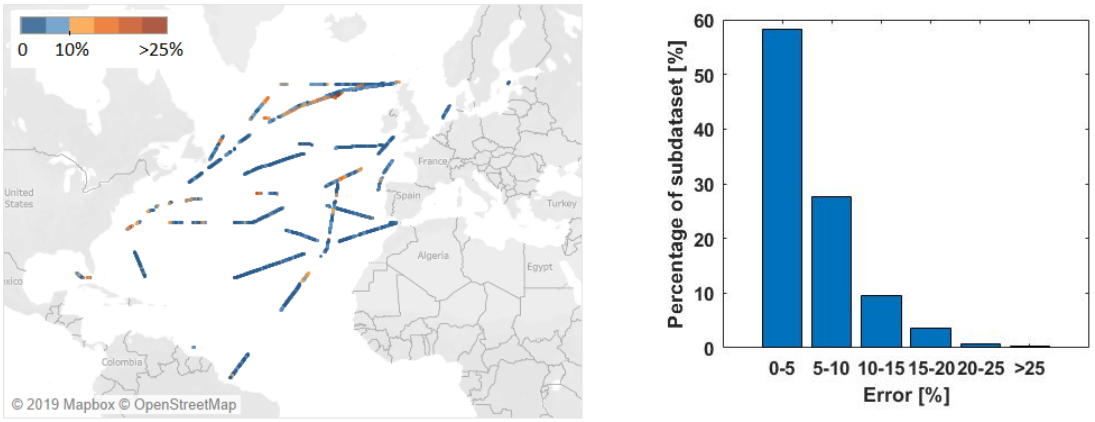

Figure 5.29: Error distribution (by BBM) for the subdataset (9289 datapoints) of swell height 2-3 m

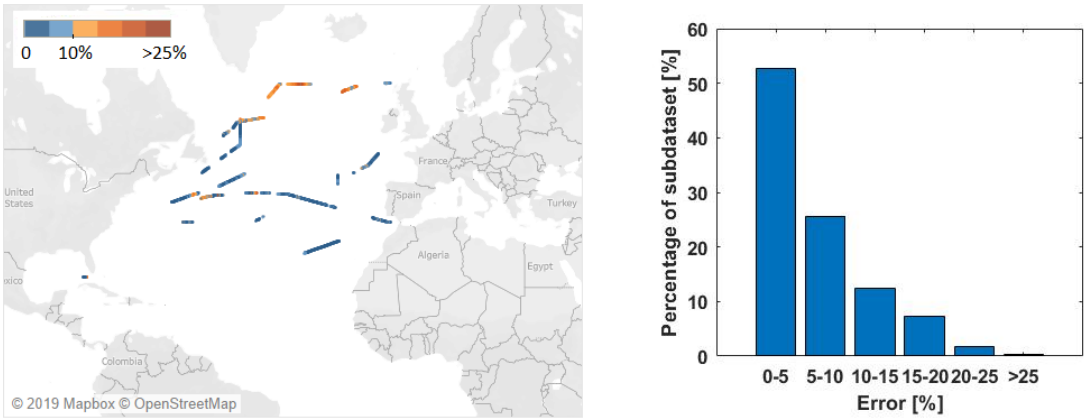

Figure 5.30: Error distribution (by BBM) for the subdataset (3342 datapoints) of swell height 3-4 m

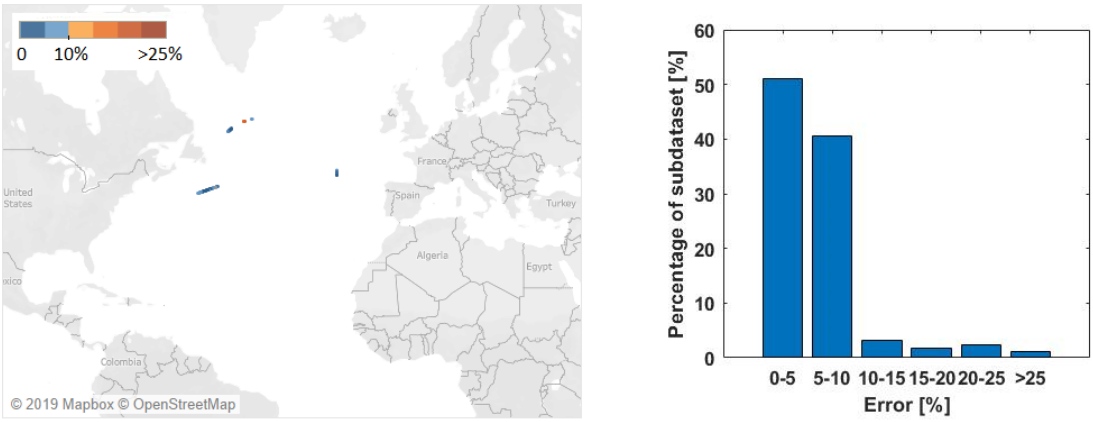

Figure 5.31: Error distribution (by BBM) for the subdataset (284 datapoints) of swell height 4-6 m

Error distribution based on the wind speed

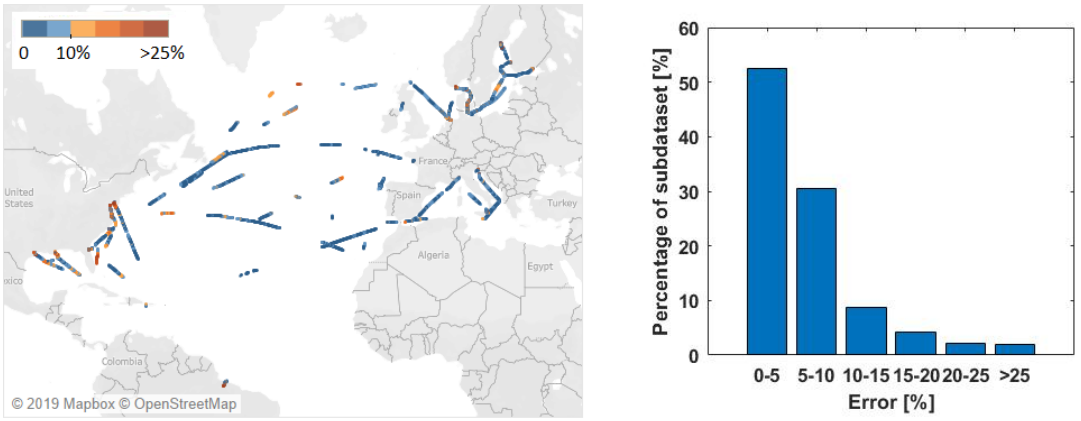

Figure 5.32: Error distribution (by BBM) for the subdataset (11213 datapoints) of wind speed 0-10 kts

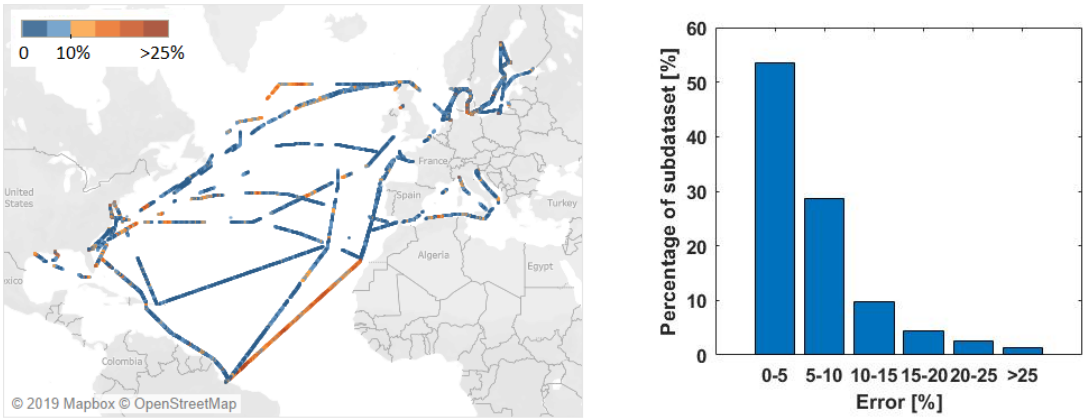

Figure 5.33: Error distribution (by BBM) for the subdataset (30716 datapoints) of wind speed 10-20 kts

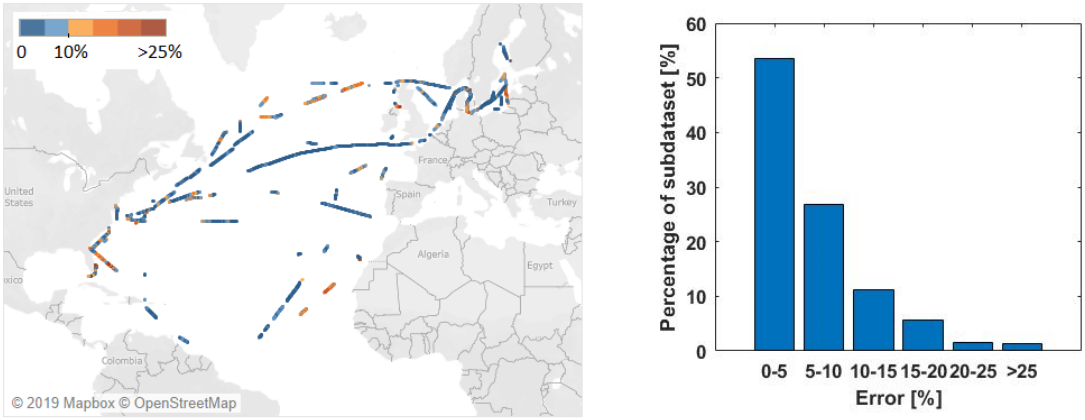

Figure 5.34: Error distribution (by BBM) for the subdataset (10279 datapoints) of wind speed 20-30 kts

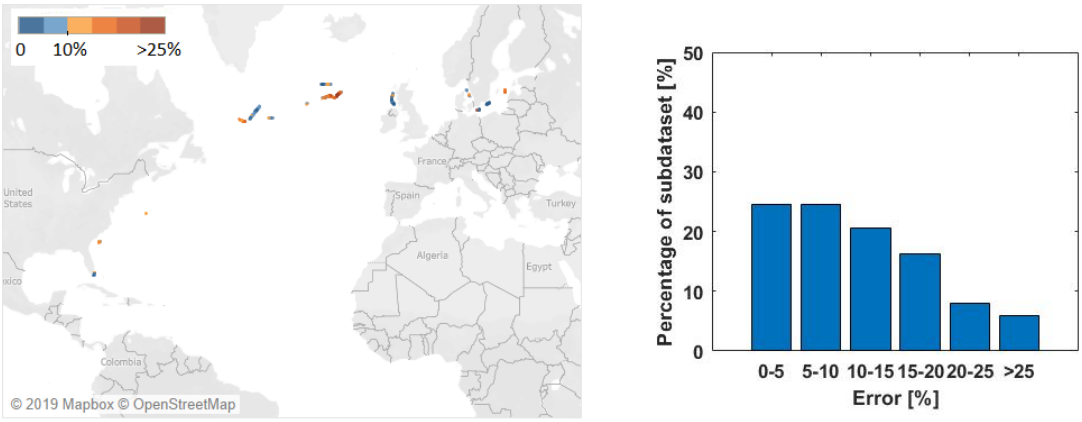

Figure 5.35: Error distribution (by BBM) for the subdataset (649 datapoints) of wind speed 30-40 kts

6

Comparison of the developed models

In this chapter the advantages and disadvantages of the models developed in the previous chapters will be discussed and comparisons will be made regarding their performance. In addition, their performance will be further examined by calculating how well the daily fuel consumption and the total fuel consumption over a voyage can be predicted. Both calculations will be done based on the data regarding Schippersgracht's last year of operation.

6.1. Comparison of models

In Chapter 4 and 5, the accuracy of the models was examined and presented. In this section the focus is to make comparisons regarding the performance of the models, both in terms of accuracy but as well in terms of time efficiency, since models which require enormous time to produce results are impractical. Thus some of the results presented in the previous chapters will be summarised here and additional performance metrics will be presented.

In Table 6.1, performance metrics are presented for all the four models. In addition, in the table 6.2 results regarding the accuracy of the models which were presented in the previous chapters are summarised. From the results presented in the Table 6.1, it is concluded that the accuracy of the models is comparable. However, in terms of time efficiency, there is an enormous difference between the performance of the BBM and that of the rest models. The WBM needs approximately 1.3 seconds for the prediction of a single datapoint which means that for the dataset regarding Schippersgracht's last year of operation (around 45000 datapoints), 16 hours were needed for the calculation. Thus the GBM-1 and GBM-2 which require the prediction of the WBM in order to give their final prediction, require as well enormous time for the calculation of a large dataset. On the other hand the BBM performed the calculation for the entire dataset regarding Schippersgracht's last year of operation in about 4 minutes. Thus it is concluded that the methods used to develop the grey box models, did not improve the accuracy of the BBM or that of the WBM. Especially the GBM-2, which appears to have slightly lower accuracy compared to the BBM and GBM-1, does not have additional benefit compared to the rest models. The GBM-2, results in accuracy of the same level with the BBM however it is questioned if there is has additional benefits compared to the pure BBM.
Regarding the performance of the WBM, it is observed that is slighlty less accurate compared to the BBM (however the difference is negligible), and requires enormously more computational time. However it offers a step by step calculation which is valuable.The step by step calculation offers the opportunity to get more outputs (i.e added resistance due to weather, efficiency of the propeller) compared to the BBM which can also lead to a better understanding of how the energy is distributed within the propulsion plant. In addition the step by step approach of the WBM, offers the opportunity to apply modifications in the sub-systems of the propulsion plant and examine the influence to the overall efficiency.

	WBM	BBM	GBM-1	GBM-2
R^2	0.655	0.758	0.759	0.718
RMSE [kg/h]	136.9	114.7	114.5	123.64
Max error [kg/h]	957.6	705	675	871.7
Time	16 hours	4 min	16 hours	16 hours

Table 6.1: Performance metrics for WBM, BBM, GBM-1, GBN-2

Error band	Percentage of datapoints within the band for WBM	Percentage of datapoints within the band for BBM	Percentage of datapoints within the band for GBM-1	Percentage of datapoints within the band for GBM-2
5%	49.25%	53.04 %	53.24%	48.63%
10%	78%	81.45%	81.34%	78.15%
15%	89.39%	91.43%	91.50%	89.71%
20%	94.48%	96.16%	96.24%	95.49%
25%	97.32%	98.49%	98.68	98.32%

Table 6.2: Percentage of datapoints within the given error bands for WBM, BBM, GBM-1 and GBM-2

6.2. Daily and voyage fuel consumption

In order to further examine the performance of the models, the results regarding the last year of operation of Schippersgracht will be used to examine the error of the models regarding the daily fuel consumption, and the fuel consumption for an entire voyage. Based on the information presented in the previous paragraph it is decided further examine the performance of the WBM, the BBM and the GBM-1, leaving outside the case of the GBM-2 since it was proven that it performs worse compared to the other models. The daily fuel consumption is calculated based on the 5-minute interval data stored in the PMS for the entire dataset regarding Schippersgracht's last year of operation (Figure 6.1. Regarding the fuel consumption per voyage, 5 voyages were selected and the total fuel oil consumption will be calculated based the predictions of the 3 models and based on the measured data. The results are presented in Table 6.3.

	Error in calculation based on WBM predictions	Error in calculation based on BBM predictions	Error in calculation based on GBM-1 predictions
Voyage 1 (7 days)	3.28%	1.15%	1.36%
Voyage 2 (10 days)	0.21%	0.1%	-0.08%
Voyage 3 (9 days)	2.11%	1.63%	1.81%
Voyage 4 (11 days)	2.95%	0.93%	0.085%
Voyage 5 (4 days)	0.16%	-0.57%	0.07%

Table 6.3: Error in the fuel oil consumption for an entire voyage

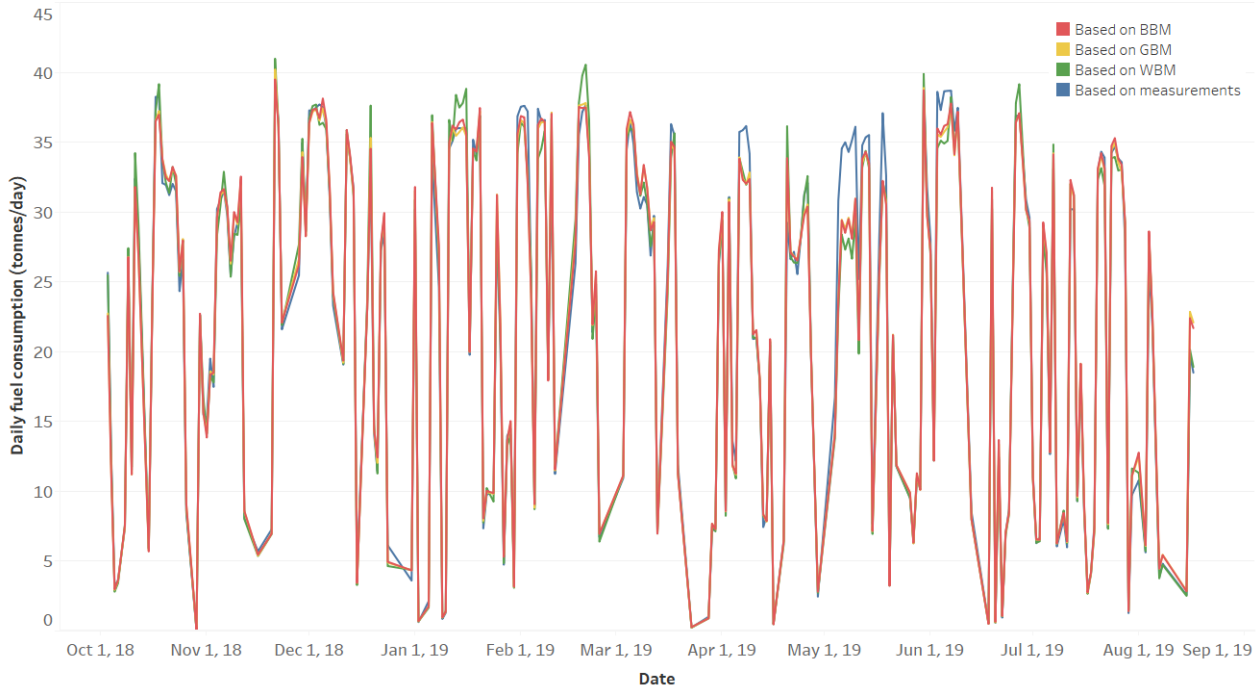

Figure 6.1: Daily fuel consumption for Schippersgracht's operation during last year

It is observed the fuel consumption of all the five voyages was predicted with an error less than 4 % by all the three models. More specifically, the error lies between 0.07-1.81 % regarding the predictions based on the BBM and GBM-1, while the WBM resulted in an error of 0.16-3.28%.

Regarding the daily fuel consumption, in Figure 6.1 it can be seen that in most cases the daily fuel consumption based on the predictions of the models is close with the daily fuel consumption based on the measurements. A few cases can be identified where the measured daily fuel consumption is higher compared to that based on the predictions of all the three models. The larger difference is observed around May,19 and is about 20%. The date corresponds to the voyage from Brazil to Canary islands, which was discussed in section 4.3.9. However, in Figure 6.1 it is difficult to make further conclusions about the predictions of the daily fuel consumption and thus the Figures 6.2-6.3 are presented to give more information. It is important to mention that in Figure 6.3, a density plot is presented. A density plot is a smoothed continuous version of a histogram estimated from the data, the difference compared to a histogram is that the in the y-axis a density is given and not a count/percentage. In order to calculate the equivalent count/rate the area under the curve and the specific interval of x axis should be found. Figure 6.3, does not add additional information compared to the Figure 6.2, however makes the comparison between the results of the three models easier. It is clear from the Figures 6.2-6.3, that the results of the daily fuel consumption based on all the three models are slightly negatively skewed (with the results of the BBM presenting a higher skewness compared to those of the GBM and WBM).
Based on the Figure 6.3 the calculation of the daily fuel consumption based on the predictions of the WBM lead in betters results. Fact which contradicts with the findings presented in the Table 6.1, where the accuracy of the WBM (regarding the 5-minute interval predictions) are slightly lower compared to that of the BBM and that of the GBM-1. Although, it should be noted that despite the fact that both calculations (performance metrics in Table 6.1 and the daily fuel consumption 6.2) refer to the same dataset, in the calculation of the daily fuel consumption, the data are summed to create the daily fuel consumption and this could be possibly explain the mismatch. In order to examine that, the total fuel consumption was calculated for the entire dataset. This calculation is in agreement with the findings regarding the performance of the models 6.1.,

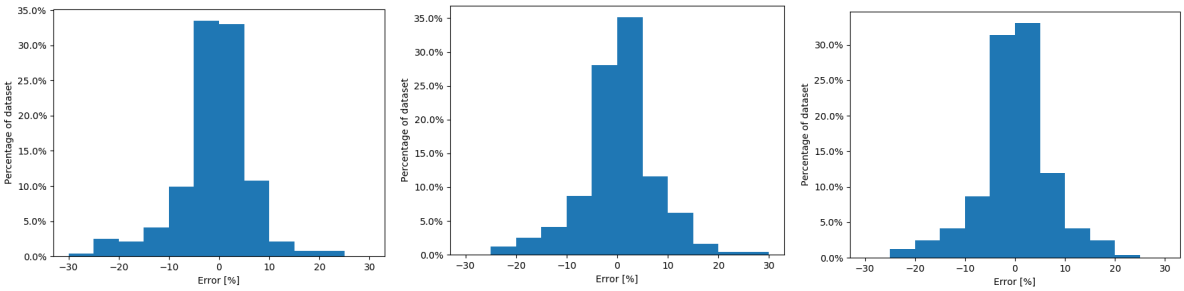

Figure 6.2: Histogram for daily fuel consumption error from WBM (left), BBM (center), GBM(right)

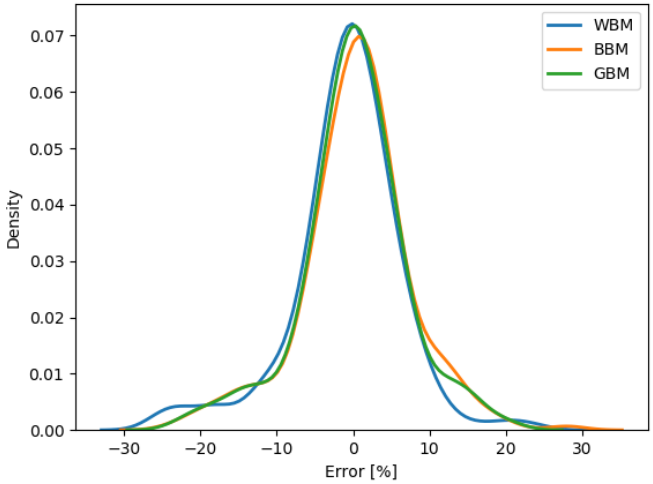

Figure 6.3: Density plot for daily fuel consumption error

Error in total fuel consumption based on the results of WBM	**Error in total fuel consumption based on the results of BBM**	**Error in total fuel consumption based on the results of GBM**
-1.031 %	-0.523%	-0.73%

Table 6.4: Error in the fuel oil consumption

In the case where the fuel consumption of the five voyages was calculated, it was observed that all the three models resulted in estimation of the entire voyage fuel consumption with error less than 4%. However, in the case of a 5 min interval or even in the case of the daily fuel consumption the error between the measured value and the predicted can take values up to 20-25 %. Thus, it is clear that when the five-minute interval predictions are summed up over a time window, the contribution of the bad predicted values becomes negligible and the error between the measured value and the predicted one becomes smaller. Fact which is useful for applications regarding the vessel's performance assessment since in the case of the five minute interval the probability for a large error is higher compared to the case where a time window is used. However, it is important to find the right value for the time window, since in a small time window (or the five minute interval) the probability of a large error is higher while on the other hand in a very large time window more time is needed until the identification of an incident. Thus the right balance should be found regarding the value of the time window, which will not make the identification tool sensitive, but on the other hand will not cause a very large delay until the identification of an incident. It is also important to mention that the value of the time window is related to the type of the application. For instance in an application where the target is to identify the state of the hull in terms of fouling a large time window (i.e 10 days) would be reasonable. Various time windows were tested and the results are presented below for all the three models (WBM,

BBM, GBM-1).

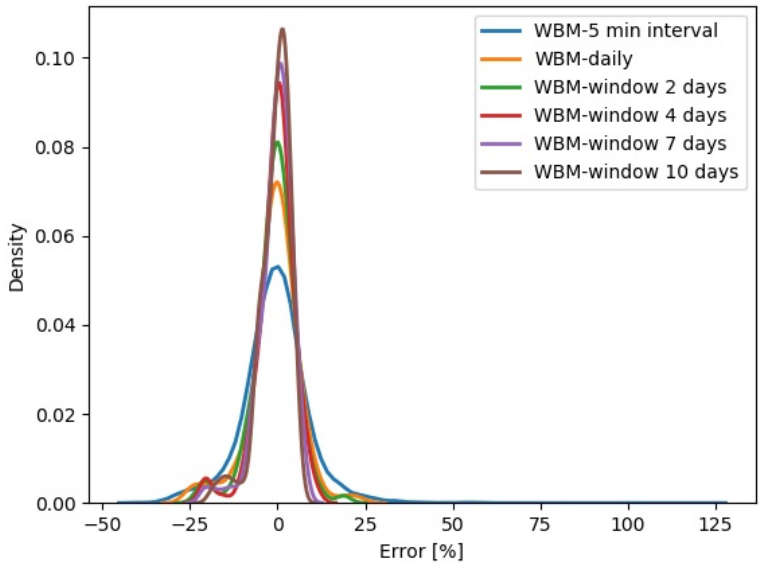

Figure 6.4: Density plot for WBM results and various time windows

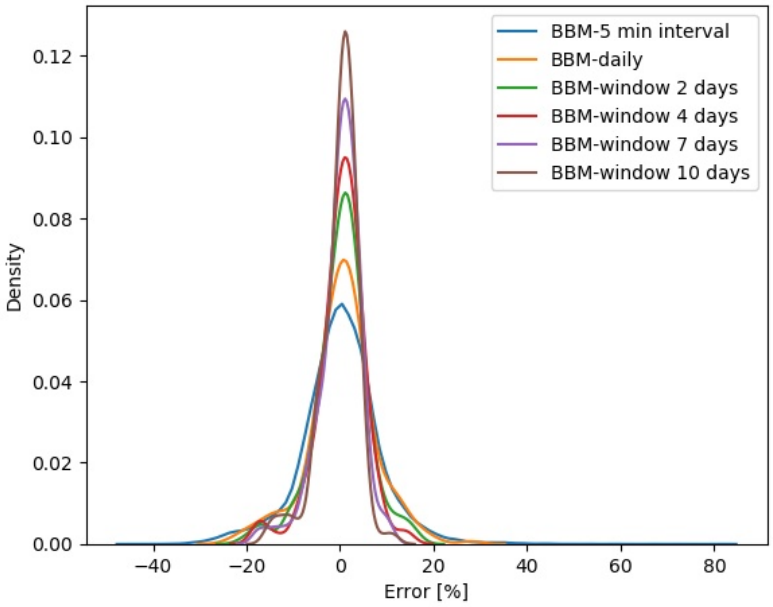

Figure 6.5: Density plot for BBM results and various time windows

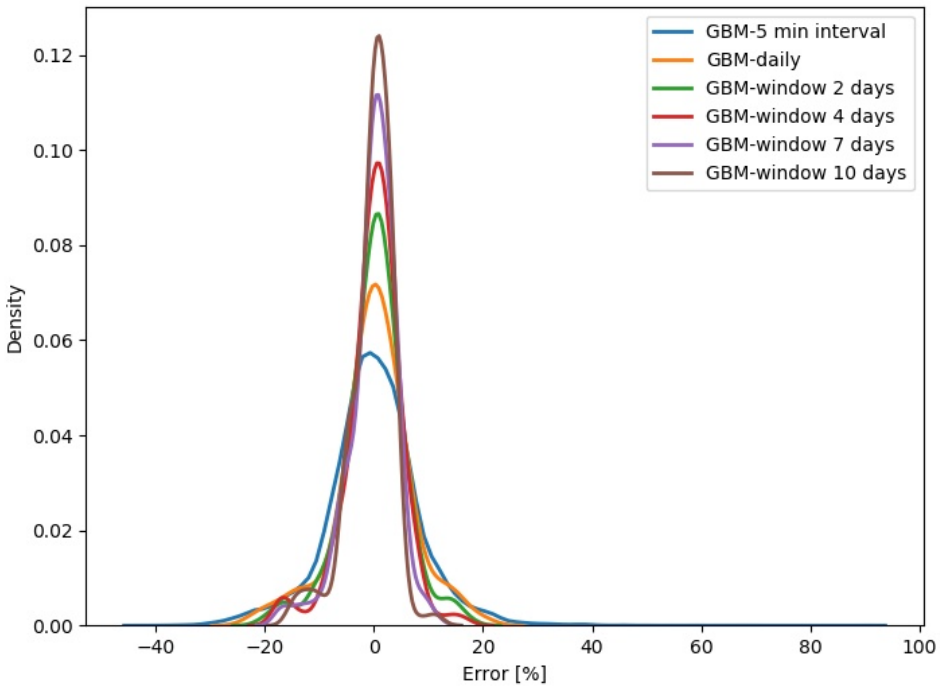

Figure 6.6: Density plot for GBM-1 results and various time windows

7

Applications and Case studies

In this chapter possible applications of the models will be discussed, to prove how the developed models (in Chapters 4 and 5) can be used to create value within Spliethoff. In addition, two case studies will be presented. It should be noted that the original plan was to create the voyage simulation algorithm. However, the case study of the variable rpm system, which was a real case problem within the company, was examined.

7.1. Applications

A general description about the applications of the performance models was given in Chapter 2. In this section, it will be discussed how the models developed in the Chapters 4 and 5, taking into account their characteristics can be used within Spliethoff.

In Chapter 6, the advantages and disadvantages of the developed models were discussed. The comparison of the models highlighted their main characteristics. The BBM is superior in terms of time efficiency compared to the WBM. On the other hand, the WBM, in which a step by step approach is followed, gives more information about the energy distribution within the propulsion system. In addition, the WBM can easily be modified, which means that it can be used to examine the impact of possible modifications in the propulsion system on the fuel consumption. Based on these characteristics, two main directions are identified regarding the applications of the developed models. The first category contains the applications which are related to the technical department while the second category contains the applications which are related to the department of operations.

As it was explained in the above paragraph, the strong point of the WBM is that it offers more information compared to the BBM and it can be modified. Thus, the WBM can be used from the technical department to examine how possible modifications in the propulsion plant or installation of additional systems will influence the fuel consumption. In addition, it can be used to create knowledge regarding the distribution of energy within the propulsion plant. This will lead to an identification of the areas where there is room for improvement in terms of energy efficiency.

The BBM is characterized mainly by the superior time efficiency compared to the WBM. Due to this fact it is more suitable to be used for applications in which a large number of iterations should be performed within a short period of time. An example of such an application is the speed or voyage optimization. In addition, tools can be created which will provide to the operators information about the estimated time of arrival to the next port and the estimated fuel consumption until the arrival to the port based on the selected speed. In the same tool it can also be enabled the examination of different speed settings and their influence on the arrival time to the port and the fuel consumption until the arrival. It should be noted that tools for the aforementioned applications are already available within the company. However, in these tools oversimplified performance models are used and due this fact, they are not very accurate. Therefore, the company has to decide whether the already available tools will be modified based on the new performance model, or a

new tool will be developed in-house which will give more freedom for development based on the company's needs and the end user's preferences.

As was mentioned in Chapter 2, there is increased interest in the development of performance models for the evaluation of the large amount of data collected from the PMS. The results from the performance model are used as the vessels reference performance, and based on the deviation between the results from the model and the actual measurements conclusions are derived for the condition of the hull, the propeller and the rest equipment. Usually these tools are focusing on the identification of the influence of fouling on the performance of the vessel, but also in the identification of faults in the equipment which cause a sudden change in the performance. Therefore, the tools which are currently used within Spliethoff for vessels' performance evaluation can be enriched with the models developed in this thesis.

Another application of the performance model which is closesy related to the concept of the digital twin is described in the following paragraph. Within the company a weather routing tool (SPOS, Meteogroup) is used, which is based on a simplified performance model. This tool provides the captains with suggestion for the route and speed to be followed during the voyage. It is observed that the captains many times do not follow the suggestions they receive from the tool. There are two reasons for that, the first one is that some captains are not motivated enough to participate in the efforts of the company to make effective use of the weather routing tool, and realise the benefit of it. On the other hand it is also observed that many captains do not trust the weather routing system and believe that based on their experience they can make better decisions. Thus, based on this fact a new application for the performance model is proposed.

The performance model can be used onboard to make comparisons on real time between the vessel's fuel consumption and the one that would be achieved if the suggestions from the weather routing system was followed. In this way it will be easier for the captains that are not willing to be part of the effort to make effective use of the weather routing system, to realise the cost of their actions. In addition, regarding the captains that do not trust the weather routing system, with this application it can be examined if they indeed make better decisions based on their experience. If this is proven then they can be part of the process to improve the existing weather routing system, and be rewarded for their contribution. If the opposite is proven, then this application will be a part of the process to strengthen the captain's trust on the weather routing system.
Two case studies will be presented in the next paragraphs. The first one is an example on how modifications within the propulsion can be examined. The modification that will be examined is an actual system that the company is considering to install. The second case study is the voyage simulation algorithm which was described in Chapter 1.

7.2. Case study 1 - Variable rpm system

As it was aforementioned, the WBM offers the opportunity to examine how modifications in the propulsion plant will influence the overall fuel consumption. In this case study the WBM will be used to examine the case of a modification in the propulsion plant which will enable to operate in variable rpm. The examined system ensures that the propeller is always operating in the most efficient point (for the conditions that the vessel is encountering) by adjusting continuously the engine's rpm and the propeller's pitch without violating the operating limits of the engine and the propeller. This system is examined from the company as a solution for the loss of efficiency which takes place (due to the fixed rpm configuration of the propulsion plant) when the vessel is operating out of the design speed and especially in very low speeds. It should be noted that if this system is installed in the propulsion plant, then the shaft generator will not be possible to be used to supply the electric power demand (the shaft generator is actually the reason why the fixed rpm configuration is used). Instead, the auxiliary generators will have to be operated in order to provide the required electric power. A second option is to add a frequency converter in the propulsion plant, which will enable to use both the shaft generator and the variable rpm system in parallel. Historical data for the vessel Schippersgracht will be used to examine how the fuel consumption will be influenced in each case. Finally, the results will be compared with the results of the WBM regarding the existing propulsion configuration to examine if the potential savings are enough to make the investment viable. The cases that will be examined are summarised in the Table 7.1.

	Configuration A (current situation)	Configuration B	Configuration C
Rpm control	fixed rpm	variable rpm system	variable rpm system
Electric power supply	shaft generator	auxiliary engines	shaft generator + frequency converter

Table 7.1: Modifications examined in the variable rpm system case study

Modifications in the WBM

Two components of the WBM need to be modified to model the operation of the vessel under the configuration B and C. The first component is the matching code. In the current situation where the vessel is operated with fixed rpm, the matching code is used to find the pitch setting of the propeller for which the required power can be delivered in order the vessel to sail in the required speed under the encountered conditions. Thus, there is one degree of freedom in this system, meaning that all the operating conditions will be handled by adjusting the pitch while the rpm are fixed.
As it was explained above, the variable rpm system which is considered as an option from the company, adjusts both the pitch and the rpm and it automatically finds the combination of the pitch and rpm value which gives the higher propeller efficiency. The limitations that are taken into account from the variable rpm system are the operating limits of the propeller and the engine.

The current system was designed to offer optimum or near optimum efficiency during the operation in design or close to the design conditions. Thus, the variable rpm system which is examined will lead to significant savings in conditions which are far from the design conditions. Figure 7.1 will be used to explain why there is a loss of efficiency in low speeds in the case of fixed rpm, and how a better propeller's efficiency is achieved with the variable rpm system. Two hypothetical cases will be used during the explanation, case-A and case-B. Let us assume that the ship's curve which is plotted in the graph corresponds to the conditions of case-A. Let us also assume that in case-A the speed of the vessel is V_A. Since the propeller operates fixed at 105 rpm, and the speed of the vessel is V_A, the advance coefficient is J_A (about 0.56). In the graph it is depicted that the ship's K_T curve intersects with the $Kt-8$ curve at J_A, which leads to a propeller efficiency of about 0.58. Now if it is assumed that the ship's K_T curve corresponds to the conditions of the case-B (due to simplicity the same ship's K_T curve is used for both case-A and case-B) where the speed of the vessel is V_B, with $V_B < V_A$. Then the J_B is about 0.38 and the ship's curve intersects with the K_t-4 curve at J_B, resulting in a propeller efficiency of 0.43. Thus, in the case of fixed rpm and variable pitch, the lower the speed, the lower the efficiency of the propeller will be. In the case where both the rpm and the pitch can be adjusted, the combination of pitch and rpm is selected properly in order to achieve the highest efficiency.

The matching code is modified according to the principle of operation of the variable rpm system. Thus, both pitch and rpm are adjusted in order to find the combination which leads to the highest efficiency. It is also taken into account that the operating limits of the engine and the propeller should not be violated.

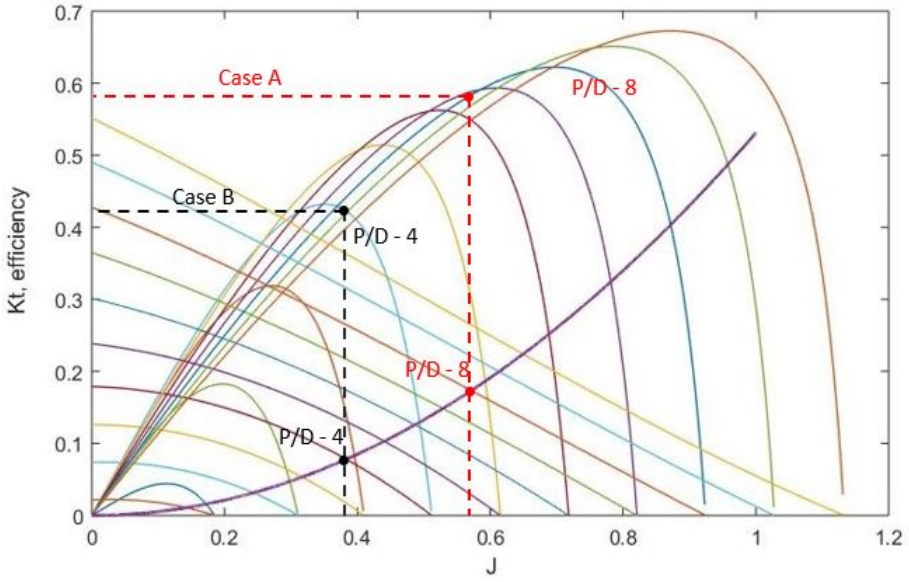

Figure 7.1: Explanation of losses in low speeds

The second component of the WBM which needs to be modified in order to model the alternative configurations of the propulsion plant is the diesel engine fuel consumption model. In the WBM a simple model about the fuel consumption of the engine is used, which is developed based on the information which were collected form the engine's product guide and the measurements of the PMS. It was observed that the fuel consumption curve from the product guide was about 10-15 % lower than the measured values in the PMS. Thus, the measurements of the PMS were used to correct for that difference.

However, the information that is provided in diesel engine's product guide about the engine's fuel consumption in variable rpm operation is not enough to develop a model that will determine the fuel consumption of the engine for every combination of engine's rpm and load falling within the engine's operational limits. In addition there are not such data in the PMS either, since the S-type vessels never sailed in variable rpm. Thus in order to create a model for the engine's fuel consumption under variable rpm, information from another diesel engine had to be used [13], which was adjusted to match with the technical characteristics of the engine used in the S-type vessels. The engine's fuel consumption in variable rpm operation is calculated according to the Figure 7.2, where the operating limits of the engine are also presented. It should be mentioned that in the results of the WBM regarding the current configuration of the propulsion plant, the updated fuel consumption method will be used as well. Thus, in all three configurations, the fuel consumption was calculated according to the Figure 7.2. It should be noted that further research is recommended regarding the engine's fuel map. The manufacturer could possibly provide additional data to verify that the developed fuel map is a sufficient approximation.

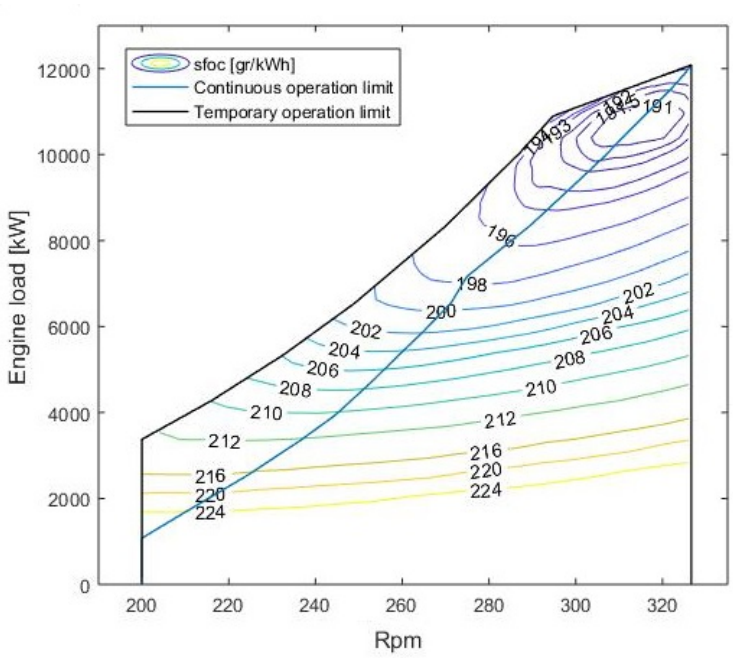

Figure 7.2: Engine's fuel oil consumption in variable rpm operation

The fuel consumption was calculated for a four month period from the data about Schippergracht's last year of operation, for all the three configurations of the propulsion plant. The results are presented in the Table 7.2.

	Configuration A (current situation)	**Configuration B (variable rpm)**	**Configuration C (variable rpm +freq. converter)**
Main engine fuel consumption [tonnes]	1,808.49	1,554.14	1,644.76
Auxiliary engine fuel consumption [tonnes]	-	131.4	-

Table 7.2: Fuel consumption for each configuration (four-month period)

In Table 7.3 the cost of the investment and the yearly fuel cost is presented for every configuration. In order to calculate the yearly fuel consumption it was assumed that the 4 month period which was presented above is repeated to form a year.

In Table 7.4 the costs of the systems and the fuel prices that were used in the calculation are presented. It should be noted that in the cost of the systems it is also included the cost of installation. The fuels prices that were used correspond to the current prices in the port of Rotterdam. In addition, it should be mentioned that maintenance costs were not taken into account.

	Configuration A (current situation)	**Configuration B (variable rpm)**	**Configuration C (variable rpm + freq.converter**
Total investment cost	-	150,000 €	450,000 €
Yearly fuel consumption	HFO: 11,677.6 tonnes	HFO: 10,035.2 tonnes MGO: 848.4 tonnes	HFO: 10,620.4 tonnes
Yearly cost of fuels	2,962,093€	2,987,488€	2,693,928€
extra cost/benefit compared to current situation (Configuration A)	-	+25,395€	-268,165€

Table 7.3: Yearly fuel consumption and total cost of fuels for all configurations

	Cost
Configuration A	-
Configuration B	variable rpm system: 150,000 €
Configuration C	variable rpm system: 150,000 € frequency converter: 300,000€
Fuel price	HFO: 253.656 €/tonne MGO: 520.98 €/tonne

Table 7.4: Cost of equipment and bunkers cost

As it can be seen in Table 7.3, switching from configuration A to configuration C requires a cost of 450,000 €, while the savings per year were estimated to be around 260,000 €. Thus, in that case (configuration C) the investment's payback time is around 2 years.
Regarding the configuration B, it is observed that the yearly total fuel cost is higher compared to the current situation despite the fact that the amount of fuels needed is lower. This is caused by the price difference between the HFO and the MGO. Due to that difference, there are cases where the fuel savings from the variable rpm system are not high enough to counteract the extra cost caused by the price difference. Therefore, it is concluded that the configuration B should be used in combination with the configuration A. Therefore a hybrid system with the configuration A and B will be examined as well. The variable rpm system and the auxiliary engines (configuration B) will be enabled only when the vessel is sailing in conditions where the fuel savings from the system can cancel out the higher price of the MGO, in all other cases the propulsion plant will operate under the configuration A. It is clear that the lower the speed, the higher the potential for savings from the variable rpm system is. Thus in the hybrid system configuration B will be used in the low speeds and configuration A in the high speeds. It should be examined in which speed value, switching to the variable rpm system is most profitable. Various cases were examined and the results are presented in Figure 7.3, where in x axis it is presented the speed value for which the system is switched from Configuration A to configuration B and in y axis the yearly fuel cost that this situation is resulting in. For example if the configurtion B is used whent the vessel is sailing with speed lower than 6 knots and configuration A when the vessels is sailing with speed higher than 6 knots, the yearly cost of the fuel will be about 2,955,000 €.

As it can be seen in Figure 7.3, in the case that configuration B and configuration A are used in a 1/2 system (using conf.A or conf.B), the yearly fuel consumption has a minimum when the configuration B is used for speeds lower than 12 knots and configuration A otherwise. This combinations results in a yearly fuel cost of about 2940000 €and the savings compared to a pure operation under configuration A are about 22000 per year. The payback time for the investment in this hybrid system is about 7 years.

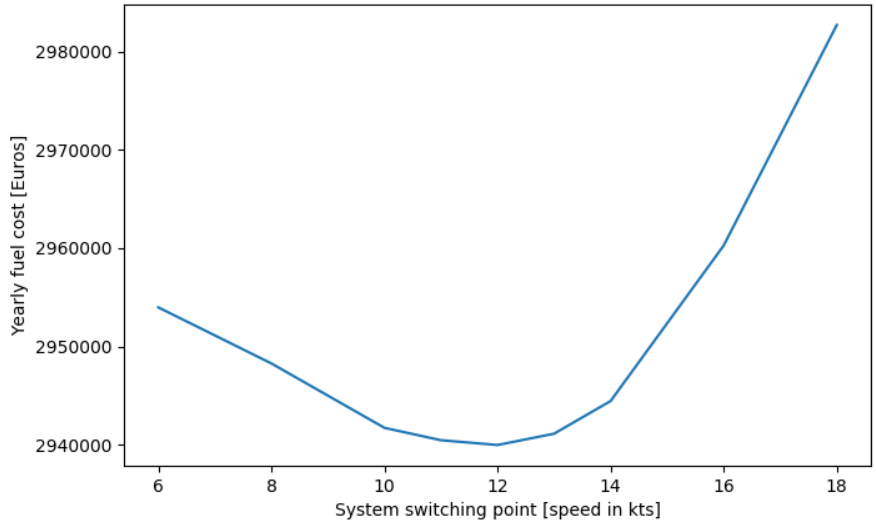

Figure 7.3: Total fuel cost for the hybrid configuration (Conf A and Conf B) versus the systems' switching point

Therefore, after analysing the alternatives which are examined from the company, it is concluded that switching to configuration C (frequency converter and the variable rpm system), will result in yearly saving of 260000 €with a payback period of about 2 years.
Regarding the case of switching to configuration B (variable rpm system and auxiliary engines), only the hybrid scenario is profitable (1/2 system with configurations A and B). In that case the minimum yearly fuel cost is achieved when the configuration B is used for speeds lower that 12 knots and configuration A otherwise. The yearly savings are around 22000 €resulting in a payback period of about 7 years. It is important here to mention that if the price difference between the MGO and HFO change significantly then different results will be obtained.

7.3. Case study 2 - Voyage simulation algorithm

In this case study an algorithm will be developed which will predict the fuel consumption for a future voyage based on the planned route and planned speed. In addition, the weather influence will be taken into account based on weather predictions. The algorithm to be developed, is the first step to examine how the models developed in Chapters 4 and 5 can be used in applications such as speed or voyage optimization. Meaning that first it should be examined how accurately a future voyage fuel consumption can be predicted with the developed algorithm, before starting the development of an speed/voyage optimization algorithm.

The voyage simulation algorithm will receive as inputs the plan of the route and the speed to be followed during the voyage. The route is given as a set of waypoints. Based on the time of arrival at each waypoint, the weather data are loaded. Afterwards, by using one of the developed performance models the fuel consumption at the waypoint can be calculated. When the fuel consumption in each waypoint is determined, the vessel's total fuel consumption in order to sail from the waypoint A to the waypoint B can be calculated by taking into account required time to sail this distance. The algorithm that is used can be seen in Figure 7.4. Regarding the electric power demand, a value of 375 kW is used except if the vessel is sailing within a SECA zone where an additional load of 75 kW is taken into account for the needs of the scrubber. These values were determined based on the available historical data and they refer to the average situation. Thus, in every waypoint it is checked whether the vessel is within a SECA zone and the electric power demand is determined accordingly.

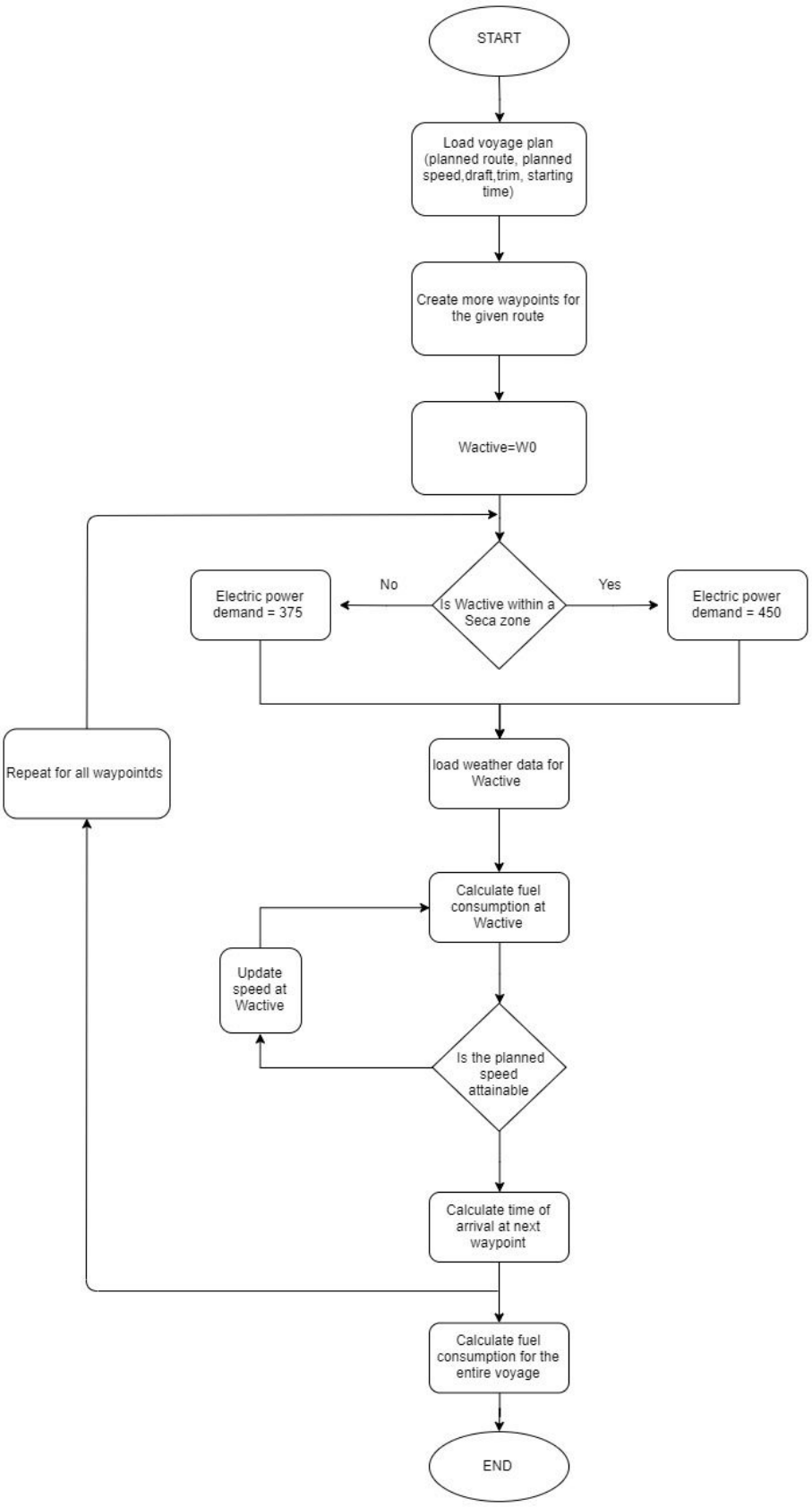

Figure 7.4: Voysge simulation algorithm flow chart

Two important aspects in the future voyage fuel consumption algorithm that have to be mentioned are

the following. Firstly, as it was aforementioned, the planned route is divided in smaller parts by the algorithm, however the size of the intervals should be determined properly. A very small time interval will result in large computational time, while a large time interval will result in larger deviation between the actual and the predicted value. The second issue is related with the weather predictions. It should be examined how the result of the algorithm is affected by the time window that is used. In that way knowledge will be created about which is the time window for which reliable predictions about the vessel's fuel consumption can be performed.

As it was aforementioned a weather routing system is used within the company. This tool provides a plan for the route and the speed to be followed during a voyage. The result of the weather routing system is given to the captains as the proposed route and speed to be followed. In order to give answers to questions presented in the previous graphs, a few voyages will be selected and the results of the voyage simulation algorithm based on the planned route and speed (from SPOS) will be compared with the actual measured values after the completion of the voyage. However, the following challenges are identified in this process. In a leg which lasts many days, the route is sometimes updated based on the updated weather conditions. Thus, sometimes the final route that is followed is significantly different from the one initially planned. In addition, except from the mismatch which is caused in the route due to the updated weather conditions, it is observed that sometimes the captain decides not to follow strictly the planned route. Therefore, it is quite rare that the planned route is identical with the one finally sailed, especially for a leg that lasts many days. A second issue is related with the speed of the vessel. In the voyage plan, the route is divided in smaller parts, which correspond to 6 hour time intervals, and a speed over ground is proposed for every interval. However, the captains do not always follow this suggestion or in some cases they update their speed setting every 12 hours or more. Thus there is a mismatch between the planned speed (which is the one that is used for the prediction of the voyage fuel consumption) and the one that the vessel was finally sailing with. Apart from the mismatch due to the fact that the captain is not following exactly the proposed plan, there is also a mismatch in the predicted weather conditions and those that the vessel actually faced during the voyage. Finally it is also observed that some captains do not trust the weather routing tool and prefer to rely on their experience

Thus it is clear that it is difficult to determine how accurately the fuel consumption of a voyage can be predicted with the developed algorithm, mainly because of the fact that the planned route and speed do not match completely with the route and speed that the vessel finally sailed.

In order to tackle this problem, the vessel Singelgracht was selected and the voyage was tracked the last days before the arrival at the port. A prediction was performed every day for the last 3 days of the voyage. The fact that the last days of the voyages are examined offers the opportunity to eliminate the differences between the planned and the actual route. However, this has as a drawback that only a small time window is examined, while a voyage lasts much longer. However, a time window strategy is followed as well in many speed/voyage optimization algorithms, since weather predictions many days in advance are not reliable, and thus it is preferred to use a time window of a few days. On the other hand it was proven in the previous Chapter that a larger window will possibly lead to a smaller error, but in that case the uncertainty of the weather forecast was not an issue since historical data were evaluated. In order to examine how well the method followed in the voyage simulation algorithm performs, the voyage's predicted fuel consumption will be compared with the actual measured fuel consumption. In addition the prediction from the voyage simulation algorithm will be compared with the fuel consumption calculated with the performance model based on the data which were recorded from the PMS (speed and weather conditions). In this way, the influence of the deviations, regarding the route, the speed and the weather conditions, between the planned and those actually sailed from the vessel can be quantified. The calculations that were performed can be seen in Figure 7.5, where for the calculations that were performed based on the voyage plan (route and speed) and weather predictions a grey box is used, while a green box is used for the calculations that were performed based on the actual data that were recorded in the PMS. The results are presented in the Table 7.5.

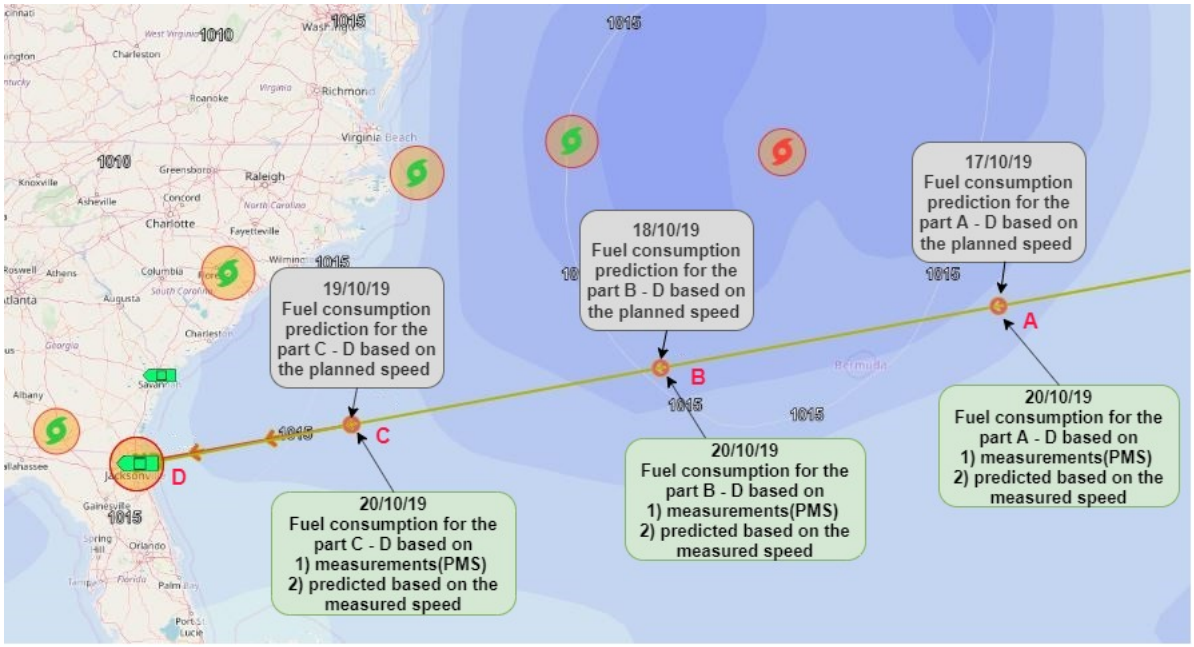

Figure 7.5

	Part A-D	**Part B-D**	**Part C-D**
Time until the end of the voyage	2.5 days	1.5 days	9 hours
Measured fuel consumption [tonnes]	79.15	38.89	12.61
Calculated by the performance model based on actual route and speed (PMS) [tonnes]	74.23	35.08	11.41
Calculated by the performance model based on voyage plan and weather predictions [tonnes]	76.34	36.07	11.52
Deviation between measured fuel cons. and predicted based on measured speed [%]	-6.21	-9.79	-9.59
Deviation between measured fuel cons. and predicted based on planned route and speed [%]	-3.55	-7.26	-8.71
Deviation between prediction based on actual route and speed and planned route and speed [%]	2.84	2.81	0.97

Table 7.5: Results for the last days of Singelgractht's voyage

From the results presented in Table 7.5, it is observed that the deviation between the measured fuel consumption and the one predicted from the performance model based on data stored in the PMS is larger compared to the deviation between the measured fuel consumption and the predicted based on the planned speed. However, the opposite situation is expected. Due to the fact that the planned speed is not exactly the same with the one recorded in the PMS we cannot make conclusions from this comparison. Regarding the deviation between the measured fuel consumption and the fuel consumption predicted based on the data recorded in the PMS, the deviation is about 5-10 %. The results presented in Figures 6.4-6.6, for the case of time window of 2 days show that errors in that range can occur. It is also important to mention that the examined leg is in an area where the prediction of the currents is not very accurate and it was connected with a

high concentration of errors during the assessment of the models (i.e Figures 4.66-4.71 regardng the WBM).

In order to examine the influence of the time-step on the accuracy of the prediction, the voyage simulation algorithm was used to predict the total fuel consumption of the vessel Slotergracht for a time window of two days based on the planned route and speed of the vessel. Three different options were considered for the time-step as it is presented in the Table 7.6. The actual fuel consumption for the examined period was also calculated after the completion of the voyage. In addition, the fuel for the examined period was calculated from the performance model based on the data recorded from the PMS (the speed and the route that was actually sailed, and the actual weather conditions and not predictions). In that case it was decided to examine a leg in the open sea, to minimize the possibility for bad currents' data. The resuslts are presented in Table 7.6. As it can be seen, in that case the deviation between the measured fuel consumption and the predicted one based in the PMS data is 0.9 %. Regarding the predictions based on the planned route and speed, it is observed that even when a 5-minute interval is used, the deviations is about 4%. This deviation is caused due to the differences between the planned speed and the one finally the vessel was sailing with. The deviations in the planned and the route finally sailed from the vessel are negligible since a small time interval was examined in which the vessel was following a straight line. In addition, part of the deviation may caused by the fact that the estimation was performed based on weather predictions.

		Fuel consumption [tonnes]	Deviation from measured fuel consumption [%]
Measured		76.1	-
Predicted from performance model based on the data recorded in PMS		76.8	0.9
Predicted from performance model based on the planned speed and route	5 min interval	79.4	4.3
	30 min interval	80.5	5.8
	1 hour interval	80.8	6.2

Table 7.6: Time interval examination

Finally the time window for which reliable predictions can be performed, will be examined. It is already known within the company that the weather predictions are reliable for a time window of 4 days. For the time window 4-7 days the predictions are still provided but the uncertainty is higher. For 7 days and longer the weather provider cannot provide predictions anymore but only an estimation based on statistical data. It should also be noted that the weather provider updates the weather data every 6 hours and provide the final data with elapsed time of 48 hours. The final data (48 hours after the examined time) are those that are stored in the PMS.

In order to examine the time window for which reliable predictions can be made, an hypothetical 7-days route to be sailed with a constant speed over ground was created. The hypothetical route will be used to examine how the weather predictions change over time and how the calculated fuel consumption is affected. Every day (from day 1 to day 7) a calculation for the daily fuel consumption based on the weather predictions was performed, from the current day until the end of the voyage (day 7). Finally after 48 hours elapsed from day 7, the final weather data (they do no be updated after 48 hours) were available and were used to perform the calculation of the daily fuel consumption from day 1 to day 7, which will be used as reference. The results are presented in Table 7.7, where in every cell of the table, the deviation compared to the reference daily fuel consumption. A general observation is that within a time window of 4 days, despite that the weather predictions are updated, the influence on the fuel consumption is in most cases less than 2%. A second observation is that in some cases (i.e. day 5 and day 7) even the predictions regarding the same day (weather predictions on beginning of day 5 for day 5) changed in a way that resulted in a deviation of around 1-1.5% compared to the daily fuel consumption calculated based on the final data, while for the rest days (day 1, day 2, day3, etc) the corresponding deviation was lower than 0.5%.

Predicted day / Current day	day 1	day 2	day 3	day 4	day 5	day 6	day 7
day 1	0.13%	-0.10%	-0.06%	1.77%	7.78%	-5.05%	-3.21%
day 2	-	-0.32%	0.24%	1.85%	4.01%	-2.16%	-3.82%
day 3	-	-	-0.18%	0.54%	3.43%	-0.76%	1.66%
day 4	-	-	-	0.99%	1.97%	-1.01%	2.31%
day 5	-	-	-	-	1.09%	-0.49%	2.06%
day 6	-	-	-	-	-	-0.38%	-1.88%
day 7	-	-	-	-	-	-	-1.69%

Table 7.7: Deviation of the fuel consumption calculated with weather predictions and final weather data

The fact that the planned route and speed for a voyage do not match with those that the captain finally followed makes it difficult to derive conclusions about how accurately the fuel consumption of a future voyage can be predicted based on the weather predictions. However, based on the findings presented in the previous paragraphs it appears that a calculation for a time window of 3-4 days it appears to lead in a deviation less than 2%.

In this case study only a few cases were examined and due to this fact, a clear conclusion cannot be derived. Thus further investigation is needed.

8

Conclusions and recommendations

8.1. Conclusions

The goal of this research is the development of performance models for the S-type vessels and the identification of ways in which these models can be used to increase operational efficiency. It should be noted that the term "optimization of operational efficiency" does not only refer to applications such as voyage/speed optimization but also in knowledge creation, which will help the operators and captains to make better decisions, or the technical department to minimize the losses in the propulsion plant.

The performance models developed in this research can be categorized into two main categories. The WBM which follows the traditional step by step approach and was tuned based on the data recorded from the PMS, and those that were developed entirely based on the data from the PMS (BBM, GBM-1, GBM-2) following the Machine Learning (ML) approach. Significant differences between the accuracy of the developed models cannot be identified. However in terms of time efficiency the BBM outperforms the rest of the models. Regarding the grey box models, both methods that were examined (GBM-1 and GBM-2) did not further improve the accuracy compared to the pure BBM. However it should be mentioned that the performance of the models was not examined regarding their extrapolation capabilities, thus it is still a question whether the grey box models (GBM-1 and GBM-2) have enhanced extrapolation capabilities compared to the pure black box model (BBM).

The dataset regarding Schippersgracht's last year of operation was used to make comparisons about the accuracy of the models. It is observed that about 80% of the dataset was predicted with less than 10 % error. In addition, the error distributions that were examined showed that the errors follow a normal distribution type, and thus, it is concluded that the models are well-tuned. Based on the error distributions, it is identified that there is room for improvement in the data-driven models (BBM, GBM-1, GBM-2) in the speed range [0-10] kts.

Based on the main characteristics of the performance models, two main directions are identified regarding the applications in which they can be used. The WBM is more suitable for applications in which knowledge creation is the priority. The step by step approach that is used in the WBM offers the opportunity for more outputs than just the fuel consumption. In addition, the WBM can easily be modified in order to account for modifications in the propulsion chain. Thus, the WBM is a tool that can create knowledge about the energy distribution within the propulsion plant and about how possible modifications in the propulsion plant will influence the fuel consumption. The case study about the variable rpm system proves the value of the WBM and how it can be used to create knowledge and value within the company. In this case study it was calculated that installing the variable rpm system and a frequency converter will result in annual savings of around 250,000€, while the investment's payback time was estimated to be about 2 years.

The BBM is more suitable for applications in which the time efficiency is the priority. Thus, it is more suitable for applications within the department of operations, such as voyage and speed optimization. In the second case study, the BBM was incorporated in the voyage simulation algorithm, which was developed to estimate the fuel consumption of an upcoming voyage based on the voyage plan (route and speed), by considering the

weather predictions. In this case study, the impact of the time interval, that is used in the algorithm, on the final result was examined. It was observed that a 5-minute time interval is preferable in terms of accuracy; however, a 30-minute or 1-hour time interval, which significantly reduce the computational time, result to comparable accuracy. In addition, it was examined the time window within which the fuel consumption can be reliably calculated, due to the uncertainty of the weather predictions, however a clear conclusion could not be derived and further examination is suggested.

An interesting observation from the case study described in the previous paragraph is that the main bottleneck in the effective use of the weather routing tool is identified in the mismatch that is observed between the proposed speed and route and the those that finally the captains choose to follow. It is reasonable that there will be deviations between the proposed speed and route and those that the vessel finally sailed with, but in Spliethoff the situation is different since large deviations are observed. Based on this observation, a new application for the performance models is proposed. The vessel's performance model can be used on board to make a real-time comparison between the vessel's fuel consumption and the one that would be achieved if the proposed by the weather routing tool, route and speed were followed.

In this research, the availability and the quality of the PMS data are of great importance. In the WBM, the data were used to validate the model and tune the sub-models in cases where it was necessary. The data-driven models would not be feasible to be developed without the availability of the data. Thus the main conclusions regarding the PMS data should be discussed. A general observation about the quality of the data recorded in the PMS is that the quality is sufficient for the type of applications examined in this research. Both the accuracy of the data and the frequency is sufficient, and there is no need to switch in a higher recording frequency or more accurate sensors. Also, the fact that the stored weather conditions are not based on measurements but instead on weather predictions does not create significant issues. The part which can be further improved is related with speed through water. As it was described, speed through water signal from the loggers is not of good quality, and thus it is not used within Spliethoff. Instead, speed through water is calculated from the speed over ground and the predictions about the currents. The calculated speed through water proved to be a better solution compared to the signal from the speed loggers. However, even in the case of the calculated speed through water, there is room for improvement. The issue that is mainly observed with the currents is mainly the bad predictions at areas close to the shore.

This research examined how the historical data collected from the Performance Monitoring System (PMS), can be used to develop a vessel's performance model. It was proven that a model developed based on the traditional approach is not lacking significantly in accuracy, compared to a Machine Learning model, if operational data are used for verification, and tuning when necessary, during the development process. In addition, it was identified that a model based on the traditional approach can be used in a wider range of applications, and provides more information compared to a Machine Learning model. On the other hand, it should be noted that a Machine Learning model will always be superior in terms of time efficiency. It is also observed that despite the fact that only the main parameters influencing the vessels resistance are taken into account by the models, when the daily fuel consumption, or the fuel consumption for an entire voyage is calculated, these simplifications have minor impact. Finally, applications of the models were discussed and the value of the models was proven with case studies.

8.2. Recommendations

In order to further improve the research the following recommendations are given.

It was observed in the research that the calculated speed through water is of better quality compared to the measured speed through water. However the need for further improvement is identified. Thus it is recommended to develop a method where the data from the speed logger will be used to apply corrections on the calculated speed when it is observed that the latter is faulty. As it was shown in Figure 4.60, the identification of faulty calculated speed through water values is not difficult, since it can be handled with event detection algorithms. Reasearch is needed on how the two signals can be used in combination, to result in a better quality data regarding the speed through water.

In addition, it was observed that in the PMS data there is no consistency regarding the water depth data. For many vessels the water depth was not recorded at all, while for others the water depth was recorded periodically. Thus, the water depth was not used as an input to the data-driven models since the sample was small to give sufficient data both for the training and the testing phase. In the WBM, despite the fact that Lackenby's model was used for the added resistance due to shallow water, it was not used in the phase where the Schippersgracht's last year of operation was tested, since the water depth was not recorded for this dataset. Thus it is recommended to start recording the water depth as well, for all vessels, in order to examine in more detail the influence of the latter on the fuel consumption.

Regarding the methods that were used to create the models, the following are proposed. In the WBM the added wave resistance is taken into account with the STAwave-2 method. However the method is suitable to be used in Froude number [0.1-0.3]. It should be examined, whether this method lead to significant overestimation of the added resistance in speeds which correspond in Froude number lower than 0.1. In addition, in the data-driven models, the SV regression was used in all models. It is worth to examine whether other algorithms (i.e. ANN) can result in higher accuracy.

In the results presented in Table 6.3 the fuel consumption of 5 voyages was calculated based on the predictions of the three models (WBM, BBM, GBM-1) and was compared to the measured one. It is recommended to examine more voyages to minimize the influence of chance. The same applies in the second case study, where the deviation between the prediction of the developed algorithm and the measured fuel consumption was tested only for a few voyages. The examination of a larger number of voyages will lead to more reliable results.

Regarding the applications of the models, it is recommended to the company to examine the case of a in-house developed voyage optimization tool. In the second case study it was proven that the models have the potential (however a deeper examination is proposed) to be used for such applications. An in-house developed voyage optimization algorithm will give more flexibility to the company to choose the risk of exposure to harsh weather conditions. In addition, the revenues can be involved as well, which will lead to the development of a profit maximization algorithm instead of a fuel minimization algorithm.

In addition, it is recommended to continue the research towards the development of tools which will be used in the performance assessment. The following steps are proposed. Development of algorithms which detect events for which the model does not account for (i.e maneuvering) and non stable periods (i.e vessel is accelerating). The data corresponding in the aforementioned cases will be filtered out from the dataset to be processed from the performance tools. Then the performance model can be used as a baseline to make comparisons with the actual fuel consumption of the vessel.

Bibliography

[1] Reducing emissions from the shipping sector. URL :https://ec.europa.eu/clima/policies/transport/shipping_en.

[2] *Second IMO GHG study*, 2009.

[3] *Shipping, world trade and the reduction of CO2 emissions*$_2$014.$International Chamber of Shipping(ICS)$,2014.

[4] *Third IMO GHG study*, 2014.

[5] L.G Aldous. *Ship operational efficiency: Performance models and uncertainty analysis*. PhD thesis, University College London (UCL), 2015.

[6] Volker Bertram. *Some Heretic Thoughts on ISO 19030*. 2017.

[7] Werner Blendermann. Wind loadings of ships - collected data from wind tunnel tests in uniform flow. 1996.

[8] John Carlton. *Marine Propellers and Propulsion*. Butterworth-Heinemann, 1994.

[9] Andrea Coraddu, Luca Oneto, Francesco Baldi, and Davide Anguita. Ship efficiency forecast based on sensors data collection: Improving numerical models through data analytics. *OCEANS 2015 - Genova*, 2015. doi: 10.1109/oceans-genova.2015.7271412.

[10] Endresen O Eide, M.S. Assessment of measures to reduce future co2 emissions from shipping. DNV GL, 2010.

[11] E Eljardt. Development of a fuel oil consumption monitoring system. Master's thesis, Hamburg University of Technology (TUHH), 2006.

[12] Shipyards' Maritime equipment association. Shipbuilding market monitoring report, 2019.

[13] R.D. Geertsma, R.R. Negenborn, K. Visser, M.A. Loonstijn, and J.J. Hopman. Pitch control for ships with diesel mechanical and hybrid propulsion: Modelling, validation and performance quantification. *Applied Energy*, 206:1609–1631, 2017. doi: 10.1016/j.apenergy.2017.09.103.

[14] DNV GL. Global sulphur cap 2020, 2019.

[15] Milinko Godjevac, Joost Drijver, Leo de Vries, and Douwe Stapersma. Evaluation of losses in maritime gearboxes. *Proceedings of the Institution of Mechanical Engineers, Part M: Journal of Engineering for the Maritime Environment*, 230(4):623–638, 2016. doi: 10.1177/1475090215613814.

[16] Rob Grin. On the prediction of wave-added resistance with empirical methods. *Journal of Ship Production and Design*, 31(3):181–191, 2015. doi: 10.5957/jspd.31.3.130060.

[17] Roeland Grutterink. Development of a ship performance monitoring system and data analysis of spliethoff vessels. Master's thesis, Delft University of Technology, 2017.

[18] Isabelle Guyon and André Elisseeff. An introduction to variable and feature selection. *Journal of machine learning research*, 3(Mar):1157–1182, 2003.

[19] S.V Hansen. *Performance Monitoring of Ships*. PhD thesis, Technical University of Denmark (DTU), 2012.

[20] J. Holtrop and G.G.J. Mennen. An approximate power prediction method. *International Shipbuilding Progress*, 29(335):166–170, 1982. doi: 10.3233/isp-1982-2933501.

[21] J. Holtrop and G.G.J. Mennen. An approximate power prediction method. *International Shipbuilding Progress*, 29(335):166–170, 1982. doi: 10.3233/isp-1982-2933501.

[22] International Towing Tank Conference (ITTC). Analysis of speed/power trial data. 2004.

[23] Johan M Journee. Review of the 1979 and 1980 full-scale experiments onboard containership m.v. hollandia. 2003.

[24] Johan M Journee. Review of the 1985 full scal calm water performance tests onboard m.v. mighty servant 3. 2003.

[25] S Sathiya Keerthi and Chih-Jen Lin. Asymptotic behaviors of support vector machines with gaussian kernel. *Neural computation*, 15(7):1667–1689, 2003.

[26] Hans Klein Woud and Douwe Stapersma. *Design of Propulsion and electric generation system*. IMarEST - The Institute of Marine Engineering, Science and Technology, 2003.

[27] Jan Kulczyk and Tomasz Tabaczek. Coefficients of propeller-hull interaction in propulsion system of inland waterway vessels with stern tunnels. *TransNav, the International Journal on Marine Navigation and Safety of Sea Transportation*, 8(3):377–384, 2014. doi: 10.12716/1001.08.03.08.

[28] H Lackenby. The effect of shallow water on ship speed. *The ship builder and the marine engine builder*.

[29] Wee Sun Lee, Peter L Bartlett, and Robert C Williamson. The importance of convexity in learning with squared loss. *IEEE Transactions on Information Theory*, 44(5):1974–1980, 1998.

[30] Leifur Þ. Leifsson, Hildur Sævarsdóttir, Sven Þ. Sigurðsson, and Ari Vésteinsson. Grey-box modeling of an ocean vessel for operational optimization. *Simulation Modelling Practice and Theory*, 16(8):923–932, 2008. doi: 10.1016/j.simpat.2008.03.006.

[31] K.P Logan. Using a ship's propeller for hull condition monitoring. 2011.

[32] J.Pyorre M.Antola, A.Solonen. Notorious speed through water. *Hullpic 2017*, 2017.

[33] Anthony F Molland, Stephen R Turnock, and Dominic A Hudson. *Ship resistance and propulsion*. Cambridge University Press, 2017.

[34] O'Connor F.R.C Moor, D.I. Resistance and propulsion factors of some single screw ships at fractional draught. *Transactions of the North East Coast Institute of Engineers and Shipbuilders*, 80:185–202, 1963.

[35] Hideo Orihara and Masaru Tsujimoto. Performance prediction of full-scale ship and analysis by means of on-board monitoring. part 2: Validation of full-scale performance predictions in actual seas. *Journal of Marine Science and Technology*, 23(4):782–801, 2017. doi: 10.1007/s00773-017-0511-5.

[36] Egon S. Pearson. Further note on the "linear correlation ratio". *Biometrika*, 19(1/2):223, 1927. doi: 10.2307/2332188.

[37] B. Pedersen. *Data-driven Vessel Performance Monitoring*. PhD thesis, DTU Mechanical Engineering, 2014.

[38] J.P Petersen. *Mining of Ship Operation Data for Energy Conservation*. PhD thesis, Technical University of Denmark (DTU), 2011.

[39] ITTC Reccommended procedures and guidelines. Prediction of power increase in irregular waves from model test. 2014.

[40] Harilaos N. Psaraftis and Christos A. Kontovas. Ship speed optimization: Concepts, models and combined speed-routing scenarios. *Transportation Research Part C: Emerging Technologies*, 44:52–69, 2014. doi: 10.1016/j.trc.2014.03.001.

[41] Bernhard Schölkopf. The kernel trick for distances. In *Advances in neural information processing systems*, pages 301–307, 2001.

[42] Clarkson Reserarch Limited Services, 2019. URL `https://www.crsl.com`.

[43] W Shi, D Stapersma, and H T. Grimmelius. Analysis of energy conversion in ship propulsion system in off-design operation conditions. volume 1, pages 461–472, 06 2009. ISBN 9781845641917. doi: 10.2495/ESU090411.

[44] Alex J Smola and Bernhard Schölkopf. A tutorial on support vector regression. *Statistics and computing*, 14(3):199–222, 2004.

[45] C. Spearman. Demonstration of formulae for true measurement of correlation. *The American Journal of Psychology*, 18(2):161, 1907. doi: 10.2307/1412408.

[46] Ao N Tikhonov and V Ya Arsenin. Methods of solution of ill-posed problems, 1979.

[47] RL Townsin and D Byrne. Speed, power and roughness: the economics of outer bottom maintenance. 1980.

[48] Masaru Tsujimoto and Hideo Orihara. Performance prediction of full-scale ship and analysis by means of on-board monitoring (part 1 ship performance prediction in actual seas). *Journal of Marine Science and Technology*, 24(1):16–33, 2018. doi: 10.1007/s00773-017-0523-1.

[49] Max van den Berg. Ship performance management and the added value of a ship performance monitoring system. Master's thesis, Delft University of Technology, 2018.

[50] P Van Oossanen. *Calculation of performance and cavitation characteristics of propellers including effects on non-uniform flow and viscosity*. PhD thesis, Delft University of Technology, 1974.

[51] Vladimir N. Vapnik. *Statistical Learning Theory*. Wiley-Interscience, 1998.

[52] Xiaoyu Wang and Chee-Chong Teo. Integrated hedging and network planning for container shipping's bunker fuel management. *Maritime Economics Logistics*, 15(2):172–196, 2013. doi: 10.1057/mel.2013.5.

[53] D. Wouters. The accuracy of spos. Master's thesis, Amsterdam University of Applied Sciences, 2017.

[54] Zhaoqiang Zhang, Alexey Matveev, Sigurd Øvrebø, Robert Nilssen, and Arne Nysveen. State of the art in generator technology for offshore wind energy conversion systems. In *2011 IEEE International Electric Machines & Drives Conference (IEMDC)*, pages 1131–1136. IEEE, 2011.